HOCHSCHULE ZITTAU/GÖRLITZ
University of Applied Sciences

Program: N2612 Electrical Engineering and Informatics

Branch: Mechatronics

CAPACITIVE SENSORS IN PROSTHESIS

THE THESIS DEALS WITH ANALYSIS, PROBLEMATICS AND IMPLEMENTATION POSSIBILITIES OF CAPACITIVE SENSORS IN PROSTHESIS.

MASTER THESIS

Performed at the company Otto Bock HealthCare GmbH, Duderstadt

department of Developement prosthetics lower extremites

Grant recipients: Hochschule Zittau/Görlitz

Author: Bc. Martin Kopeček

Thesis Supervisor: Prof. Dr.-Ing. Alexander Kratzsch

Thesis Consultant: Dipl.-Ing. Herman Boiten

Date of entry of thesis: 02. 06. 2011

Date of submission of thesis: 19. 12. 2011

HOCHSCHULE ZITTAU/GÖRLITZ
University of Applied Sciences

Task of Master Thesis

Surname and name of the student (personal number - optional)	Martin kopeček
Abbreviation workplace	IPM
Date of entry MT	02. 06. 2011
Date of submission of thesis	19. 12. 2011
Range of graphics	by appropriate documentation
Range of thesis	cca 75 pages
Název Diplomové Práce (Czech)	Kapacitní senzory v protetice
Title of Master Thesis (English)	Capacitive sensors in prosthesis

Principles for the preparation Diploma Work

1) Analysis capacitive sensors.

2) Analysis of possible aplications of capacitive senzors in prosthesis.

3) Analysis of adverse ambient effects and their minimization.

4) Design of smart capacitive sensor concepts for prosthetic applications.

5) Development and implementation of one or two model sensor prototypes.

6) Testing and measurement of prototypes.

7) Benefits, disadvantages and use of sensors in practice.

Thesis Supervisor	Prof. Dr.-Ing. Alexander Kratzsch
Thesis Consultant	Dipl.-Ing. Herman Boiten Experte Knie- und Hüftgelenke Otto Bock HealthCare GmbH Max-Näder-Str. 15, D-37115 Duderstadt Telefon: +49 5527 848-3038, Fax: +49 5527 848-83038 boiten@ottobock.de | www.ottobock.de

Affidavit

I declare that I developed this diploma thesis independently only with cooperation of my supervisor and consultant and that I said all of the used literature.

Date: 14. 12. 2011, Zittau .....

Acknowledgement

I would like to express my appreciation to my consultant Dipl.-Ing. Herman Boiten and my supervisor Prof. Dr.-Ing. Alexander Kratzsch. Thanks for giving me the opportunity to be part of this interesting research. My deepest gratitude goes to Dipl.-Ing. Boiten for his time, patience, and understanding. Your ideas and recommendations were a motor for my work and it has been an honor to work with you. My special thanks belong to Prof. Kratzsch for his invaluable advice during the colloquiums. Also, thanks to the Otto Bock company for making this study and experience possible.

My gratitude also goes to the department of Developement prosthetics lower extremites, Hardware and Electronics Lab and manufacture department, there are not enough words to describe your excellent work. Special thanks to Stefan for your hardware advice and for acting as a mentor to me. Alexander, thanks for helping me run the experiments.

Then, sincere thanks to Cara, Elmar and Andreas for the help with the practical parts of the design process.

I also thank the Technical University of Liberec for their support and technical advice and literature for this topic.

Annotation

Martin Kopeček, Master thesis

In the first part of the literature analysis is focuses on problems with walking for people after amputation of a lower extremity and briefly examines the biomechanics of the human leg. Also described will be the creation of artificial prosthesis, their description and their basic functions. In the second part of this thesis, attention is generaly applied to capacitance and capacitive sensors. Here will be discussed their properties, connections and use in practice. The third part deals with the possible use of capacitive sensors for applications in prosthetics. A testing evaluating board was made called "EBWorkspace". Tested and investigated are all sensors on the immunity against external adverse ambient effects on transfer of measuring signal and their possible supression. The Matlab program and Microsoft Office Excel is used for vizualize and calculations. In the fourth part is the design of the concept of smart sensing unit- adapter for C Leg prosthesis in software ProEngineer using knowledge from previous measurements. There is emphasis on design and sensor arrangement in the tube of prosthesis and on the change of construction of supporting element prosthesis based on the patented parts of the company OttoBock. For the visualization of several models analysis, the programme ProMechanic and Ansys were chosen. The quality of the model prototype is verified also in this part, and its functionality, mechanical resistance and resistance against adverse ambient effects tested. Output data were measured and the obtained measurement evaluated. A general discussion on the usability of these sensors in prosthesis applications on the base of knowledge from the developed prototype is on the end this part. Benefits and disadvantages of capacitive sensors are analysed in comparison with other sensors. In the last part are most important knowledge from developement summarised and also proposed an outline for further innovation and development of capacitive sensors in the C -Leg prosthesis or other use.

Key words:

sensor; capacity; design; Evaluating Board; prosthesis; model; PicoCap; extension; flexion; lower extremity; temperature; humidity ; C-Leg; moment; vertical force; electrode; expansion; contraction

Anotace

Martin Kopeček, Diplomová práce

V literárním rozboru je v první části zdůrazněn problém s chůzí u lidí po amputaci dolní končetiny a stručně rozebrána biomechanika lidské nohy, dále způsoby vytvoření umělé protézy, její popis a základní funkce. V druhé části této práce je pozornost věnována obecně kapacitě a především kapacitním senzorům. Zde jsou rozebrány jejich vlastnosti, zapojení a využití v praxi. Třetí část se zabívá možným využitím kapacitních senzorů v aplikacích pro protetiku. Je vyrobeno testovací zařízení "EBWorkspace" , kde jsou testovány jak vlastní sensory tak jsou zde zkoumány vedlejší negativní vlivy prostředí na přenos měřeného signálu a jejich možné potlačení. Vývojové prostředí pro vizualizaci je vytvořeno v programu Matlab a Microsoft Office Excel. Ve čtvrté části je v programu ProEngineer navržen koncept speciální snímací jednotky, adaptéru pro protézu C-Leg, kde je využito poznatků z předcházejících měření. Je zde kladen důraz na návrh a uspořádání senzorů v trupu protézy a na změnu konstrukce nosného prvku protézy vycházející z patentovaných částí firmy OttoBock. Pro analýzu a zatěžovací vizualizace modelu byl vybrán program ProMechanic a Ansys. Je zde také prověřována kvalita vyrobeného modelu, testována jeho funkčnost, mechanická odolnost, odolnost proti vnějším vlivům, jsou zde změřena výstupní data a zhodnocena získaná měření. V této části je také obecná diskuse o využitelnosti těchto senzorů v protetických aplikacích na základě poznatků z vytvořeného prototypu. Jsou zde rozebrány výhody a nevýhody kapacitních senzorů v porovnání s jinými senzory. Závěrem jsou nejdůležitější poznatky z výzkumu shrnuty a je zde nastíněna další inovace a vývoj kapacitního senzoru v protéze C-Leg nebo podobné využití.

Klíčová slova:

senzor; kapacita; návrh; Evaluating board; protéza; model; PicoCap; extenze; flexe; dolní končetina; teplota; vlhkost; C-Leg; moment; vertikální síla; elektroda; expanze, kontrakce

Content

List of Abbreviations

GRF	Ground reaction force
GRFV	ground reaction force vector
M	Moment
EB	Evaluating board
EBW	Evaluating board workspace
C (1...5)	Capacitive sensor (1...5)
S (1...5)	Capacitive sensor (1...5)
PCB	Printed circuit board
FR 4	Flame resistant composit of fiberglass with epoxy resin
COP	Center of pressure
DC	Direct current
AC	Alternating current
PicoCap	PC01-AD microchip
Tab.	Table
Fig.	Figure
FEM	Finite element method
MB	Main body
PCapØ1-EVA-KIT	PCapØ1- microchip and evaluating kit
SPI	Serial Peripheral Interface Bus
A (1234)	Attachment (1234)
CCG	Central circle ground
CE	Circle element
TE	Tube element
MA	Moment arm
GND	Ground (electricity)
RME	Root mean-square
AT	Aluminium tube
WAK	Thermal expansion coefficient
NTE	Negative thermal expansion

Introduction

In the case that someone is healthy, they usually try enjoy life to the fullest. Unfortunately, not everyone has such luck. An inborn defect, sudden illness or serious injury can completely change a person's life. Most people will try to influence the situation when in a tight spot with their mobility and autarchy.

One of the biggest changes in life is when losing a lower extremity. The reasons may vary, but it is always a radical situation and one which needs to be tackled.

Nowadays people dont remain in the confines of a wheelchair or walk on one leg with crutches. Help for these patients is provided by prosthetics and the field of biomechanics. This field finds solutions so that one can still go on to lead a very active life without any restriction with the use of artificial limbs/prosthesis. This is a very expensive and complicated device that went through many decades of development and has gradually provided many disciplines. Nowadays you can choose from a lot of possible types of prostheses that meet the essential requirements for copying human walking and trying to bring near natural movement in most daily situations. To achieve this it is necessary to equip special prosthesis sensors that are able to locate the position of prosthesis, and at the right moment, to ensure safe and smooth movement.

This work focuses on the development of capacitive sensors in prosthetics. In cooperation with the OttoBock company in Germany it was suggested to explore in detail the possibility of using these sensors, especially in the latest versions of the knee prosthesis of the C-Leg system. C-Leg system is designed as a substitute for transfemoral amputation and it allows the patient very natural and safe movement.

The task of this work is to analyze, design, implement and test the system with capacitive sensors for prosthetic applications, resolve the issue of interference external adverse ambient effects and assess the benefits and disadvantages of this technology. The knowledge gained will be used primarily for scanning and motion control system in the C-Leg. For visualization of the proposed model the program ProEngineer was chosen and for stress tests and mechanical tests the ProMechanic program was selected. To develop this sensor, internal information from OttoBock company was used along with available literature and my own experiences.

1 Biomechanics and Prosthetics

This chapter is attempt to briefly sumarize the facts and ideas in the field of biomechanics which have already been, or which should be used, in the construction of prosthesis of lower extremity. For a better understanding of this complex issue the basic therminology and basic analysis of human gait is explained. Focus is given to biomechanical requirements in prosthetics, which can integrate prosthesis in to normal gait without occasion enormal compensation of movements.

Biomechanics is the interdisciplinary science which is specifically focussed to describe application of mechanical principles to biological systems.

"Biomechanics is the study of the structure and function of biological systems by means of the methods of mechanics". **description by Herbert Hatze, 1974* [20]

Biomechanics provides key information on the most effective and safest movement patterns, equipment, and relevant exercises to improve human movement describes Knudson, D [1]. Is the study of motion and its causes in living things. It is closely related to engineering and biological systems. Applied mechanics, most notably mechanical engineering disciplines such as continuum mechanics, mechanism analysis, structural analysis, kinematics and dynamics and today still more and more electronics, mechatronics and sensor techniques play one of the most important roles in the study of biomechanics as is expained in [2,5,32].

Prosthetics

Since ancient times, people have tried to find possible solutions for artificial replacements, and the emerging knowledge of medicine allows a larger use of new knowledge to develop better equipment for the treatment of patients after amputation. To better understand the function of certain parts of the human body it was necessary to investigate human movement. Based on this knowledge more sophisticated compensation copying, replacing and mimicking of the human body has been developed. This gave the basis for dealing with the field of artificial replacement - prostheses[11].

1.1. Biomechanics analysis of the lower extremity and gait

In this part is shown how mutual cooperation systematically operating external moments flexion and extension during gait, which arise due reaction powers from platform, inertia forces and internal moments of muscles forces.[4]

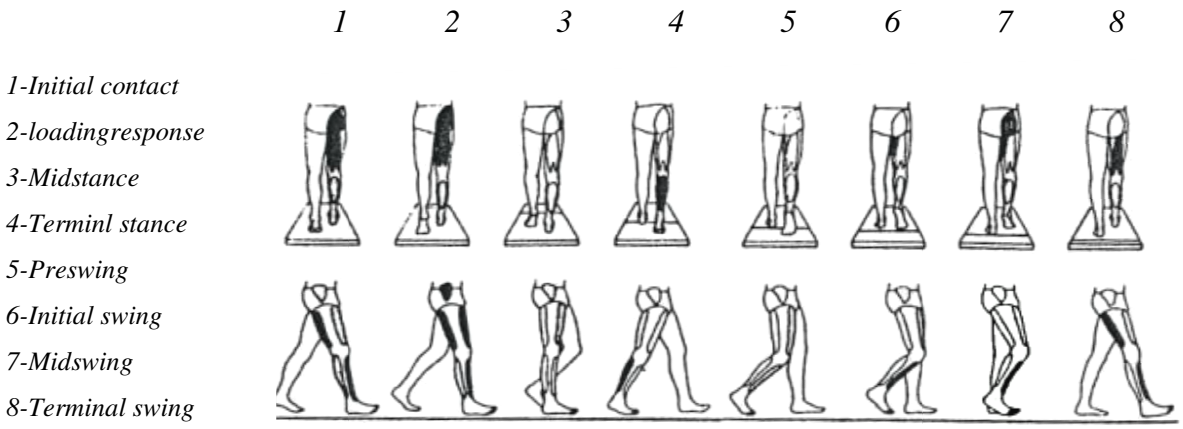

Fig. 1: Muscle study in gaitcycle

The study of muscles of the lower extremity during gait is be shown on Fig. 1. It is a complex interplay of several muscles and muscle groups that use bones and joints to create support for the weight of the human body. All joints are connected and strengthened by ligaments and joint capsules. The function of the legs is divided into static, supporting, which provides the body with solid foot support and transfers weight to the straight, as well as unstraight or slippery surface, and a dynamic part of the leg provides reliable support while walking, running, jumping and carrying loads.[6] During the gait, several forces act on the lower limbs. Fig. 2 shows how forces, moments and vectors interact with the human body. Many examples exist of how the gait cycle with vectors of forces and moments is

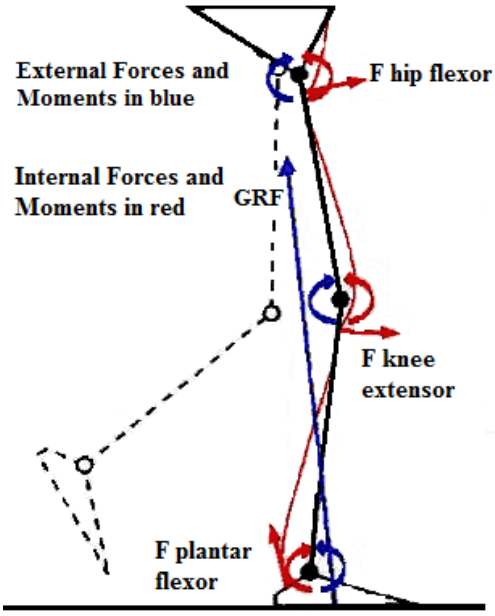

Fig. 2: Gait pattern-force and moment vector diagram

described. For our demonstration will be this description sufficient, this diagram is in sagital plane (it is usually explained as a 2D cut of the human body).

Ground reaction force GRF

The size of the ground reaction force (GRF) is changed according to the possition of the leg during the stance phase (Fig 2). The GRF is equal in magnitude and opposite in direction to the force that the body exerts on the supporting surface through the foot. The ground reaction force vector (GRFV) passes upward from the foot and produces movement at each lower extremity joint. The GRFV differs from a "gravity line," which is a vector that extends vertically from the center of gravity of a static body. [12,14] Instead, the GRFV is a "reflection of the total mass-times-acceleration product of all body segments and therefore represents the total of all net muscle and gravitational forces acting at each instant of time over the stance period".

**description by Winter, 1984*[21]

It can predict muscle activity quite accurately if it takes the view that the ground reaction force (GRF) and the muscles produce equal and opposite moments (M) around each joint. The ground reaction force is not the only force reacting on joints during gait. The weight and inertia of a moving segment has an effect on the segments distal and proximal to it. Moving the upper extremity influences movement in the lower extremity. These joint reaction forces can be in some case important. However, joint reaction forces are relatively small in the lower extremity, at least during stance phase. Therefore, clinicians can use the GRFV's position by itself to understand the forces that human muscles must control during gait's stance phase. For our developement it will be worked with GRF, because this describing of forces helps set and control the settings of right position of prosthesis on the measuring surface and calculation vertical forces and moment in prosthesis. [12,13,14]

"The lower extremity is served as a connection body with the environment and proprioception feedback maintain upright posture. Each step begins with the foot as a flexible structure do not know the surrounding environment, and completes it as a rigid lever, maintaining balance of the body ".

** description by P.Dungel and collective*[6]

Knowledge of the biomechanics of human gait will help during the following tests, measurement and development. The next part of the thesis focuses on knee joint problematics where it is connect to the C-Leg prosthesis and especially capacitive sensors. Also explained is the difference between normal gait and gait with prosthesis.

1.2. Flexion and extension of knee joint

For the movement of a lower extremity it is necessary to show what parts of human body are responsible for it. This part shown the influence and work of ligaments and bones.

The knee joint (articulatio genus) (Fig. 3) is one of the biggest part of a lower extremity. The main movement is in the sagittal plane. Maximal passive range of flexion knee joint in rotation movement is 120-160°. For our daily mothorical system it is important to have extension and flexion in the knee joint in both an unloaded and loaded condition. [4]

The muscle strength and right possition and force of ligaments do a right possibility to fix the bones in extension (flexion). Functionless of one of these parts can create a problem for walking, standing and other movements. [4]

A. basic position-fullextension (locked knee)

B. at flexion 5° associated with initial rotation ("unlock") shall be released collateral ligaments (4, 5) and crucial ligaments (2)

C. continued to flexion again collateral ligaments (5) and cruciate ligaments (2) and they provide protection and strength knee in motion[25]

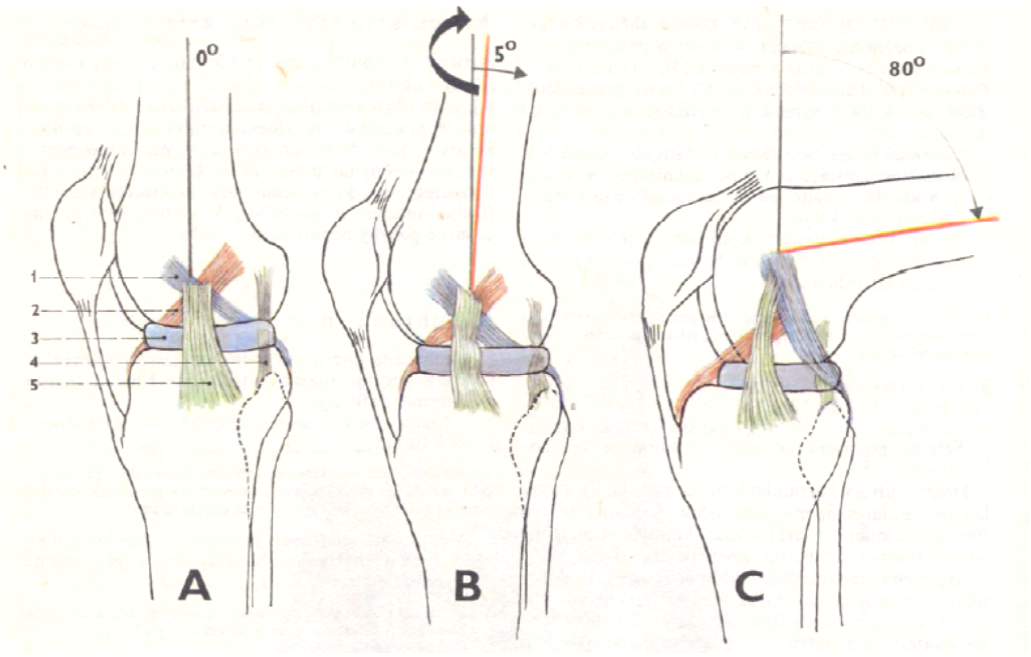

Fig. 3: Knee diagram

1,2: cruciate ligaments *3:* meniscus *4,5:* collateral ligaments

The knee joint consists of several parts. To name just a few fundamental ones, Jírová, J[25] writes: To compensate of the curvature is meniscus-cartilage plates crescent shape, attached to the tibia (shin bone). The joint capsule is strong and reinforced lateral ligaments. Inside of the knee are two separate cruciate ligaments. The stability is a prerequisite for the stability of the whole lower extremity.

1.3. Muscle study of the lower extremity

There are a large number muscles which are divided into the following groups: Muscles of the hip joint, Thigh muscles, Lower leg muscles and Foot muscles. In to the detail, it is presented only following muscle group as thigh muscles. For this thesis is this part, one of the most important in terms of transferring forces and moments, as can be determined from the biomechanical studies above. The lower extremity is a work of art composed of 26 bones, 107 ligaments and 19 muscles.[4, 11]

1.3.1. The quadriceps

Also called the quadriceps extensor is a large muscle group (Fig. 4) that includes the four prevailing muscles on the front of the thigh. The great extensor muscle of the knee, forming a large fleshy mass which covers the front and sides of the femur, the strongest muscle in the human body and together with glutes muscles the most important muscle for walking. [28]

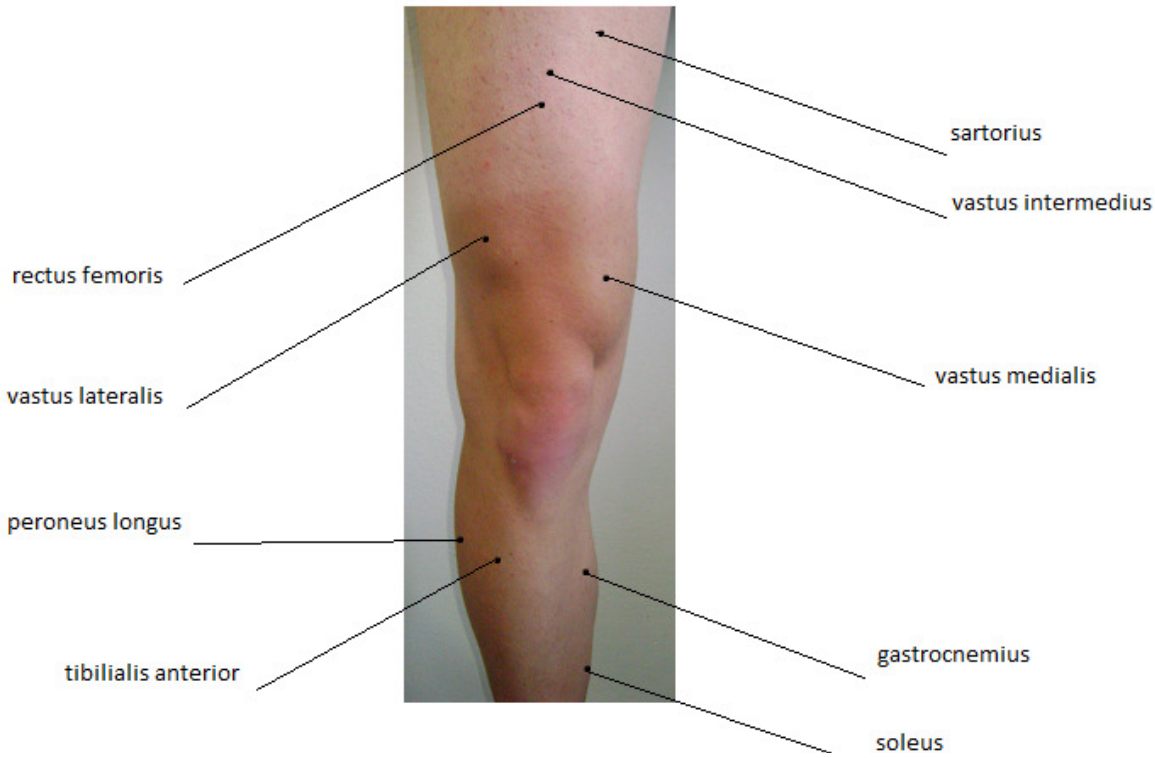

Fig. 4: Lower extremity-quadriceps

Rectus femoris occupies the middle of the thigh, covering most of the other three quadriceps muscles. It originates on the ilium. It is named from its straight course.

The other three lie deep to rectus femoris and originate from the body of the femur, which they cover from the trochanters to the condyles:

Vastus lateralis is on the *lateral side* of the femur (i.e. on the outer side of the thigh).

Vastus medialis is on the *medial side* of the femur (i.e. on the inner part thigh).

Vastus intermedius lies between vastus lateralis and vastus medialis on the *front* of the femur (i.e. on the top or front of the thigh). [28]

1.3.2. Range of motion measured during walking

During walking the knee joint is never in full extension (Tab. 1). At the start and the end of the stance phase there is almost maximal extension -5°. Maximal flexion 75° is in the midle of phase.

Range of joint motion during common activities:

Activity	Range of motion from knee extension to knee flexion(degrees):
Walking	0-67 *
Climbing stairs	0-83 #
Descending stairs	0-90
Sitting down	0-93
Tying a shoe	0-106
Lifting an object	0-117

Tab. 1

** Data from Kettelkamp(1970).Mean for 22 subjects. A slight difference was found between right and left knees (mean for right knee 68.1 degrees; mean for left knee 66.7 degrees).* [22]

#These and subsequent data from Laubenthal(1972).Mean for 30 subjects. [23]

1.3.3. Amount of knee flexion

(during stance phase of walking and running in Tab. 2)

Activity	Range in amount of knee flexion during stance phase (degrees)
Walking	
Slow	0-6
Free	12-18
Fast	6-12
Running	18-30

Tab. 2

Data from Perry et al., 1977. Range for seven subjects. [24]

Thanks to this biomechanical knowledge it is possible to try to produce an artificial substitute which can compensate the movement of a healthy human.

1.1. The issue of gait after amputation

The loss of part or all of a lower (upper too) extremity can be a dramatic interruption to a person's life. All care, beginning with preoperative psychological care, operations and ending with rehabilitation measures in specialised institute, are influenced by the patient's physical and mental condition.[11] However, with a team approach by the medical staff, the negative effects can be minimized and the positive benefits emphasized. Equipping the patient with a prosthesis not only greatly improves the patient's functional status but also helps his or her psyche.[1, 2, 3]

Patients who have undergone amputations often adapt a unique way of ambulating with a prosthesis, but these adaptations also bring about challenges in diagnosing problems with their gait. By understanding the biomechanics of the patient's gait, most problems can be discerned by means of observation, by measurement and testing. Basically we can say that lower amputation means less problems how to do a gait more naturally.

Nowadays amputations are divided in to the following levels (Fig. 5):

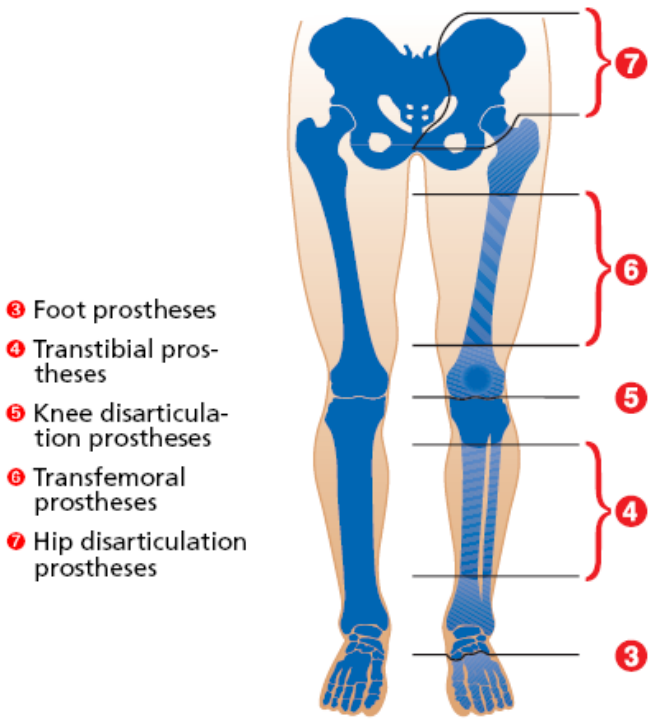

Fig. 5: Amputation levels

1.2. Lower Extremity Prosthetics

In source [11] the problematics are described in greater depth. Because each level of amputation needs a different type of prosthesis (Fig. 6) all companies who are developing and inventing prostheses need to standardize their products to the most universal range for most universal uses. Of course there exists special types of prosthesis for special events(especially for a sport, touristic), but we have to understand that each development costs a lot of money for the company = the patients and insurance companies have to pay much more money. A strategy is to produce universal equipement which can work around the world during different weather, temperature, wind outside influences, different work uses etc.

Fig. 6: Otto Bock modular prostheses for different amputation levels

The multi connection provided by the “adjustable connection element," is an Otto Bock invention. Inside the adapter there are four screws connected to the cross. They are fixing the pyramidshaped core, fixed on the convex attachment surface. Fixing can be made in all three dimensions, independent of each other. It is a big advantage which compensates the biologically bad position of the legs, set the right angle for foot prostheses. [11]

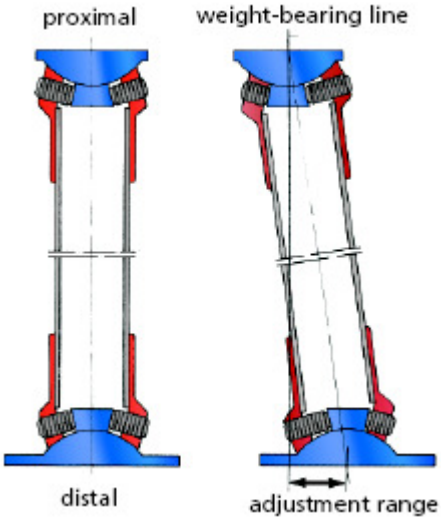

The horizontal plane should be modified by rotational adjustment at the

Fig. 7: Adjustment possibilities of the modular system

socket adapter or the tube clamp fixation. The right position may be fixed simply by loosening two screws, which lie at right angles to each other (Fig. 7).[11]

For the connection between several parts of prosthesis and parts other connectors can be used too.

Fig. 8: Adapter, proximal view

This connector (Fig. 8) is one of the most commonly used parts in prosthetic legs. It is used for testing new prosthesis in laboratory, because the assembling of new parts and manufacture possibilities are coming from previous experiences. The adapter from Fig. 8 is usually connected with the pyramidshaped core (Fig. 9) with female and male connectors. During development, new parts for prostheses are connected with this connectors. There exists several types of design, but the main idea is always the same. This special attachment used by other companies too and it is now the prosthesis technical standard around the world. [11]

Fig. 9: Pyramid adapter

2 Capacitive sensors

Capacitive sensors are contactless devices capable of high-resolution measurement of the position and/or change of position of any conductive (or nonconductive) target. A variety of things can be directly sensed - motion, chemical composition, electric field and, indirectly, sense many other variables which can be converted into motion or dielectric constant, such as pressure, acceleration, fluid level, and fluid composition. [15,16]

The range of application of capacitive sensors is extraordinary and very large. [15]. In [16] is explained that capacitive sensors use the electrical property of "capacitance" to make measurements. Capacitance is propertie two conductive objects with a space between them and respond to a voltage difference. Changes in the distance between the surfaces changes the capacitance. It is this change of capacitance that capacitive sensors use to indicate changes in position of a target. High-performance displacement sensors use small sensing surfaces and as result are positioned close to the targets (0.01-2 mm). [16]

Basic equation for calculation of capacity

$$C = \varepsilon_0 \varepsilon_r \frac{S}{d}$$

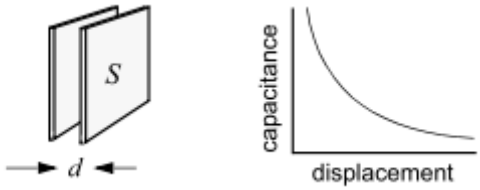

Fig. 10: Motion sense with spacing variation *

C [pF]	capacitance 1F=1C/V=1 $(A^2 \cdot s^4)/(kg \cdot m^2)$
ε_0[As/Vm]	electric constant - vacuum permittivity ($\varepsilon_0 \approx 8.854 \times 10^{-12}$ F m^{-1})
ε_r [1]	relative permittivity of the material (air ≈1.0005898 ± 0.0000005)
S [m^2]	surface of overlap of the two plates
d [m]	distance between the plates

From this equation it can be shown that capacity depends only on the size of the parallel-plate capacitor *(S)*, the type of insulator - dielectric properties (ε_r) and the distance between the plates *(d)*. The capacitance is therefore greatest in devices made from materials with a high permittivity, large plate area, and small distance between the

plates (says Baxter, L [15]). Typical dielectric materials such as plastic, glass or oil have dielectric constants of 3-10 as describe graphicaly [31] , and some polar fluids such as water have dielectric constants of 50 or more.[31,16] Around 10 % change in capacitance is produced by a 10 % spacing change, so with small distance between electrodes this system is very sensitive to spacing changes. [15]

*(*The extend of the capacitance depending on displacement is exaggerated for illustration purposes - Fig. 10)*

2.1. Advantages of capacitive sensors

In comparision with other contactless sensing technologies, such as optical, inductive, laser, and eddy-current, high-performance capacitive sensors have some distinct advantages which have more smart and easier solutions for measurement and use. There can be higher resolutions of sensing, some microchip including subnanometer resolutions and the small weight of electrodes can be in some case essential things for the selection of this sensor. Capacitive sensors respond equally to all conductors and they are less expensive and much smaller than laser interferometers and strain gauge sensors.

In [16] is written that for some applications capacitive sensors are not a good solution. Dirty or wet environments (eddy-current sensors are ideal) and large gaps between sensors and targets is required (optical and laser are better).

Of course, many another reasons exist why to use capacitive sensors. From this thesis, the main reason for use was the contactlessness and low price.

2.2. Application

A lot of different types of capacitive sensors exist which use similar plate geometry and similar circuits and components. This part presents some of the different electrode configurations used to build various types of sensors. It is described in more detail by Baxter, L [15]. It is especially focussed on the position sensing by two parallel plates of electrodes.

For the manufacturer of production, the most important thing is having a working, smart, cheap and easy solution. This solution, as in all development, is usually the desired solution.

2.2.1. Position measurement/sensing

Capacitive sensors are basically position measuring equipments. (Fig. 11) Their outputs always indicate the size of the spacing between the sensor's sensing surface and the target - usually conductor in this type sensing. If the measurement is stationary, any changes in the output are directly interpreted as changes in position of the target – idealization (are ignored adverse ambient effects). [16]

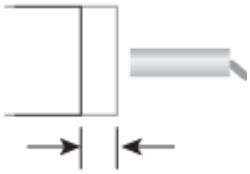

Fig. 11: Position displacement

2.2.2. Dynamic motion

The noncontact measurement is required for measuring the dynamics of a continuously moving target, such as a rotating spindle or vibrating element as in Fig. 12. Capacitive sensors are ideal when the environment is clean and the motions are small and slow, requiring high-resolution measurements.[16]

Fig. 12: Vibration

2.2.3. Thickness measurement

The common application for capacitive sensors is measuring material thickness in a noncontact fashion. A favourite application is a two-channel differential system (Fig. 13) where are used two separate sensors for each side of the product being measured. [16]

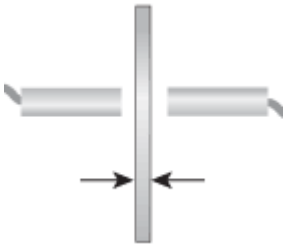

Fig. 13: Thickness

2.2.4. Testing of defectiveness

One of the properties of capacitive sensors is a much higher sensitivity to conductors than to nonconductors as in Fig. 14. Therefore, they can be used to detect the presence/absence of metallic subassemblies in the completed product. An example is a connector

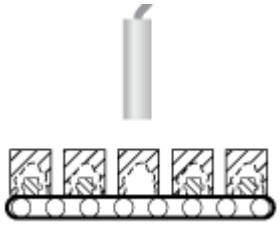

Fig. 14: Part sorting

assembly requiring an internal metallic snap ring which is not visible in the final product. The system can detect the defective part and highlight and alert the operator.[16]

2.2.1. Non-conductive thickness

Capacitive sensors can also be used to sense a thickness and/or density nonconductive materials which are placed between the probe's sensing area and a grounded back target (Fig. 15). When the distance between the sensor and the grounded surface is behind the target stable, changes in the sensor output are indicative of changes in thickness, density, or composition of the material in the sensor. [16]

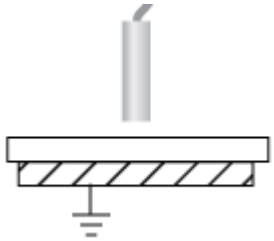

Fig. 15: Non-conductive thickness

2.3. Position detection

For common use, capacitive sensor are direct motion applications and a good solution for contactless measurement of angle, long-throw linear displacement or micro-plate spacing.

Several different arrangements of sensing electrodes are used, depending on the required measurement. For accurate measurement of small displacements, spacing variation is best, and for long throw applications, area variation is best. Three-electrode systems can improve performance, and many plates are used in parallel to increase capacitance. Multiple plates can be independently addressed to allow digital readout for better accuracy in long-throw applications-source [15,16].

For measurement with capacitive sensors a popular connection is explained in the following figure (Fig.16).

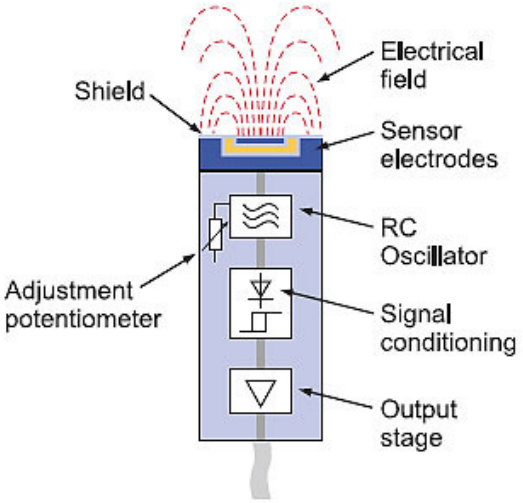

Fig. 16: Typical capacitive sensor construction

2.3.1. Principle of operation

Altendorf. R. [17] describes the principle as follows. The active part of the capacitive sensor consists of the two electrodes of measuring capacitor. The electrodes are connected in a circuit RC oscillator. When approaching the subject for the active part of the sensor will change the capacity of the capacitor and thus to change the frequency of oscillator (insulator changes the dielectric permittivity, a metallic object increases electrode surface). A change of frequency is evaluated by the sensor electronics and, after the subsequent amplification, converted as an output signal. Capacitive sensor sensitivity (range) can be continuously adjusted by a trimmer.

The capacitive sensor looks like an open condensator. For better sensing and protection against the negative influence of environment and electromagnetic field, the circular profile with the ground and compensation electrode is used. This design is now mostly in all capacitive sensors for series production, but a disadvantage of this can be the higher price and no possibility of a change or size or design of sensors. For special products, for example in prosthetics, it is better to develop our own structure of sensor, which will be done to special requirements and properties.

For this example, it was calculated with the basic structure for the sensor-parallel plates with ground, because for future work it is expected that the sensor will be inside of some completely closed system and it wont be needed to change or open it. Next text is focused only on the structure for spacing and area variation.

2.3.2. Spacing variation

Displacement variation of parallel plates is often used for motion detection if the spacing change is less than the electrode size is. The parallel plate capacitance formula (Fig. 10) shows that capacitance is inversely related to spacing. This gives a conveniently large value of capacitance at small spacing, but it does often require signal conditioning which can compensate for the parabolic capacitance-motion relationship. Measurement accuracy suffers from vanishing signal level says Baxter, L. [15]. Several sources of nonlinearity corrupt the performance of a simple parallel plate sensor. A simple two-plate Z-axis sensor with same-sized plates will have unwanted sensitivity to the transverse displacement in X or Y axes, coupling from back of plate and for

example tilt too (Fig. 17). [16] The characteristic of sensor is nonlinear describes Adámek M. [19].

Assuming that S and ε_r is constant the following equation applies:

$$C = \varepsilon_0 \varepsilon_r \cdot \frac{S}{d} \qquad C1 = \varepsilon_0 \varepsilon_r \cdot \frac{S}{d \pm \Delta d} = \varepsilon_0 \varepsilon_r \cdot \frac{S}{d1} \qquad C1 = C \cdot \frac{1}{1 \pm \frac{\Delta d}{d}}$$

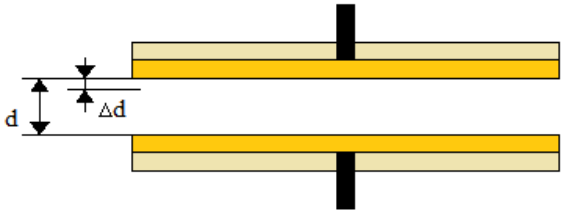

Fig. 17: Spacing variation

For an explanation of the theoretical supposition, a simple measurement was prepared with two printed circuit board (PCB) parallel plates electrodes of rectangular shape. From Graph 1 the nonlinear characteristic of capacity on the change of spacing or gap between the plates 3x3cm can be seen. This measurement was prepared from [18] for internal use in OttoBock. The signal from Graph 1 is made by one separative sensor and connected as a ground variation as is shown in chapter 3.1.4.

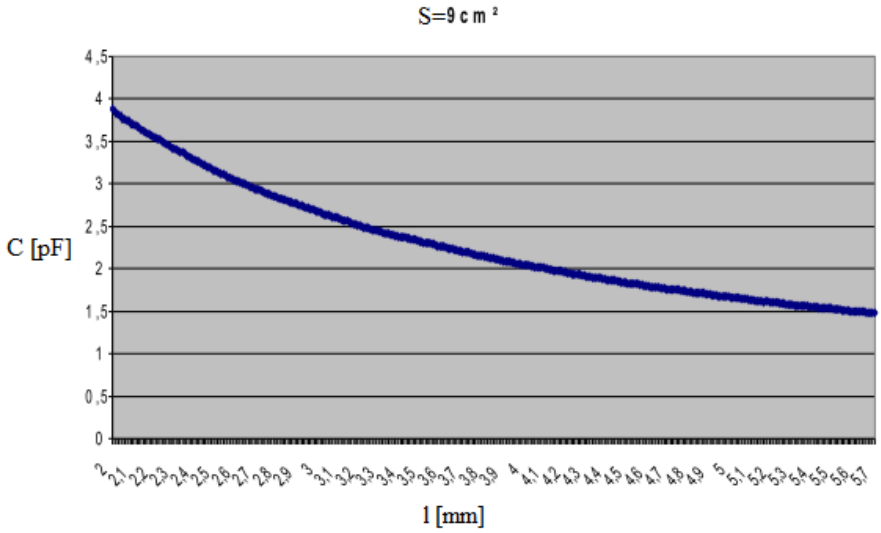

Graph 1: Spacing variation

2.3.3. Area variation

Area variation is preferred if it is possible controled the movement only on the horizontal direction and it can be really good compensated the vertical change of movement Δd. Only from this requirements it can be really good linearizated process made (Fig. 18). Area variation as these plates (Fig.18) slide transversely, capacitance changes linearly with motion - shifting. As with spacing variation, overlap is needed so

that unwanted sensitivities are minimized. This is described more precisely in [15]. Unwanted cases are for example the tilt in any axis, gap change and coupling from the back of the plate.

Adámek M. [19] assuming that d, b and ε_r is constant and the shape of electrodes is rectangular, the following equation applies:

This equation expresses the maximal capacity C_{max} for maximal overlap of electrod $l_{max.}$

$$C = \varepsilon_0 \varepsilon_r \cdot \frac{bl}{d} \qquad \frac{C}{C\,max} = \frac{l}{l\,max}$$

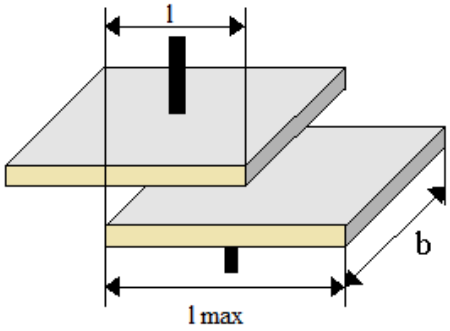

Fig. 18: Area variation

This equation expresses the maximal capacity C_{max} for maximal overlap of electrod $l_{max.}$

The characteristic of sensor is linear. With influence of spacing d and Δd is the equation following:

$$\frac{C}{C\,max} = \frac{l}{l\,max} \cdot \frac{1}{1 \pm \frac{\Delta d}{d}}$$

When is the change of spacing smaller $\frac{\Delta d}{d} \ll 1$ then it can be written:

$$\frac{C}{C\,max} \approx \frac{l}{l\,max} \cdot (1 + \frac{\Delta d}{d})$$

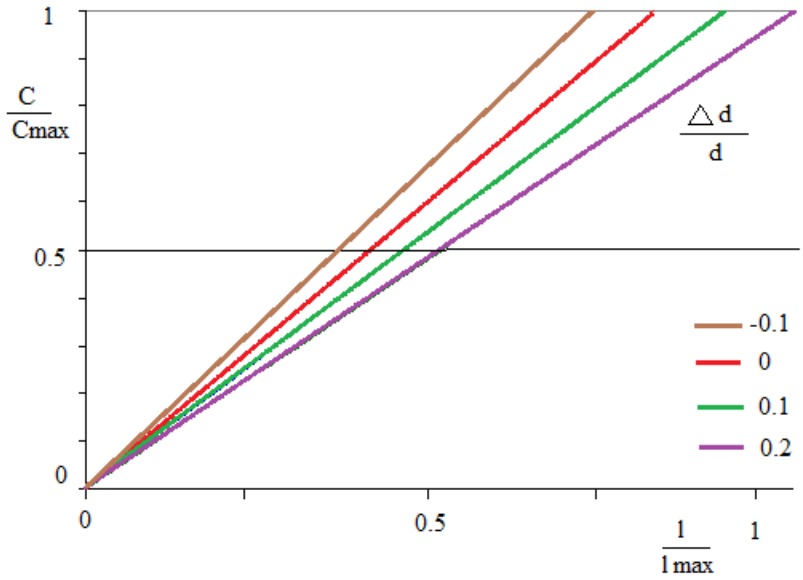

Normalizated equation of sensor with area variation of electrode is shown in Graph 2.

Graph 2: Area variation

3 Capacitive sensors for applications in prosthetics

Nowadays, sensor technology is growing in lots of types of prosthetics applications. It was written by a lot of expert researches that lot of applications use various sensing elements, but the capacitive sensors are still, in this type of development, unexplored and used only exceptionally. Due to their properties as a contactless measurement and high sensitivity, they can be used for specific measurement of a wide variety of physical phenomena such as pressure, spacing, thickness measurement, ice detection, humidity, shaft angle, linear position, balances etc. According to the basic theoretical information from the last chapter, it is known that with a change of space the capacity of sensors rises or decreases. The prosthetics replace lost, congenital defects or damaged parts of human body. Since the prosthesis manufactured from materials can be more or less deformed during movement, right here is a posibility to use capacitive sensors to measure spaces between some parts during the deformation, bending and pressure.

The next branch where capacitive sensors for prosthetics are used are various investigative methods of gait. One of them is Dynamic plantography, which uses the pressure platform for measureming pressure distribution under the foot, usually during walking or different standing modifications. For pressure measurements, platforms with high-density pressure or capacitive sensors are used. In plantography, capacitive sensors are used consisting of two flat conductors, between which is inserted an elastic dielectric. When the load is elastic, the dielectric presses, thereby changing its permittivity and the distance of both conductors. This changes the capacity of the sensor and changes the voltage. Frame rate is a maximum of 100 Hz. The hysteresis limit is given due to the slow response of the dielectric material on the change in pressure.[3]

3.1. Evaluating Board Workspace

For the verification of options used, the capacity measurement in prosthetics application was designed and developed; a testing workplace called Evaluating Board Workplace – (EBWorkspace) (Fig. 19). From the beginning of the six-month research in OttoBock was considered and worked on a special design of capacitive sensor in to

the latest prosthetic C-Leg. Before starting work on this sensor ,it was first necessary to verify the theoretical preconditions of capacitive sensors in general, to explore the possibilities of their shape, attachment and involvement, dependence on the dust, humidity and temperature, to explore the linear and nonlinear behavior of sensors so that in future application in prosthesis lengthy and frequent changes are avoided in design and editing prototype and guarantee the functionality of the final product. An important factor for the design and preparation of a simple device EBWorkspace was mostly the time saved and financial costs than to develop much more sophisticated and expensive sensors for the prosthetic C-Leg without no experiences. The workplace consists of the Evaluating Board (EB), sensors, wiring, equipment evaluation, electronics and personal notebook.

For calibration or stabilization of the right prosthesis or orthosis position it is necessary to know the pressure activity of human feed to the platform. Requirements and conditions on our testing device were chosen for the best structure of connection for capacitive sensors and their number inside of the evaluating board, toughness and material strength of the evaluating board, good deformation between the two steel parts of the board, and the right size for one human foot or prosthesis.

This EBWorkplace is used for finding the right position of prosthesis parts as the angles between ankle and knee, right length prosthesis tube, distribution of masses and volumes during the load.

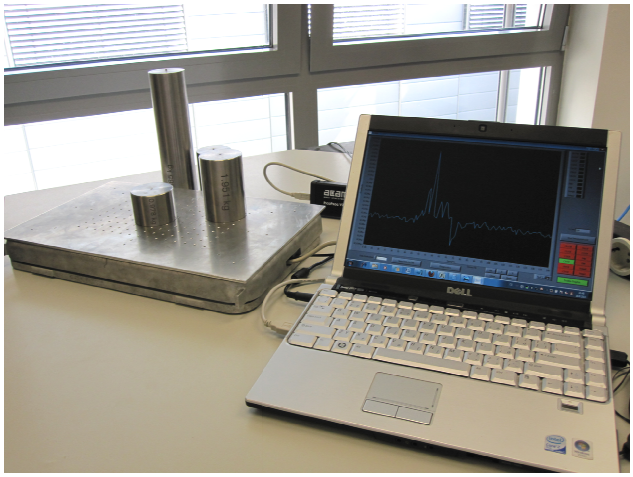

Fig. 19: Evaluating Board Workspace

3.1.1. Design of Board

Older prototype equipment from the scientist laboratory in OttoBock company (Fig. 20) was used for the development of the board and remodeled for our requirements.

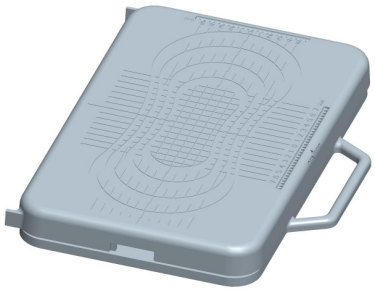

Fig. 20: Evaluating board

There are two parts of the same size (400x250mm), which are connected at the corners by elastic rubber rollers on each corner and fastened with screws. This system quarantees contactless measurement. Elastic rubber roles are dimensioned on the 40kg weight. This corresponds with the loading of the EB by one leg on which the EB is designed. More description of this problem is explained by Biemüller, P[18]. The material of EB is aluminium, on the upper site it was prepared measuring machined map for the right position of the human feet.

This enters a closed box with one hole for the output and input cables. The inner side plates have been shaped so as to alow the electrode sensors to be placed above each other. The maximal change of distance (limited of elastic properties and design of board) between these two parts is 5mm and it is equal to 100 Kg on the upper surface. Total weight of the whole board with all electronics parts is around 5Kg.

3.1.2. Sensors and sensing

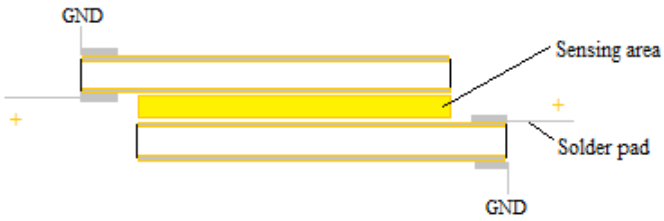

Fig. 22: Position of electrods

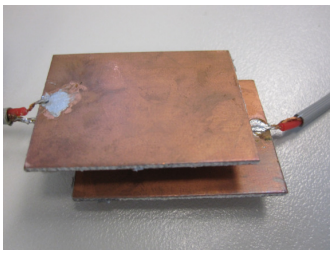

Fig. 21: Copper electrodes-double-sided PCB

For the development of the sensors it was important to design a shape of sensors – electrodes into the EB in connection for more measurement possibilities and

compare them in sensing properties and especially parasitic negative environmental influences.

Biemüller, P[18] chose a rectangular shape for four electrodes for easier measurement and verification of tests. The active rectangle parts –electrodes-were made from double-sided copper PCB 1.5mm, material FR 4 dimension of 40x30mm as in Fig. 21, which were soldered by sheeting doublewire cables from both sides. The surfaces are shifted on to each other in a horizontal position on 10mm (Fig. 22). The reason is that the solder pads have some width and has a negative influence on capacity measurement. Sensing area is the 30x30mm, meaning 900mm^2. For the connection of the sensors with EB five channels were made together (Fig. 25) and one of them as a referential (Sensor 5). Storage of sensors in EB is shown in Fig. 24 resp. Fig. 25. This diameter and the number of them was chosen for future mass measurement and load tests. This solution should make it easier for the calculation of the vertical force.

Sensor electrodes are individually placed exactly opposite from each other and form a total of 4 capacitive sensors. The dielectric is composed of an air, the reference capacitor has the air dielektrikum too.

Fig. 23: Elastic el.(A)

The Sensing is shown on Fig. 24. When the upper surface of EB is loaded, the elastic elements (Fig.23) are deformed (A) and the range between the plates of aluminium EB and the electrodes copper surfaces are closer (B). The capacity in this case growing up and conversely.

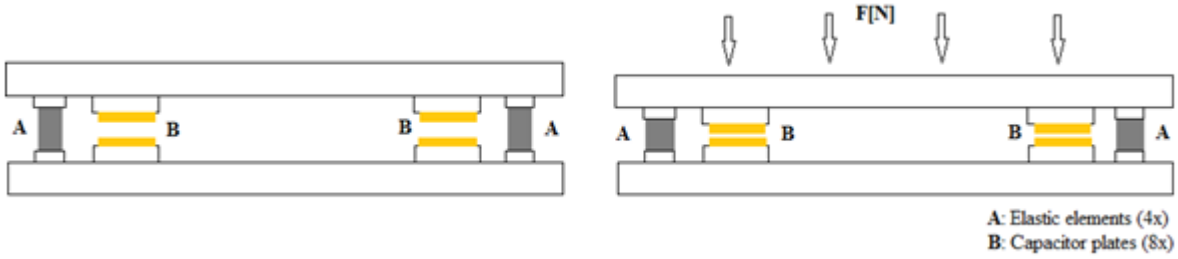

Fig. 24: Method of sensing

3.1.3. Evaluating electronics

For measurement, a Plug-in module was bought from the ACAM company. The sensors are connected to the Plug-in module and after conversion of the A/D converter the datas are processed by PicoProg V.2.0 and by a USB connected with a PC or laptop. This Kit included PicoCap01-EVA Software too.

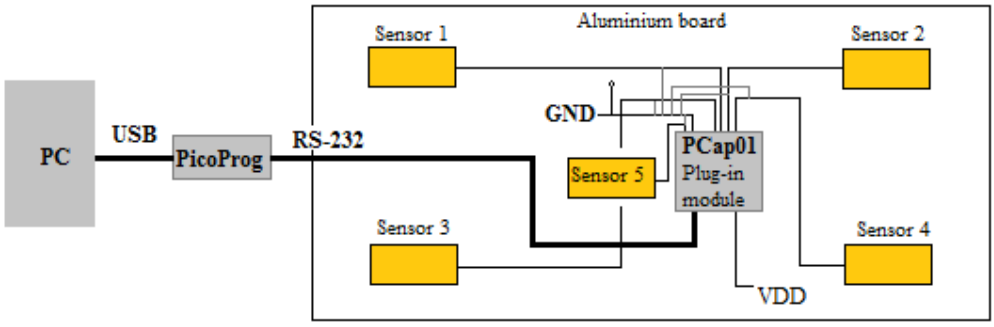

Fig. 25: Block diagram of electronicsnics

PCapØ1-EVA-KIT

A special microchip was used which can measure more channels and has higher internal capacity than our measurement range from sensor. The most important thing was good sensitivity and high accuracy and some evaluation system for connecting with computers. PCapØ1microchip (Fig. 26) was chosen from Acam messelectronic, gmbh from Germany. The benefit of this system is the included software and it is possible to immediately concentrate more time for evaluating of the sensors. The chip was ordered as a kit with control electronics**.** The kit consists of a motherboard, PC01-AD Plug-in module, PICOPROG V2.0 Programmer, High density DSUB15 cable, USB cable, Wall power supply 9 V, CD-ROM wih software. This support is used for testing Pcap01 microchip (Fig. 27) with the several connections with the sensors.

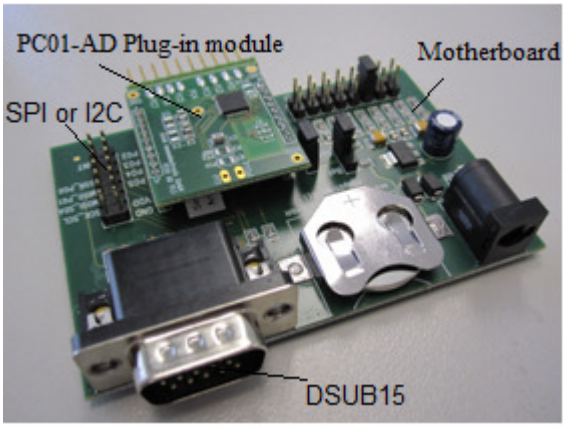

Fig. 26: EVA KIT

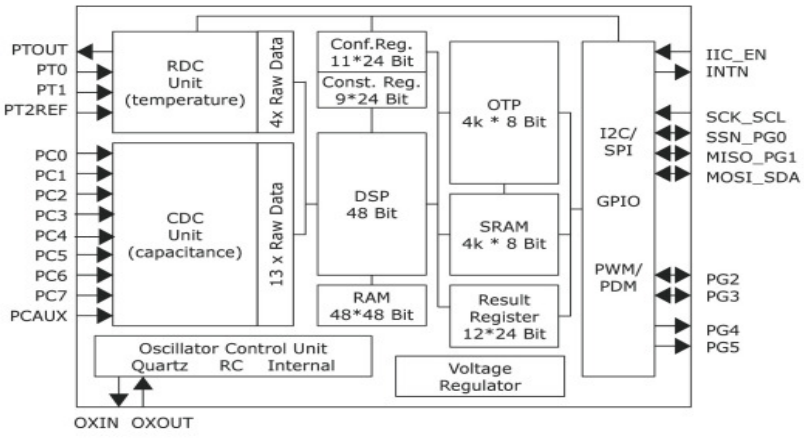

Fig. 27: Block diagram of the microchip

Measuring principle

The capacitors are charged to the DC voltage, then discharged (Fig. 28). The discharge time is then measured. The oscillator is used only as time reference. The discharge time is given by the capacitors and the discharge resistor. As a referencial capacitor is used 44 pF. Mutual comparison of the discharging times, reference capacitor and the resulting capacity indicates the capacity of the sensor (capacitor), which is displayed both graphically and in the form of values in the measuring software. [10]

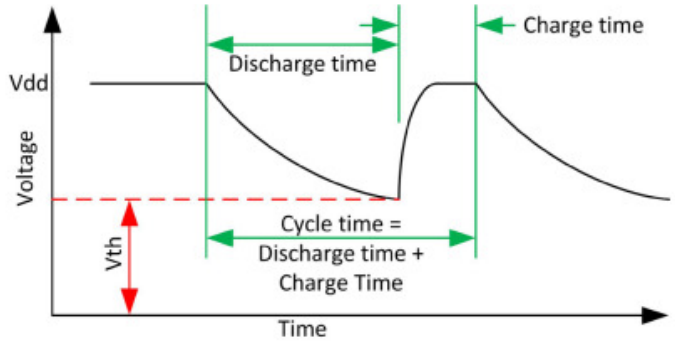

Fig. 28: Cycle time

An important notion is "cycle time", the period of one elementary discharge-and-recharge cycle, see Fig. 28. It is the time interval, set by the user, between two discharge time measurements. After measuring all channels, follow the interupt for the other measurement (temperature) or next measurement cycle.

The deducing of the measurement: discharge time ratios equal sensor to reference values:

$$\frac{\tau_N}{\tau_{ref}} = \frac{C_N}{C_{ref}}$$

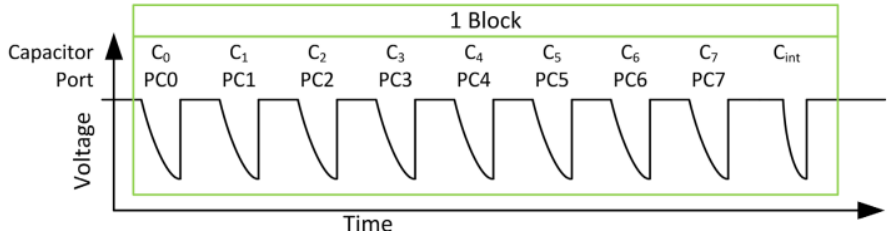

Fig. 29: Charging-/ discharging cycles grounded

One block for measurement is made of a discharge time measurement for each capacitor –sensor (Fig. 29) and an additional one for measuring the internal stray capacities and comparator delay (internal compensation). [10]

An example of how the sensors can be connected with averaging the measurements and internal compensations:

4 single grounded sensors + reference, cycle time = 200 µs: block period = 1.20 ms

$$4 \times 200\mu s + 200\mu s + 200\mu s\ intern.comp = 1.20ms$$

2 fake blocks + 10-fold averaging: measurement period = 14.4 ms

$$1.20ms \times 10Avg + 2fake \times 1.20ms = 14.4ms$$

$$f_{max} = \frac{1}{14.4ms} = 69.4Hz$$

Maximum update rate = 69.4 Hz

A detailed description is given in the datasheet [10].

The sensors can be connected floating. In this mode the two plates of the capacitor are charged alternately to DC, therefore the dielectric between the plates sees an AC field.

Connected cables

As was written in the theoretical part, the cable works as a condensator by small capacity and if it is not well shielded the measurement should have an adverse ambient effect in the cable or wire surrounding. For EB, "low noise" high density shielding cables of dimension 5mm were chosen. Schematic is in Fig. 30. Their connection with the active part of the sensor was done with the maximum accuracy and in all sensors on the same place with the same size of soldering spot. Next, cables for EBWorkspace were shielding too. With grounded capacitors the PCap01 offers the possibility to compensate for internal parasitic capacities and, having the same effect, the propagation delay of the comparator. With floating sensors there is an additional option to compensate the external parasitic capacities and noises against the ground. On the pcb the wire capacitance typically refers to the ground. For long wires it is necessary to have shielded wires with the shields grounded on the pcb connection side. Fig. 30 shows how shielded cables shall be connected for compensation of the external parasitic capacities. [10]

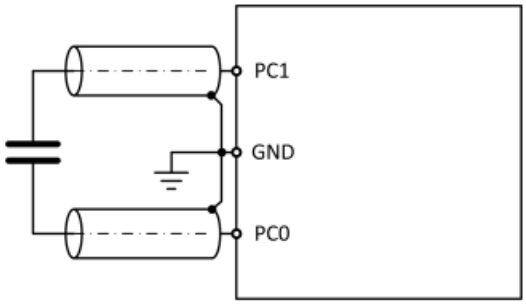

Fig. 30: Connecting sensor by shielded cables

3.1.4. Connecting the Capacitive Sensors

It exist lot of types of connection-floating mode, ground mode, differential connections etc. For our structure of the EB, the first two were chosen for testing.

Floating mode

For the EBWorkspace and PCap01 microchip it is possible to connect 3 sensors and one reference in floating mode as in Fif. 31. In our EB sensors C1 for shown behavior of the sensor and the whole system in the gradual uneven load were chosen (Graph. 3). [10]

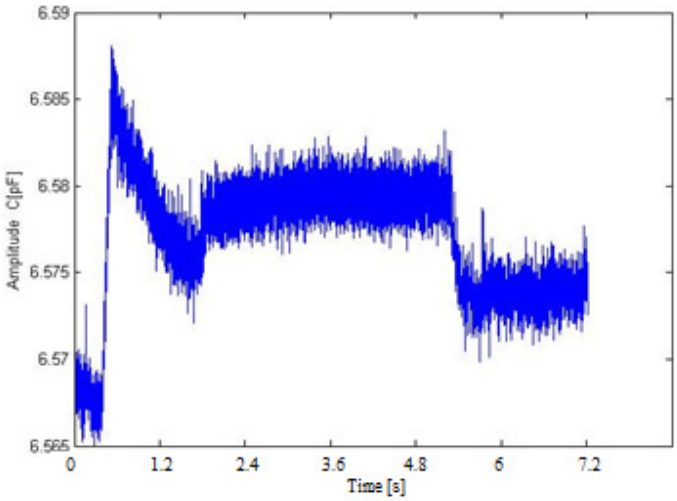

Graph 3: Reaction on touch the EB by finger

Result

The system was relatively well-sensitive, recorded loads from about 100g. The problem were shielded cables, which could not be resolved with the ubiquitous parasitic capacities around the sensors (human hand, wires and other electronics, etc.) , next problem was with not enough outputs. Therefore, more detailed measurements have already discontinued.

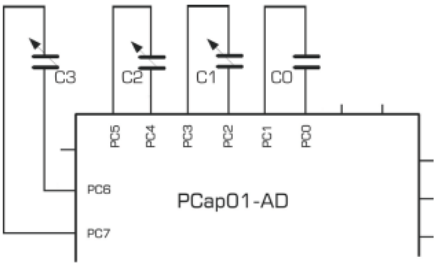

Fig. 31: Floating mode connection

Ground mode

In the EB it is possible to connect up to 7 sensors and one reference (C5) in ground mode (Fig. 32). C3 Sensors were chosen for this testing. The board was loaded by external effects and negative influences were compensated shered ground. During the measurement EB was unequally strained and was compared with the results from floating mode. [10]

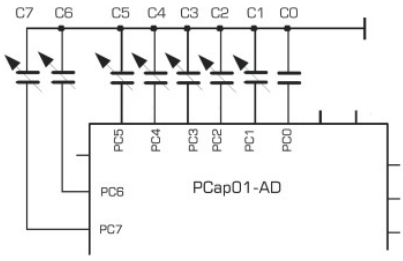

Fig. 32: Ground mode connection

Result: Graph 4 shows the sensitivity of the sensors, when all of the board is completly grounded. For testing, the sampling frequency of 50KHz was chosen. The Conversion time is 40 µs, because there is one more capacitor as a reference (together 2 channels in our test), the measuring rate was 25KHz and only small noise was measured from connected cables. This system was completely shielded to touches and vibrations. It was a big advantage against random noises from floating mode. In the Graph 4 is a small nonlinearity which was later compensated by an average of the samples. Sensitivity on the change of distance was better than in floating mode in the same settings. Noises were smaller and touching of the board did not have negative influences. Only deformation of the cables got low noise on the measured signal. For the next measureent this system was used. The accuracy and size of the basic capacities of sensors are influenced by the quality of the manufacturing and machining of parts of the sensor-active electrodes, as well as their attachment to the EB, soldering to the PCB, and especially on long cables between sensors and PCap01 EVA-KIT. For future innovation it is appropriate to have equal length cables for each sensor and choose machine production PCB. In our case, there were shortages corrected by offset. The measurement was influenced by the possibilities measure only vertical loads to the desktop. During measurement of the horizontal load the plates are deformeted cylindrical rubber pads to the side and the measurement was to a large extent degraded. In other parts of the research on EB it was suggested by several measurements, which assumed only vertical loads.

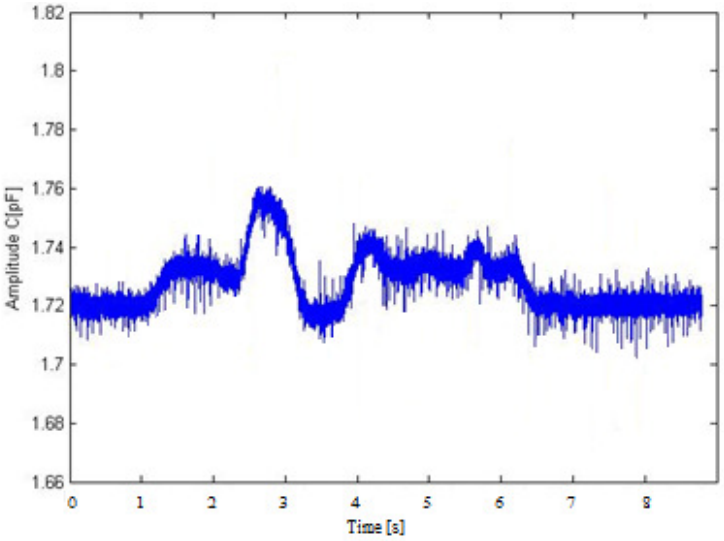

Graph 4: Reaction on shifting and gripping of cables by hand

In the future it would be not desirable to include horizontal forces in the measurements as it is necessary to anchor the plates system of two cylinders of various diameters, which fit together and include springs. This prevents displacement of plates and it is possible to measure the resulting vertical loads at one time.

3.1.5. Temperature measurement

To measure the temperature dependence at constant absolute humidity and capacity of sensors measured was prepared in climate box. The process of the temperatures were simulated from 60 °C to 10 °C for our EB. Constant absolute humidity was 8.5 g/m^3 or 0.0076 kg/kg of dry air. Constant absolute humidity was used to guarantee dependence of capacity only on temperature. Measurements from higher to lower temperatures had a reason in terms of condensation of residual water on the electrodes, which in the opposite case should spoil the accuracy of the measurement data.

Fig. 33: Temperature and climate box WKL

The temperature and climate testing box Weiss Umwelttechnik GmbH WKL64/40 (Fig. 33) has performances for temperature and humidity tests: Temp. Range was from min.-40 to max.+180°C, Temperature changing rate for cooling 5.0 K/min, Heating 3.5 K/min, Temp. constancy in time ±0.3 to ±1.0K, Temperature gradient 2 to 4K. Humidity range 10 to 98% r.h(depends on aktual temperature). Humidity constancy ±1 to ±3% r.h.

Temperature [°C]	Absolute Humidity [g/m^3]	Relative Humidity [% rH]
60.0	8.5	6.5
50.0	8.5	10.2
40.0	8.5	16.5
30.0	8.5	27.8
20.0	8.5	49.0
10.0	8.5	90.0

Tab. 3

In Tab. 3 is the verified data from general humidity table and calculated from relative values of humidity by constant absolute humidity value 8.5g/m3. According to this value, relative humidity was calculated and thus was barred the

influence of humidity from measurement. The calculated values are rounded to tenths. Absolute humidity expresses the weight of water steam contained in the unit volume of air. The most common expression is in grams of water steam per square meter of the air. If m is the weight of water steam in volume V then absolute humidity of air can be expressed in the following equation. [9] $\phi = \frac{m}{V}\ [g \times m^3]$

If m is the mass of water steam that is contained in the air, and M is the weight of water steam, which would contain the same volume of saturated air at the same temperature and pressure, then the relative humidity φ is given $\phi = 100\frac{m}{M}\ [\%]$

This relationship can be by using an expression for the absolute humidity in the rewrite form: $\phi = 100\frac{\phi}{\phi_n}\ [\%]$ where it indicates absolute Φ_n moisture saturated air (calculated form appropriate tables from this webside: *http://www.vaisala.com/humiditycalculator/vaisala_humidity_calculator.html).*[9] It means maximal quantity of humidity at a given temperature, the air is able to absorb - the water has already started to condensate. Φ is absolute humidity.[8] Since the amount of saturated steam depends on air temperature, relative humidity is changing with the the temperature even though the absolute amount of water steam stays the same. [9]

In the Graph 5 we can see the setting of the temperature with calculation of humidity.

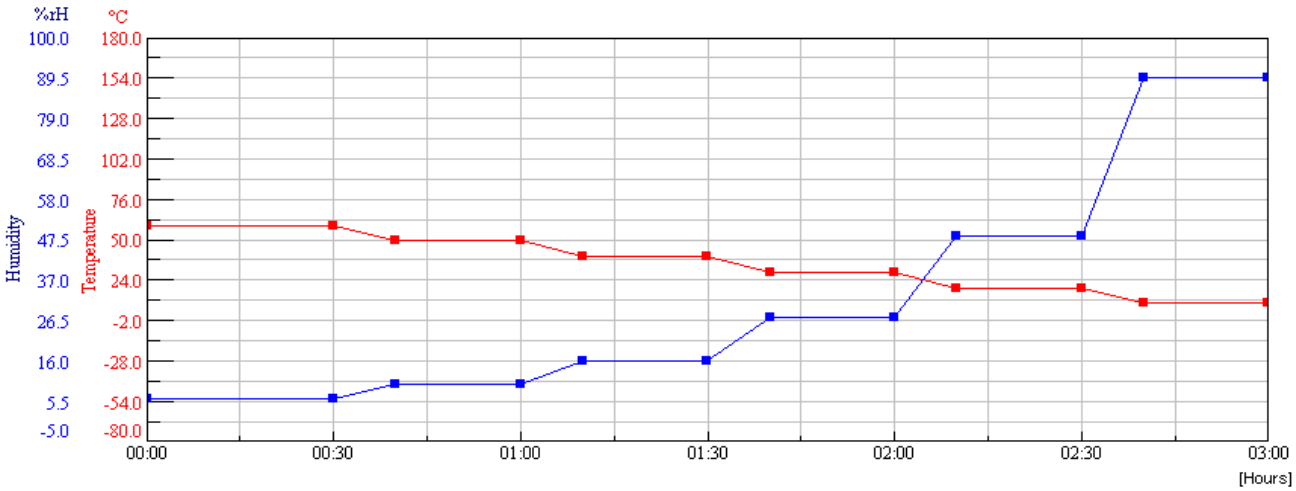

Graph 5: Required temperature (set in the climate box WKL)

The resulting process of the temperature measurement

Graph 6 shows the measured data during the measuring cycle, the response speed of the controller inside the climate box and in conjunction with the graph from the graphical interface from Acam PicoCap software it is possible to compare the dependence capacity on temperature and time. Sampling time was 10ms (100Hz) and conversion time was 60ms/6channels (1 channel = 10 ms) for more accurate data to be processed every three samples were averaged and using sequence timer was measured at 1.32 s each with a frequency of 763mHz.

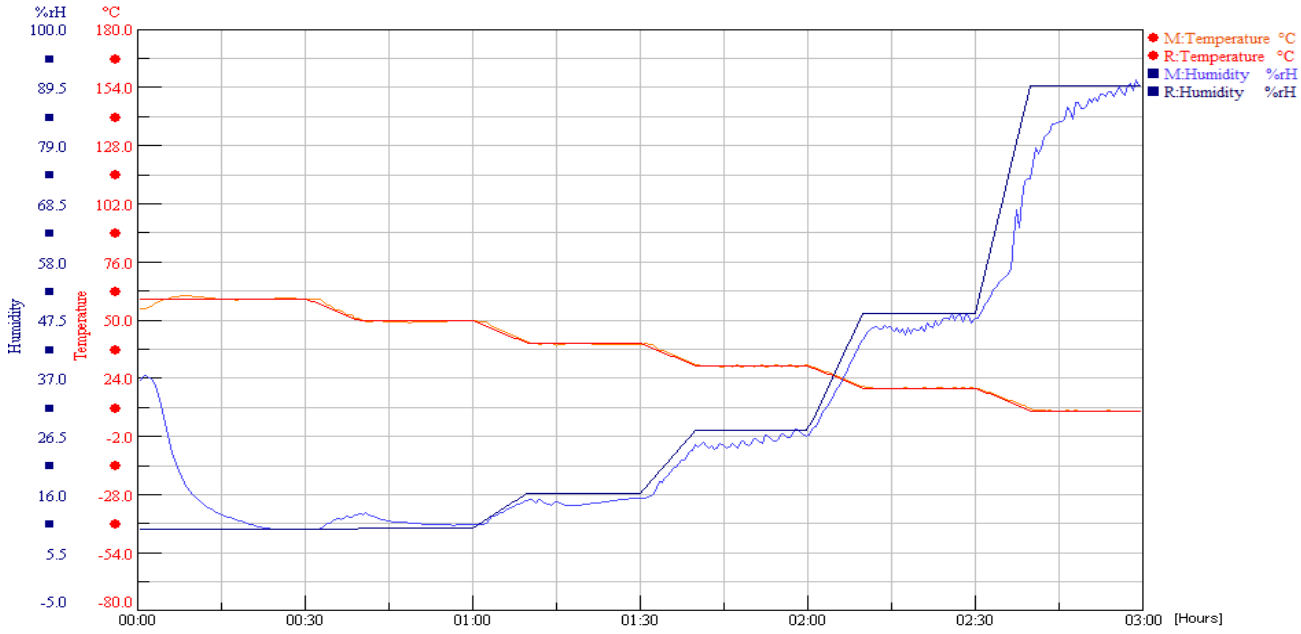

Graph 6: Real temperature measurement

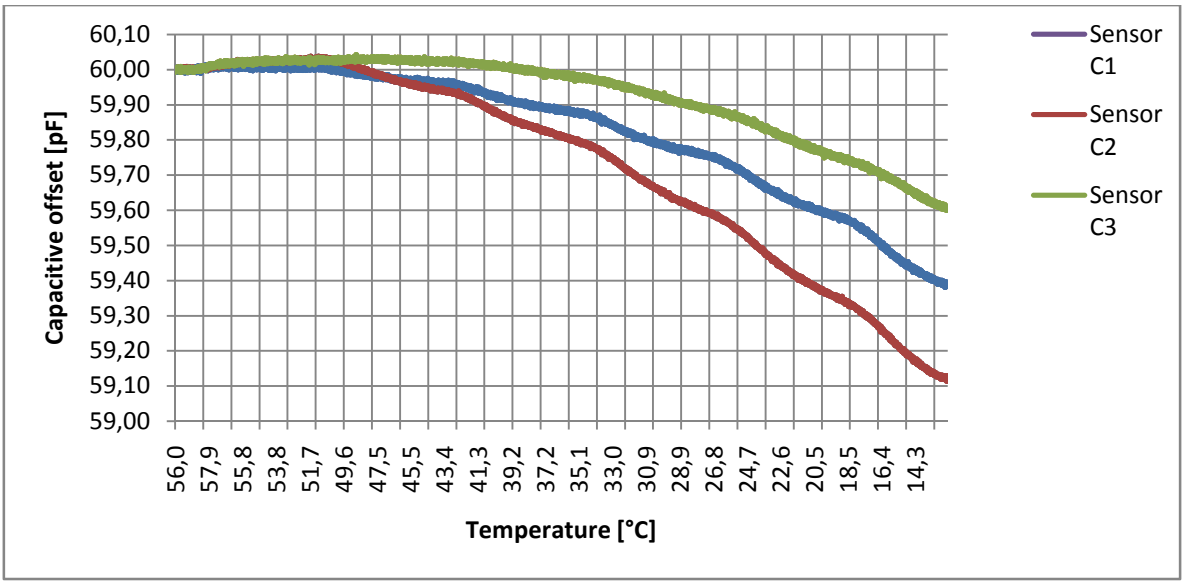

Graph 7: Process of capacities

Capacity measurement

Channel sensors C1, C2 and C3 were callibrated on one level of capacity for comparison (Graph.7). Here it is evident the nonlinearity between the spacing and area variation of each channel. For measuring the temperature dependency as a step of 20 °C (middle part of the measurement) Channel 1 was chosen. Directly speaking, the total capacity change from 60 °C to 10 °C in 3 h time for channel – Sensor 1 is 0.6 pF and by calculation 12 fF at 1 °C and 240 fF on 20 °C (Graph 8). This calculation is idealised and linearised, because the processing of measurement in real is nonlinear. For evaluation of the capacity, dependence on the temperature was deducted (from Graph 7) 20 values of the capacity on the end of each stable part for a given temperature, always closely before the next step, when the temperature capacity was slightly stabilized. For this reason the measurement was set at 10 °C with time for stabilization. The results weren‘t calculated, but only deducted from a graphs. But for verificating theoretical aspects it will suffice.

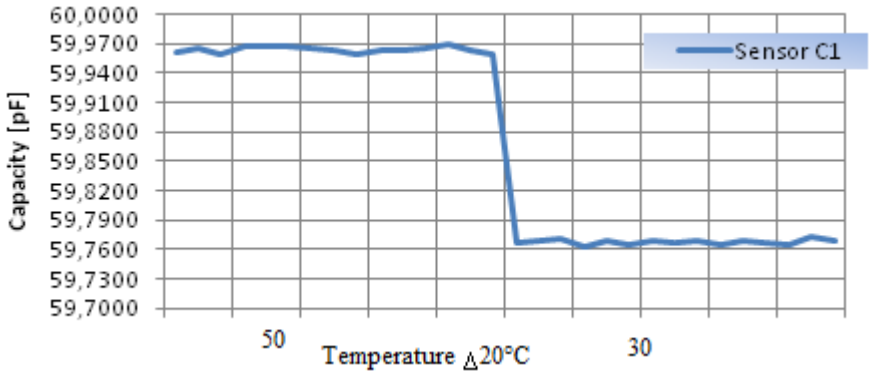

Graph 8: Temperature step of 20°C

For use in a room with a constant temperature, a temperature gradient 2 K/h does not need external compensation of the measured data. For use in applications where there are significant short-term temperature changes there must be measurements of capacity to compensate. The eventuel principle of compensation will be given in later developments in the C -Leg.

3.1.6. Humidity measurement

For the measurement of the dependency of humidity on the change of capacity the measurement period 6h was selected. For dependence of the capacity strictly on the humidity, a temperature of 20 °C was chosen. The measuring rate was from 10 % to 90 % of relative humidity with a gradient of 20 %/h -with increasing humidity is (about

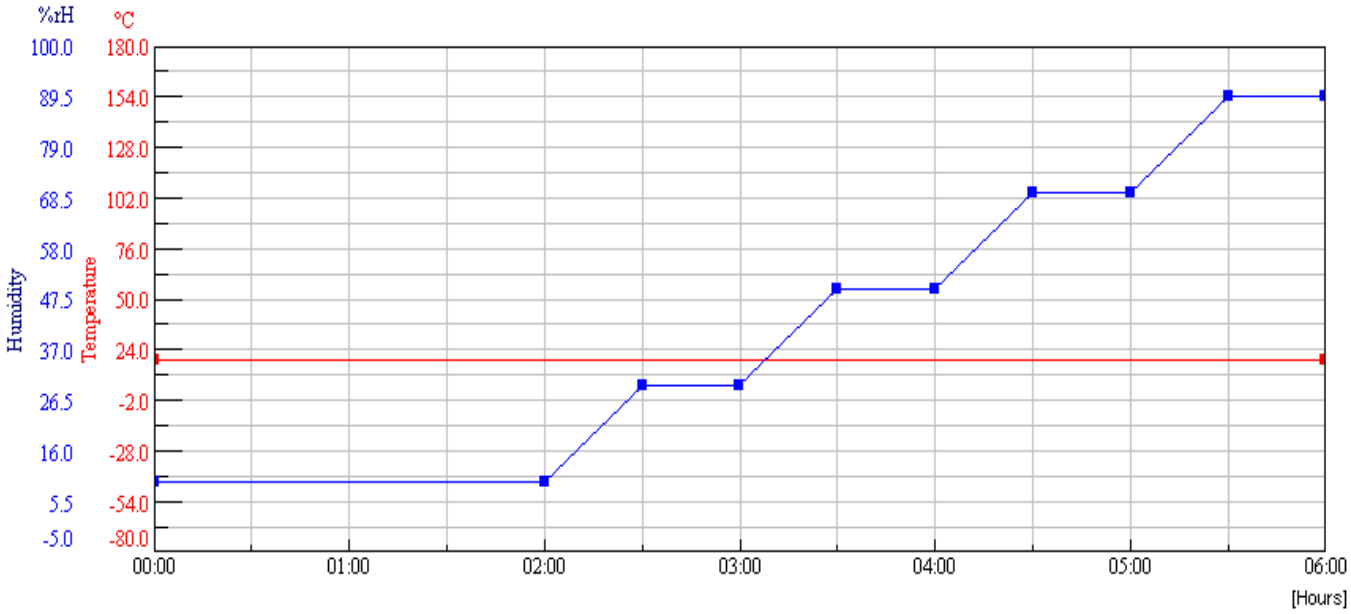

Graph 9: Humidity settings

theoretical assumption) for constant temperature in the temperature box more water, therefore a measurement was chosen in the ascending tendency to protect the measurement against the condensation of water steam on the electrodes.

In Graph 9 is set the process of chosen measurement. In Graph 10 is a real process of the measurement in the temperature box and easily it can be recognised with the result in Graph 11, where dependency of the capacity on the humidity is shown. Tab. 4 explains the calulated value of the absolute humidity in the climate box.

Temperature [°C]	Set Relative Humidity [% rH]	Relative Humidity [% rH]	Absolute Humidity [g/m^3]
20	10	17	3
20	30	16	2.8
20	50	50	8.8
20	70	70	12.3
20	90	90	15.9

Tab. 4

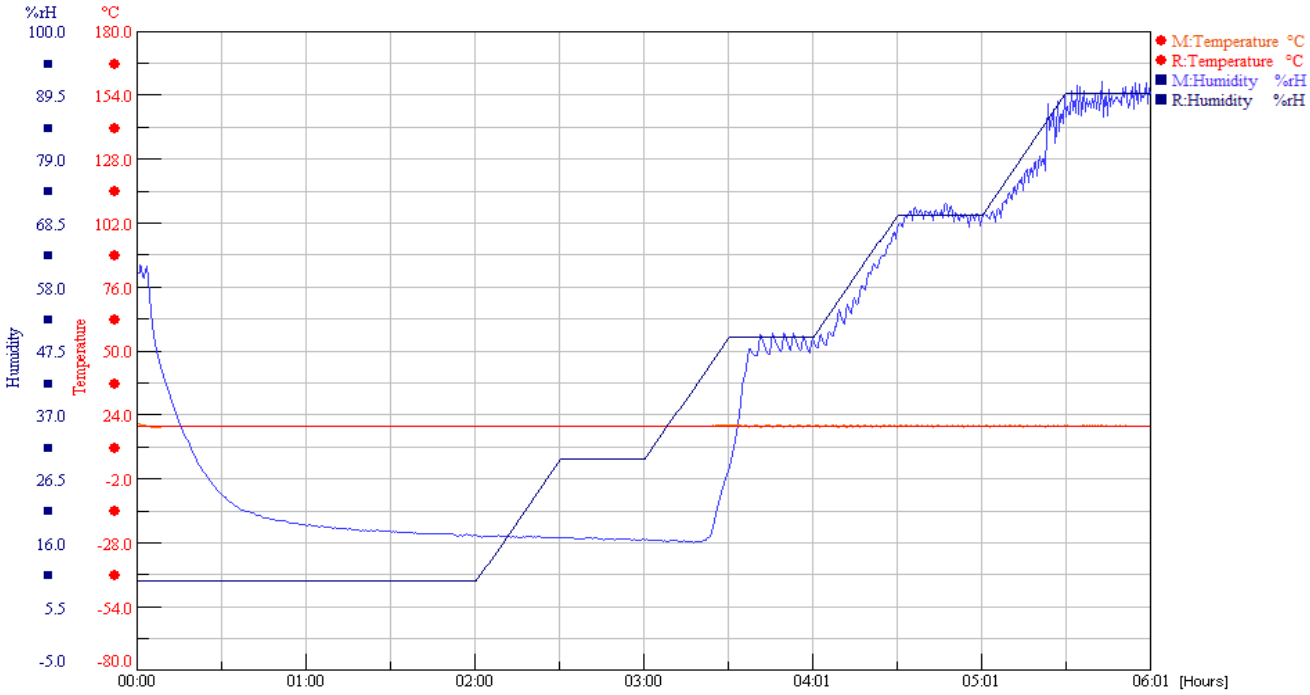

Graph 10: Real process of measurement

The real curve of humidity was influenced by the limit of the climate box. For temp. 20 °C it is not possible to simulate humidity around 10 %. min. value was 16 % of relative humidity (Graph. 10).

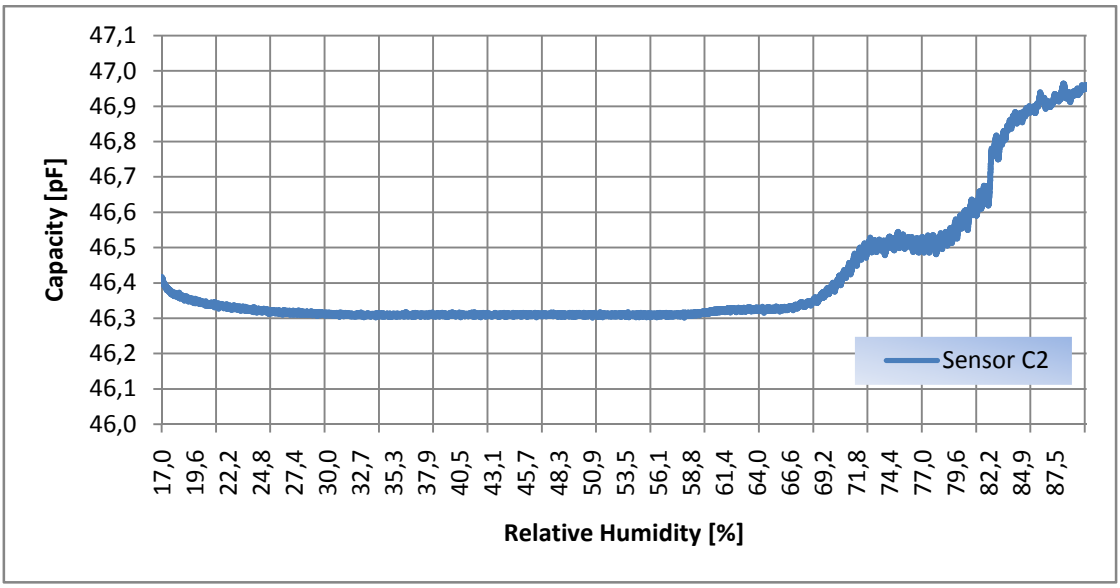

Graph 11: Humidity influence

The final behaviour of capacity very well copies the humidity curve from the regulator. On every 20 % of change of humidity, the capacity of the sensor increases around 100 fF (Graph. 11). The detail analysis of the influences will be studied in the C-Leg connector too.

3.1.7. Mass measurement

For the measurement of mass "Massmeasurement.m" program was first prepared in Matlab 2009 where it was simulated and displayed the process of loading the EB by mass. Programe was designed as interactive and dynamical move description of the load. The program code with comments is in the attachment A1.

The program can recognise a really low load - only 100 g is enough as a signal converted to the program. The purpose of this program is to evaluate the position of the prosthesis, orthosis or effected leg. Thanks to this program it is possible to imagine how the sensors reacting on the load and how the process of gait or standing works. For the display of the signals from the capacitive sensors, the Gaussian function was used (Fig. 34): [34]

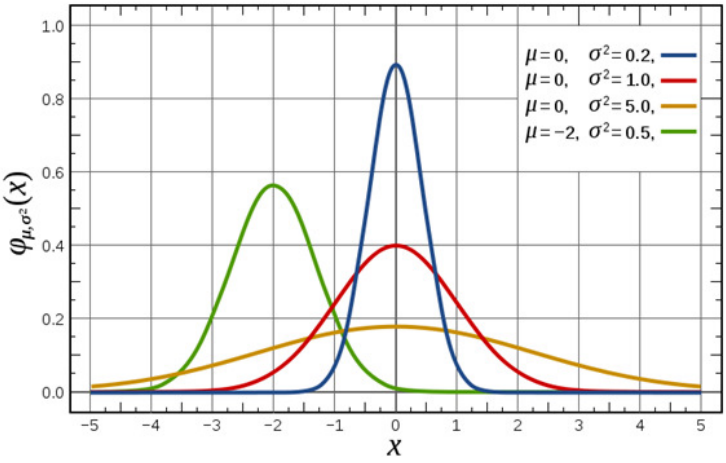

Fig. 34: Gaussian function (curve)

$$f(x) = ae^{-\frac{(x-\mu)^2}{2\sigma^2}}.$$

x= μ= coordinates

real constants a, μ, σ > 0, and e ≈ 2.718281828 (Euler's number)

after the modification:

$$f(j_x, j_y) = a \times e^{(-\sigma*(j_x - s_x)^2)} \times e^{(-\sigma*(j_y - s_y)^2)}$$

a	The amplitude, "high"of the curve = data from the measurement.
x	Coordinates in the space.
μ	Position of the centre of the peak.
σ	Controls the width of the curve = programable as needed.
j_x,j_y	Coordinates in the board.
S_x,S_y	Position of the centre of each peak. [34]

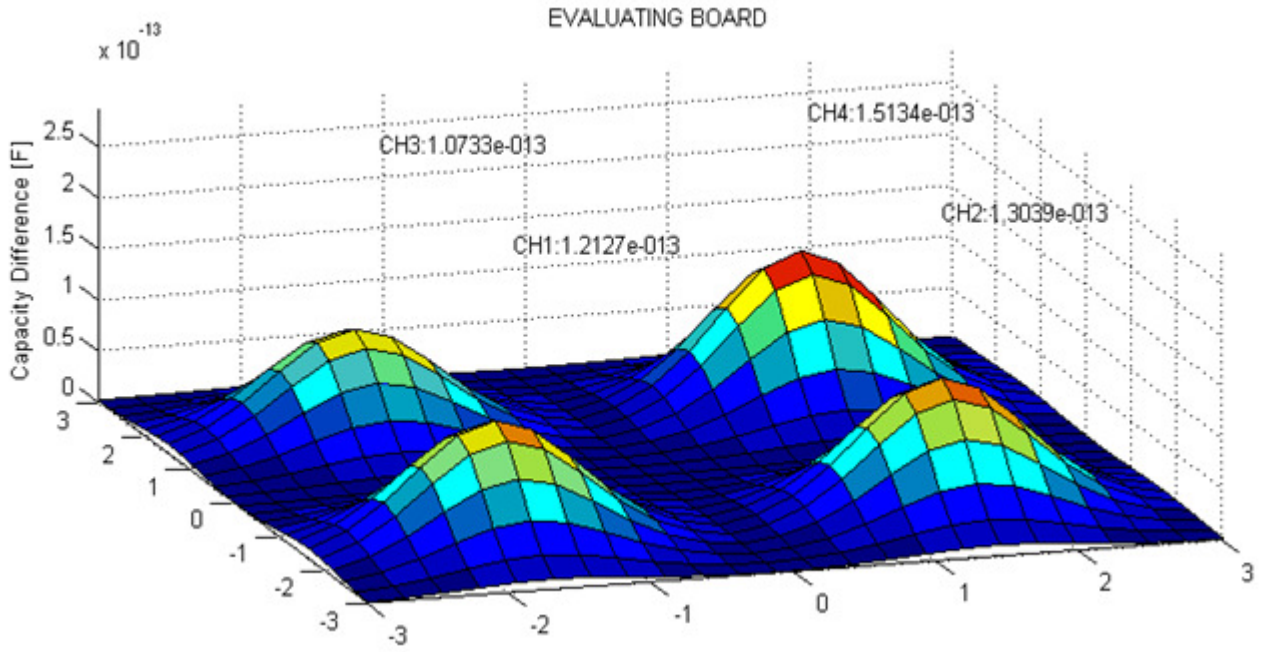

Fig. 35: Gaussian EB

After evaluation of data from Acam soft PicoCap this system reads, by "Massmeasurement.m" programe from Matlab software, measured data and displays the results as in the Fig. 35 or Fig. 36. The dynamic movement is done by a cycle of the change of the figures after each mathematical calculation. Each peak describes the value of the capacity for the given sensor. In the EB are 4 capacitive sensors. The centre point of the sensor and peaks are fixed in the same position. The offset is calculated from the minimal values of the capacity from each sensor.

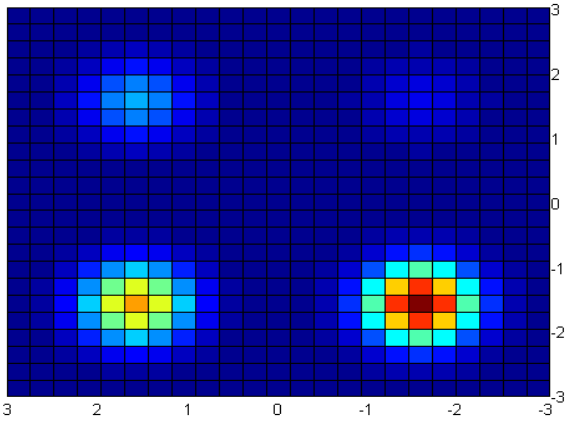

Fig. 36: Surface view

For use in real-time it is necessary in the next phase to solve the problem of communicating the EB with a personal computer for immediate processing and directly evaluation of measured data. It is possible to use a Matlab for realtime process and measurement, but this is not the main part of this thesis and unfortunately the Matlab is not supported in OttoBock company and potential development would be based on another graphical and calculating interface.

3.1.8. Center of pressure - method of ratio

The next question concerned the problem of how to find a center of pressure (COP) on our EB. Fig. 37 shows that while the foot is in contact with the ground (EB) there are acting forces between them. They can be summed up as a single-ground reaction force – vector F. Free torgue vector T_z is a second component of the movement on the board and for our measurement it will be suppressed. The COP of the GRF on the plate is our center of pressure. The sum of all big and small reaction forces together which react on the EB are our center COP. GRF is described in detail in chapter 1.1. [26]

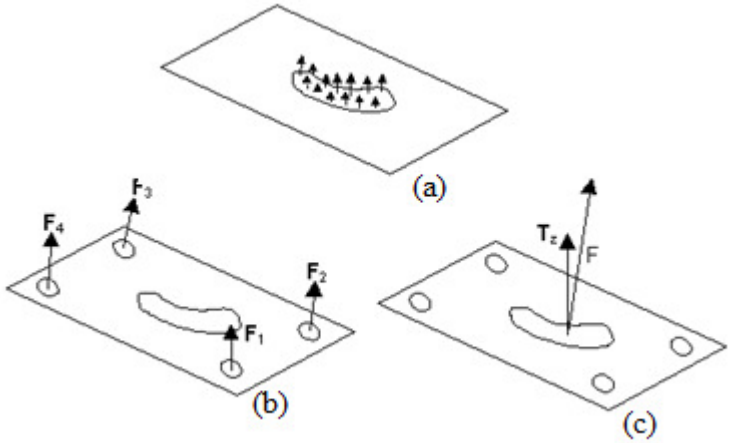

Fig. 37: Center point and GRF

Fig. 37 demonstrates where the COP is in contact, for example with human feet. The human foot produces vertical force and the horizontal force. The horizontal force is, in the end, not so bad, but for measurement it is undesirable. As the moment is suppressed the horizontal force is too. For better results and elimination of the horizontal force and torgue T_z, it is recommended for the next development to replace the polyuretan rubber element between the plates of the EB. The system of spring in concentric tubes in each corner can be used, movement is guaranteed in only the vertical plane.

Program Matlab was chosen again for calculation and displaying the results Fig. 38. The system of calculation is as follows:

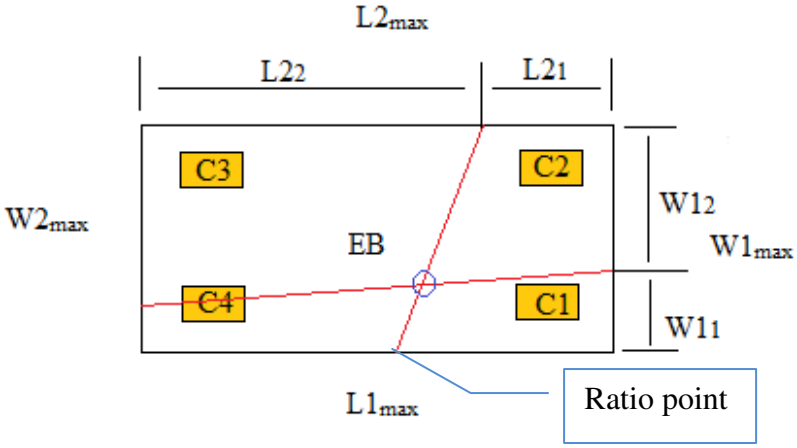

Fig. 38: COP method of ratio

Single reaction force is :

$$F = F_1 + F_2 + F_3 + F_4 \ [\mathrm{N}]$$

$L1_{max} = L2_{max} = 400$ mm

$W1_{max} = W2_{max} = 250$ mm

Basically, for calculating COP the moment of balance is looked for. Since the total distance between F1, F2, F3, F4 is fixed and known, it is possible to calculate the required distances of L or W.

Theoretical calculation

First of all, it is necessary to calculate the ratio between the neighboring sensors as from the following equations (Fig. 39). Searching values are $W1_1$, $W2_1$, $L1_1$, $L2_1$. There are the coefficients for calculations. The basic derive is as follows.

M_{load} limit loading force for balance

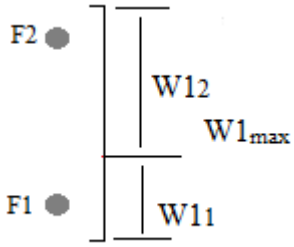

Fig. 39: Neighboring sensors

$$F_{y1} = F1 + F2$$

$$\sum M_{load} = 0 = F1 \times W1_1 - F2 \times W1_2$$

$$F1 \times W1_1 = F2 \times W1_2$$

$$F1 \times W1_1 = F2 \times (W1_{max} - W1_1)$$

$$F1 \times W1_1 = F2 \times W1_{max} - F2 \times W1_1$$

$$F1 \times W1_1 + F2 \times W1_1 = F2 \times W1_{max}$$

$$W1_1 = W1_{max} \times \frac{F2}{F1 + F2}$$

Modification to the capacity:

$$W1_1 = W1_{max} \times \frac{C2}{C1 + C2} \qquad [mm]$$

Calculation of the next coefficients:

$$W2_1 = \frac{C4}{C3 + C4} \times W2_{max} \quad [mm]$$

The result $W1_1$ and $W2_1$ is the width, ratio from the capacitor C1 resp. C2. There are points in this position where the capacity or forces are in balance. The same modification was used for calculation of length of the EB:

$$L1_1 = \frac{C1}{C1 + C4} \times L1_{max} \quad [mm] \qquad L2_1 = \frac{C3}{C2 + C3} \times L2_{max} \quad [mm]$$

The position from the width $W1_1$ and $W2_1$ from both sensors are connected by a line. It is necessary to do the same with length $L1_1$ and $L2_1$. The intersection of two stright lines found the COP. [18]

Example:

C1 = 6 pF	C2 = 2 pF	C3 = 1 pF	C4 = 4 pF

$$W1_1 = \frac{C2}{C1 + C2} \times W1_{max} \qquad W2_1 = 200 \quad [mm]$$

$$W1_1 = \frac{2}{6 + 2} \times 250 \qquad L1_1 = 150 \quad [mm]$$

$$W1_1 = 62.5 \quad [mm] \qquad L2_1 = 83.3 \quad [mm]$$

The expected result corresponds with Fig. 38. The working programme was designed around.

Practical result

From the theoretical equation, a program was made called "Massmeasurement_point.m". The measurement process eliminated the horizontal force and torque as it was possible, but the influence was evident. Vibration was compensated by ground mode connection. The size of noise was still much less than the measured signal. This negative influence was compensated by averaging. The displaying was

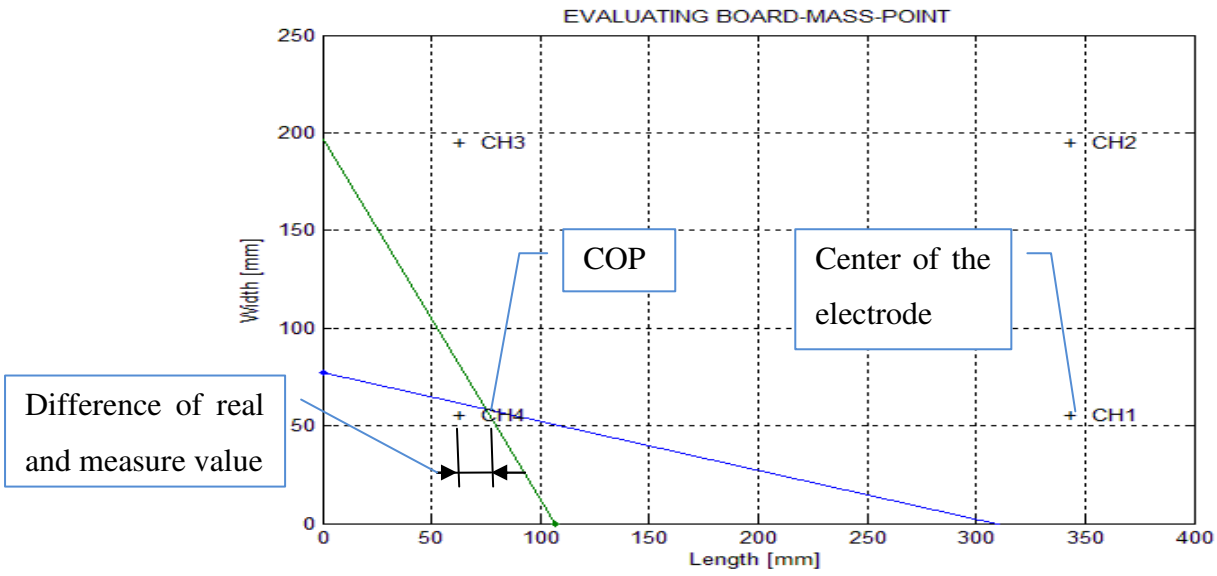

Fig. 40: COP dynamical process - ratio

again dynamical and it was possible to watch the COP really precisely (Fig. 40).

Expected was the homogeneous magnetic field and constant temperature and humidity distribution. This theorum works when the load on the EB was bigger then 5kg. For less loading there was the problem of finding the COP because there were a lot

of nonlinearities. The next problem was to test an EB on looking for COP on the edge of the board, behind the sensors. There is a different physical behavior of EB, where pressing the point behind the sensor makes the opposite direction of the force on the other side of the EB. Basically it works as a swing and the measurement loses accuracy. A solution was to measure only between the sensor area.

The nonlinear characteristic of the rubber elements had a problem with a faster changing of the position of load on the board. The problem is the perfect elasticity of the rubber roller elements. If we load and unload the board as on start of measurement, then the position of EB is same after some minutes, not imediately. With as increase of the load on the sensor it takes more time set the rubber elements back to the initial position. This makes a measurement error as in Fig. 40. The problem was partly solved using the minimal offset for setting of treshold data, as in Graph 12. This threshold set the range of minimal values for the sensors and determines the stand mode on the EB.

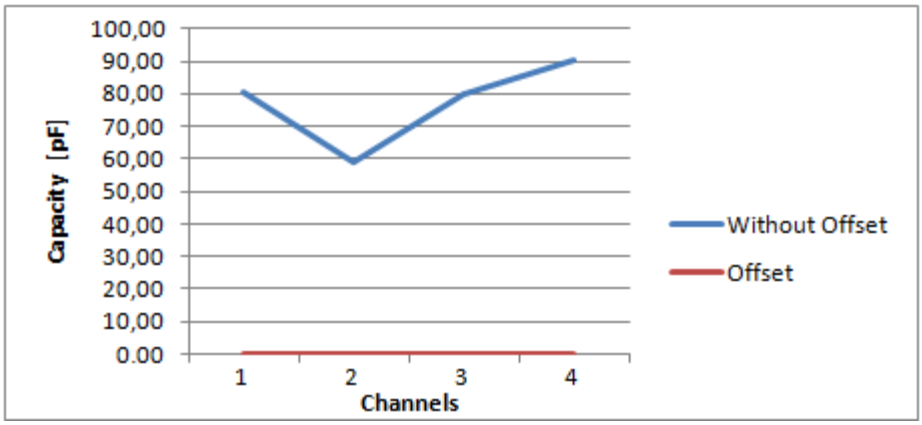

Graph 12: Offset

On Graph 12 it is shown the offset on 0 during start calibration. Without this compensation each channel was shifted and the measurement was not possible. This meant a small failure in the measurement, because the distance of nonlinearity between electrodes are reflected.

Result

The offset problems were solved by software and use for other tests in this thesis too. The error or deviation after all compensation of the measurement was maximal 9.25347 mm ≙ 5.3% (first line in Tab. 5 deducted from the Fig. 40). It was the difference between real and measured value up the center of sensor C4. This measurement was for 4.885 kg of load. Real value was constant for all measurements.

Measured value [pF]	Real value [pF]	Difference from sensor C4 [pF]	Difference from sensor C4 [mm]	Length fom Center of board to C4 [mm]	≈ **Deviation of distance [%]**
90.737379	90.579267	0.158112	9.200000 (from figure)	175.000000	5.3
90.736930	90.579267	0.157664	9.173921	175.000000	5.2
90.737356	90.579267	0.158090	9.198697	175.000000	5.3
90.737132	90.579267	0.157866	9.185657	175.000000	5.2
90.738051	90.579267	0.158784	9.239119	175.000000	5.3
90.737468	90.579267	0.158202	9.205214	175.000000	5.3
90.737132	90.579267	0.157866	9.185657	175.000000	5.2
90.736684	90.579267	0.157417	9.159572	175.000000	5.2
90.737401	90.579267	0.158134	9.201303	175.000000	5.3
90.738298	90.579267	0.159031	9.253468	175.000000	5.3

Tab. 5

The deviation was around 5.3 % of the distance from COP to the center of board. This error was growed by offset problem and nonlinearity of the sensors especially rubber cylinders basicly exhibit a high degree of elastic hysteresis.[18]

3.1.9. Center of the pressure - coordinates method

The next test of finding the COP was to build on the basic coordinates. The external board was prepared in manufacturing with the special symetrical pins for the measurement. These pins represent the coordinates of each point on the EB with a range of 15 mm between them (Fig. 41). The size of the board is 250x400 mm and 2 mm thickness. It is made from aluminium. The board was fixed with glue on the EB. The pins are prepared for the weights for right position of COP on the surface. The main idea was to find a coefficient for length and width for each pin, find the COP and convert the coefficients to the load by anexternal table.

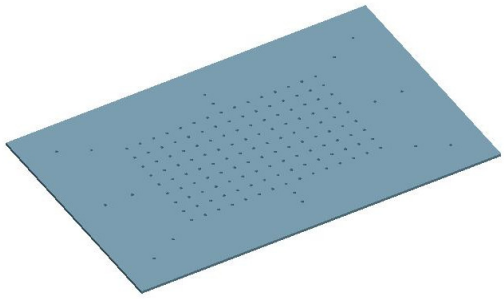

Fig. 41: Coordinates board

Every pin has got itis own coordinates x, y and coefficients for width, length and number. Together there are 151 pins where it is possible to measure. There is a higher

concentration in the center of board, where the position of prosthesis or feet will be evaluated.

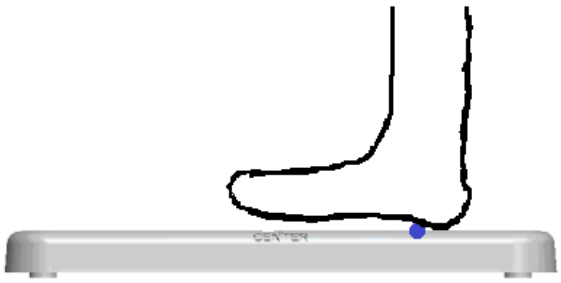

Fig. 42: COP for feet

As in Fig. 42 the COP can be measured for a disabled leg, prosthesis or for orthosis. Measurement is direct and in Matlab the process of load during stance phase is displayed.

Theoretical calculation

According to Biemüller, P. [18] was prepared calculation for the coordinates. The distribution system for the sensor is the same as in chapter 3.1.8. The measurement coefficient was pressed by 4.885kg load pin by pin.

As the sensors are nonlinear with a difference in distance-load, this method is the ratio method too. If the capacity is changed on one sensor, all sensors are changed. It means that the coefficient should be for all weights a minimum of 4.885 kg, the same. This is a hypothesis.[18] For calculation of COP by this hypothesis, an equation of coefficient for sensors was prepared.

The rectangular form:

$$\frac{F1+F2}{F3+F4}=\frac{C1+C2}{C3+C4}=Coefficient\ W$$

$$\frac{F2+F3}{F1+F4}=\frac{C2+C3}{C1+C4}=Coefficient\ L$$

From the coefficient it is possible to calculate coordinates x and y because the width (250mm) and length (400mm) is known. The calibrated calculation is shown in Tab. 6.

Pin number	Length [mm]	Width [mm]	C1 [pF]	C2 [pF]	C3 [pF]	C4 [pF]	C5 [pF]	Koeficient Width	Koeficient Length
…	…	…	…	…	…	…	…	…	…
8	-105	45	4.00980	2.92520	3.97650	4.50990	3.43200	0.81719	0.81009
9	-105	30	4.01000	2.92510	3.97620	4.51020	3.43200	0.81720	0.80999
10	-105	15	4.01020	2.92490	3.97590	4.51040	3.43200	0.81721	0.80990
11	-105	0	4.01050	2.92470	3.97570	4.51080	3.43200	0.81720	0.80978
12	-105	-15	4.01070	2.92450	3.97540	4.51110	3.43200	0.81720	0.80968
…	…	…	…	…	…	…	…	…	…

Tab. 6

Practical result

By the coefficient from the Tab. 6, we know the coordinates L and W. In Matlab the program "Massmeasurement_point_2.m" (Fig. 43) was prepared.

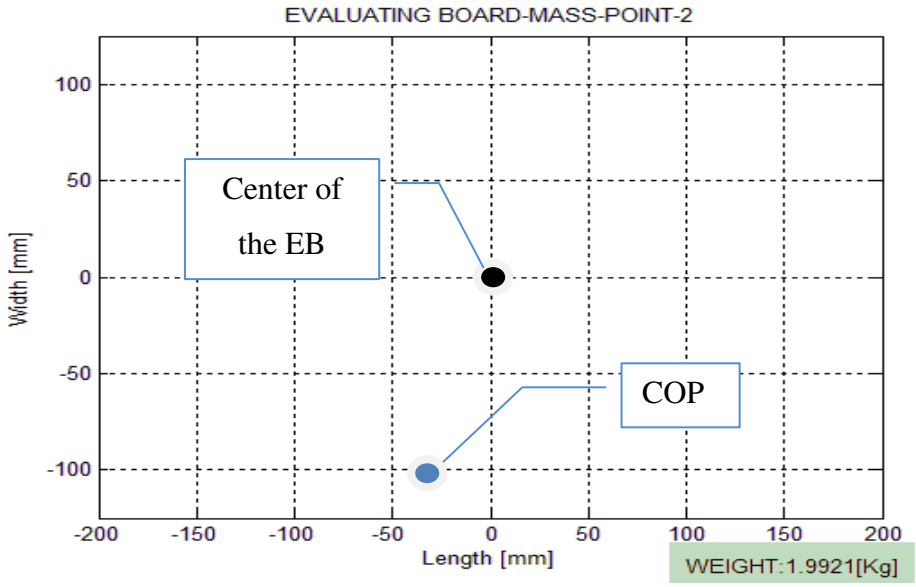

Fig. 43: COP dynamical process - coordinates

The program calculated simplify the linear dependence of weight on capacity. The characteristic of load during the measurement is shown in Graph 13. There was progressive measurement of load from 0 to 41.7 kg. This characteristic is measured in the center of EB, symetrically to all the sensors.

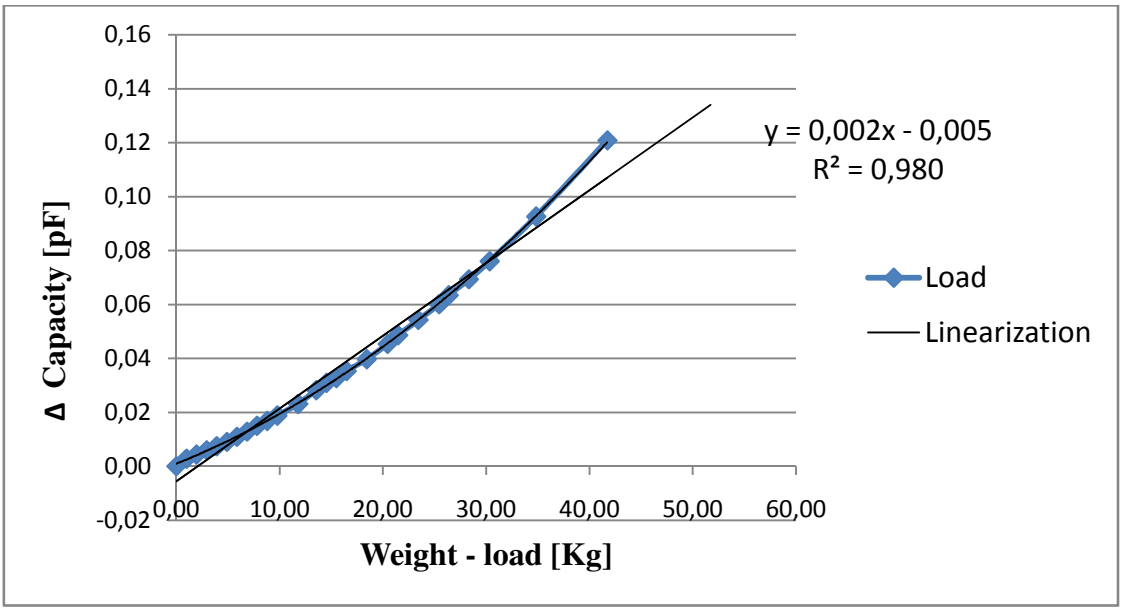

Graph 13: Linearization of load

Before linearization of load measurement for all sensors it was necessary to solve the question of temperature and humidity.

Temperature and humidity compensation in EB

It is assumed that the EB will be in a stable environment with homogenic temperature and humidity. For the calibration of the sensor in a different environment (for example transfer the EB to another room, place) it is better to use calibration capacitive sensor (C5) for compenstaion. This compensation is based also on the measurement from chapters 3.1.5. and 3.1.6. The sensor was placed in the center of the board at the same distance between electrodes with the same connection and with the same dimension as the other capacitive sensors. Capacity change on capacitor C5 depends on the change of temperature and humidity. The temperature is not measured directly, only the difference of capacity C5. There is a basic capacity C5 for the calibration (for room temperature 23 °C). If the capacity on C5 is changed, all other sensors are changed too. The difference between measured capacity and basic calibration capacity on C5 is implemented in compensation for other sensors as in the following Graph 14. The compensation of calculation was solved by program. There is evident change of temperature and humidity in the EB (blue curve) and it follows compensation (red curve).

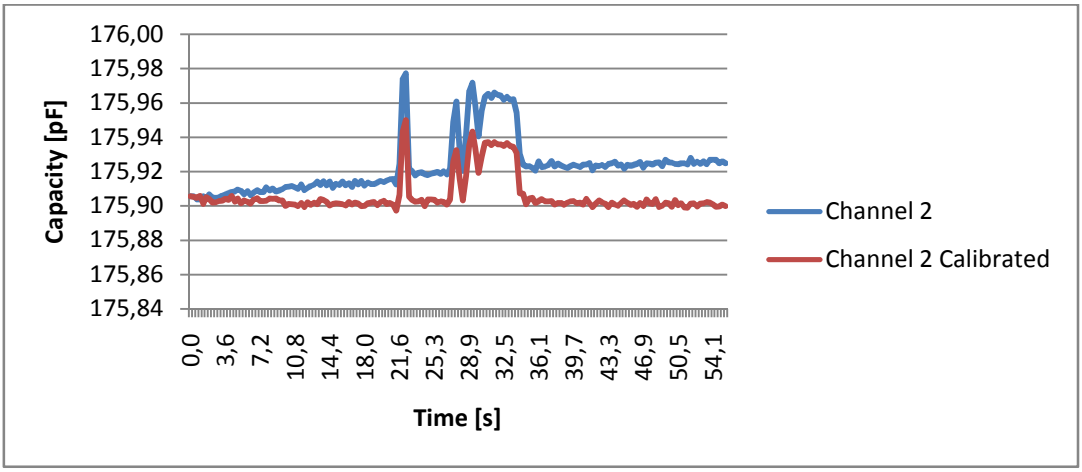

Graph 14: Temperature and humidity compensation

The dimension of the electrode C5 compensation sensor is the same, but the electric field around the sensor is not direct. With this property there was a problem with separating the temperature from the movement of the board. The movement made distortion in the temperature sensor. For complete separation a same sensor with positive electrode was chosen, but the ground plates were two times bigger (1800mm^2). This helped separate the temperature from the movement by around 50 % (electric field was more closed). Use some temperature sensor for next evaluating is also possible.

Vertical force - load

The load characteristic from Graph 15 is different for each sensor. The coordinate method calculates with the same range of capacity in all sensors. In fact, we can see that this was a mistake in the theoretical assumption, because a created error is not negligible. In simple terms the load in the center does different signals than the same load on other positions on the EB. This is a problem for determinating the right weight and force on te EB. Linearization for each sensor on the board should be prepared for compensation, separately in polynomial form. This problem is shown in Graph 15. Here is the recalculation of capacity directly on the vertical force [N].

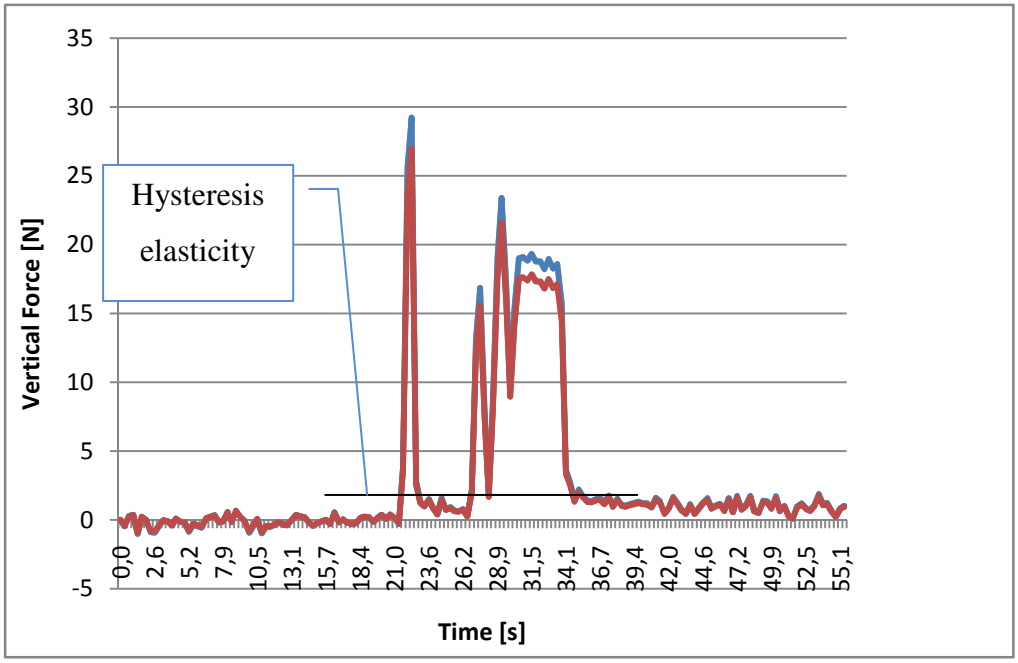

Graph 15: Hysteresis

As is evident from Graph 15, the error of test measurement for the two positions of load is about 7 % (deducted from the measurement) from the measurement range. The course was calculated with a constant weight of 4.885 kg with central and sub-central coefficient and after this it was implemented to the calculation of searching force. Coefficients are calculated as a difference of the sum of all sensors for central and sub-central position of weight 4.885 kg. The load was made in feet on the EB and it is calculated as a linear function (equation). Data are first calibrated by compensation of sensor C5. The procedure of compensation and calculation is in the attachment on the CD.

Result

The range of coefficients values for 151 pins is too small and sometimes more pin with the same coefficients exist. A higher weight than 11.4 kg has to be used for improvement. For accurancy, 1.5 mm was an incorrect measurement. Theoreticaly this method shoud work, but practical problem is with the same coefficients. It may be unsolvable with this type of hardware properties in the EB. Because of this problem, it is not possible to determine the max. deviation and difference from the real value.

Each sensor has got a different starting offset. It means a different load characteristic for every point or place on the EB. The offset was solved by software in the programme, but there was a big error in load measurement. Good result was only for measurement of load in the center of EB,because here was made a calibration.

Comparison of both method

Both methods have hysteresis elasticity of rubber as the biggest problem. This nonlinearity causes the highest error for the measurement. A technique to remove this error is to replace the rubber element with some circular concentric tube with spring. In EB only 4 rubber elements are used and in my opinion it is not enough. For really continous transfer of the center of gravity and vertical forces it will be better to use more smaller elements than 4 bigger one. It is the same principle as in the spring mattress. A mattress with more smaller springs does not sway a lot and the weight is naturally distributed. The problem of hysteresis is shown on Graph 15 too. This solution should help with the elimination of horizontal forces and torgue too.

A problem with temperature compensation was solved with the calibration sensor. It will be interesting how compensation will be better by some temperature sensor for next developement. This was a big benefit in chapter 3.1.9. against the method of ratio 3.1.8. where the temperature and humidity was neglected. Both methods can measure the COP, but from earlier measurement looks better the method of ratio (3.1.8.) in this moment. If it is solved and reduced the problem with hysteresis of rubber and will be used higher weight, will be possible to measure with max. error deviation 1.5 mm. For linearization of the sensor it is necessary to manufacture the electrodes and their position in the EB with high quality and accuracy. It is necessary to set the software in the same settings with the same types of compensation, averaging etc. Otherwise, the differing sizes of capacity measurement will be there every time.

4 New C-Leg adapter

The experiences from the EB developement were used for the evaluation of a new connector, especially for a C-Leg prosthesis. C-Leg is a new technology in lower limb prosthesis. It is a type of electronic knee joint with hydraulic stance and swing phase control (Fig. 44). The Technology is based on continually recording data from on-board sensors during each phase of gait. [27] This data forms the basis for optimizing the hydraulic resistances to movement in accordance with the gait of different patients. [11]

Fig. 44: Easy walking with the C-Leg system

Construction and function

The main idea originates from the late eighties around a research group of Kelvin James at the University of Edmonton, Alberta, Canada and has been improved by Otto Bock company to allow serial fabrication in practice. [11] The C-Leg ® is a monocentric knee joint. It consists of the following elements (Fig. 45):

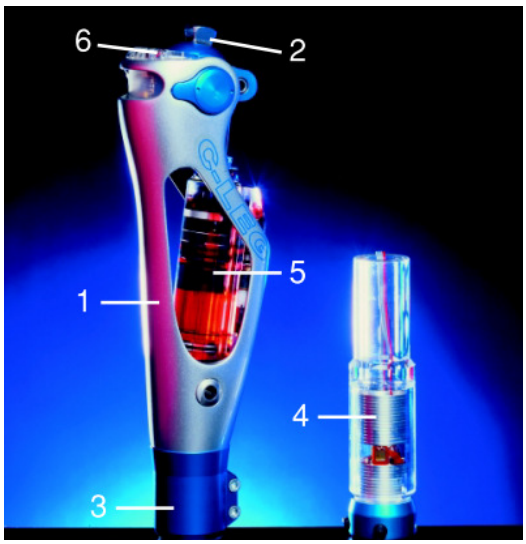

Fig. 45: C-Leg Components

" The carbon fiber frame (1) provides the supporting structure and is connected to the upper joint section (2); the distal tube clamp (3) accepts the tube adapter (4) with integrated moment sensor; the carbon fiber frame contains the hydraulics (5) with servo-motors, elec tronics (6) and battery."

** description by F.Blohmke, E.H. Max Näder, Hans Georg Näder* [11]

There are strain gauges in the shin tube and a knee angle sensor for collecting the data. The micro-controllers calculate the required signal to movement. Flexion and extension damping is regulated by servomotors that open and close the hydraulic valves.[11]

Philosophy of sensing

The philosophy of using capacitive sensors is to find possibilities for replacing the gauges and knee sensors for contactless capacity technology. One of the main reasons to change it is the lower price and relatively simple technology of sensing. This technology has already been described in the chapter 2 and 3.

The tube adapter (Fig. 45 – number 4) is important for the developement of the range of this thesis. This part of the C-Leg prosthesis is independent and it is possible to work and improve it separately.

4.1. Design of the tube adapter

The main problem was finding the right structure of the adapter tube-body, because its first purpose was based on the change of distance between some parts inside the adapter. This assumption was built on the end on the material deformation of the tube, similary as the structure for the gauges sensors as in Fig. 45. The deformation changes the distances of some parts and from the capacitive sensor the vertical force and moment should be possible to measure. The requirements for the vertical force resolution was 1 daN (approx. 1 kg), deviation over time and temperature no more than +/- 5 daN, range -150 to 450 daN. For the moment was a resolution of 1 Nm, deviation over time and temperature no more than +/- 3 Nm, Range -200 to 350 Nm. The tube needs to be water resistant.

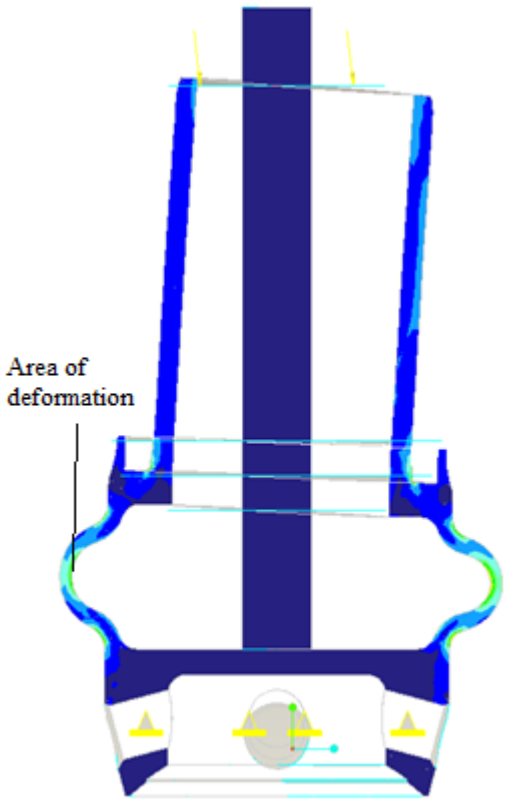

Fig. 46: Tube adapter- body cut

According to this requirement, the basic structure of the adapter was designed in the ProEngineer programme. Calculations for deformation were made by FEM in the ProMechanic programme. Fig. 46 shows how the adapter look in the cut during the deformation by vertical force and moment. Parameters for load and deformation were

1000N for vertical force and 100Nm for moment. Moment arm perpendicular distance was 100mm and it equalled the COP for GRF during the extension in midstance phase.

4.2. Inside sensor structure

Designs of the sensors structure were based on the properties of the tube adapter. The bottom part of the adapter was stable and deformation did not have influence on it (Fig. 46). In Attachment 2, at the end this thesis, are several designs how can be the solved a sensing of distance. The following structure was chosen from many designs.

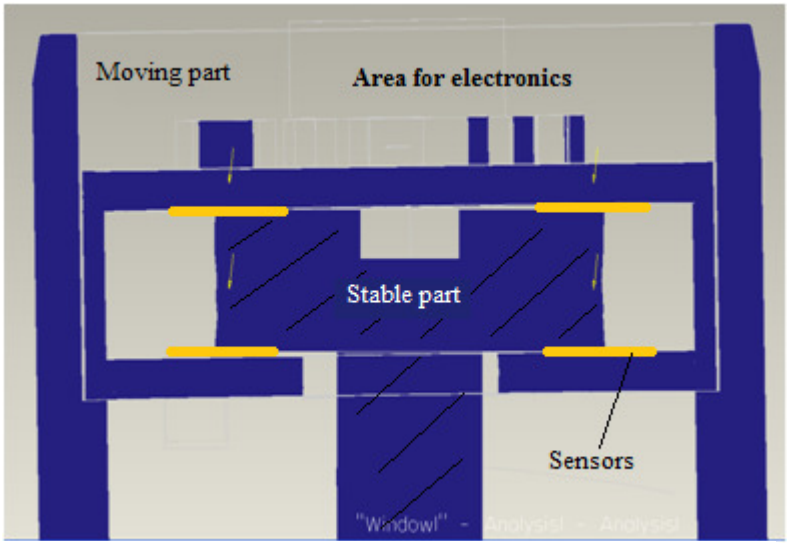

Fig. 47: Final structure of sensors

The two dimensional structure was chosen after discussion with Otto Bock experts (Fig. 47). Vertical force and moment was measured by capacity sensor as a gauge sensor and angle knee sensor in C-Leg now. The winning structure had a system of 4 parallel sensors with central shared ground- ground mode measurement as in chapter 3.1.4. This permitted really small measurement differences of 0.07 mm for the moment and 0.02 mm for vertical force with load 125 kg. During the movement, spacing and area variation in the top part of the tube adapter are included, as Fig. 47 shows.

The dielectric was chosen an air. This is better for heat transfer. The assembling and disassembling of the real model were more comfortable for testing with air than some special oil. Another dielectric made from solid substances could be problematic, because there is a danger of material deformation. An ideal material does not exist. A disadvantage of air can be the humidity influence on the difference of temperature.

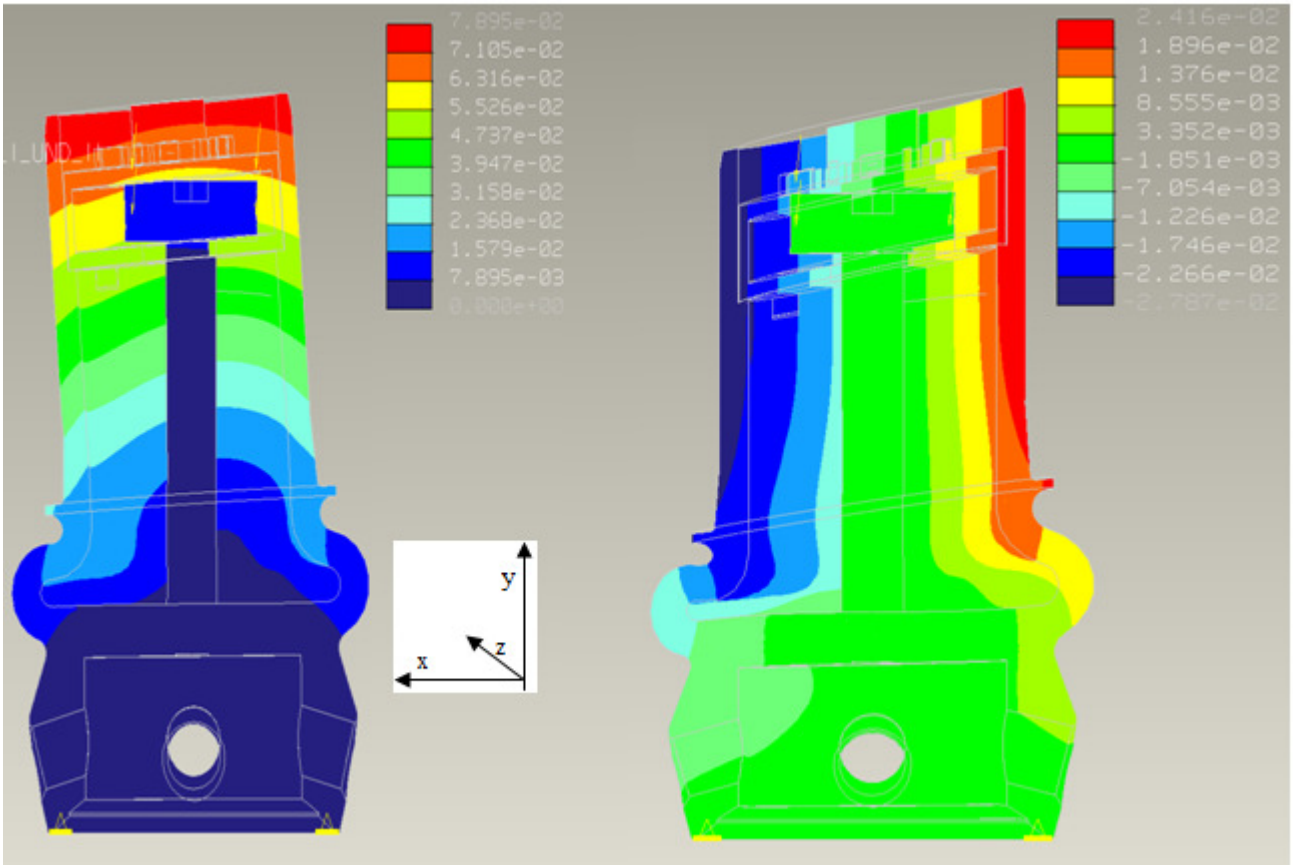

Fig. 48: FEM - displacement

Fig. 49: FEM - y direction displacement

The model was analysed by FEM in the ProMechanic program with the result about theoretical assumption.

Displacement for vertical force and moment in Fig. 48 is for the whole model (in horizontal direction) for 125 kg person equal 0.07 mm on one side and 0.14mm for both sides. The colour steps for displacement are shown

Displacement 0.02 mm for only y direction is analyzed in Fig. 49.

The torsion for this load was calculated maximal around 800 N/mm^2.

Approximate Young's modulus for various materials

The FEM analyses were calculated for the steel material. Titanium was used in the manufacture in the end. This means that the results are not correct and have to be recalculated. The lower part of the body adapter is stable.

The E-modul for steel is 200 GPa, for the titanium it is 105-120 GPa. [33] Simply written 2:1. The real result in our model had a displacement of 0.035 mm and in y direction 0.01 mm in titanium. Real torsion of assembly was around 400 N/mm^2. These results are complied with the task.

4.2.1. Moment and force analysis

The basic space between all four electrodes is same by a theoretical assumption. This position of the sensors can be calculated as a variation connection of full **bridge** for unknown capacity. The **temperature** and **humidity** can be eliminated exactly by this method.

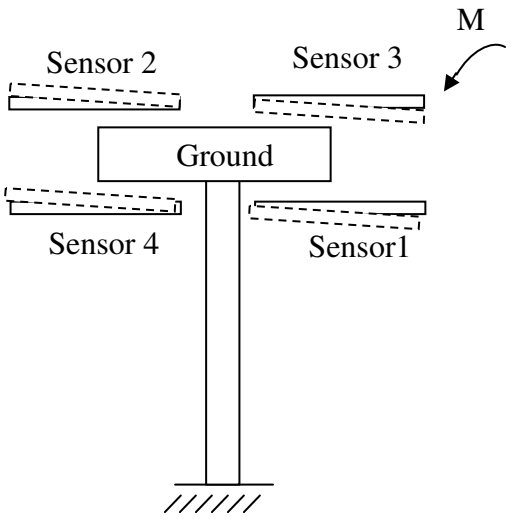

Fig. 50: Moment calculation

On Fig. 50 the moment measurement is explained. Acting moment makes a deformation of the tube adapter and this changes the position of electrodes due to the middle ground. In the real process is displacement of around 0.35 mm. This was one of the requirements on the measured system. The values of moment have got the same direction in diagonal connection.

Sum of moment equation is following:

$$M = (Sensor\ 1 + Sensor\ 2) - (Sensor\ 3 + Sensor\ 4) \qquad [Nm].$$

If has the moment reverse direction, and the result can be changed only with a negative sign.

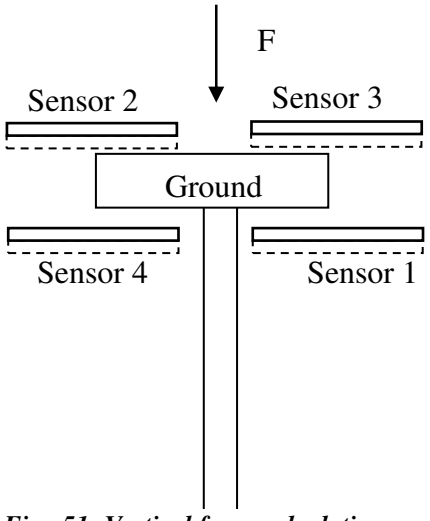

Fig. 51: Vertical force calculation

For the analysis of the vertical force a similar system of measuring was designed, but in Fig. 51 are upper or lower electrodes in the same direction.

The contactless difference in the final model has to be guaranteed between the positive electrode and the ground. Moment and vertical force in reality will correspond together. The displacement in Fig. 50 and 51 are visibly idealized for better understanding.

The sum of the vertical force equation can be:

$$F = (Sensor\ 2 + Sensor\ 3) - (Sensor\ 1 + Sensor\ 4) \qquad [N].$$

4.3. Construction

The final model was prepared in ProEngineer after the design of the right structure. This model consisted of several parts assembled together. A key to good construction was the repeatable possibility for assembly and disassembly. The accuracy was calculated with the highest manufacture possibilities in the OttoBock Manufacture and production department. All of them are now described. The drawings for the manufacture of all parts in this chapter are in Attachment A4. The material chosen was titanium for all metal parts. The next material that was chosen was FR 4 for PCB.

4.3.1. Main body

The main body (MB) part in Fig. 52 was made from titanium. This is a very hard material, with low weight and water resistance. Calculation of stress and displacement for this part has already been described in chapter 4.1. The upper part of the body adapter is a connector for the tube for connecting the C-leg knee system as in Fig. 44 and 45. A small pin inside the main body works for fixing the inside sensor in the right direction. The sensor has to have the same direction all the time because the structure is two dimensional.

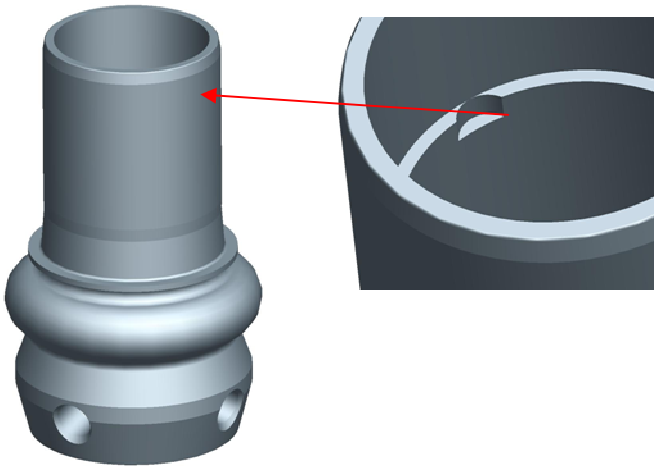

Fig. 52: Main body with pin

There were no problems during the manufacturing. The pin has a circle shape, which was easier and cheaper for the manufacturer.

During the design of this part it was supposed that the connection of the adapter with the

Fig. 53: Connecting tube

measuring tube - Fig. 53 (Highlighted the previous connector) will be fixed enough. The top part of the adapter was roughened by sandblasting for this, but it was not fixed well. There was extreme vibration during measurement. A special testing tube was made for eliminating this negative influence.

Testing tube

Due to inadequate fixation a special tube was manufactured with thread to easily separate the tube from the adapter at any time. On Fig. 54 is the titanium tube with thread and a special screw connector fixed with two component glue on the adapter. The small frame in the centre of the tube was made for connecting the cable.

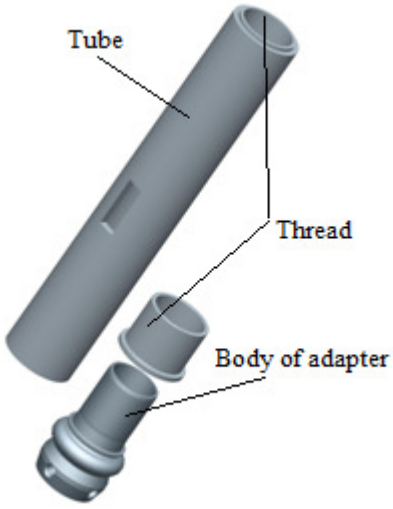

Fig. 54: Testing tube

4.3.2. Electrodes of sensors

PCBs from material FR 4 of 1.5mm width were prepared according to the sensing technology outlined in chapter 4.2.1. The PCapØ1-EVA-KIT has got a Serial Peripheral Interface Bus (SPI) communication port and it is possible to make our own PCB with microchip PCapØ1 and connect the PCB with the motherboard. On Fig. 55 the design of PCB is shown for upper and lower electrodes. The ground electrode is

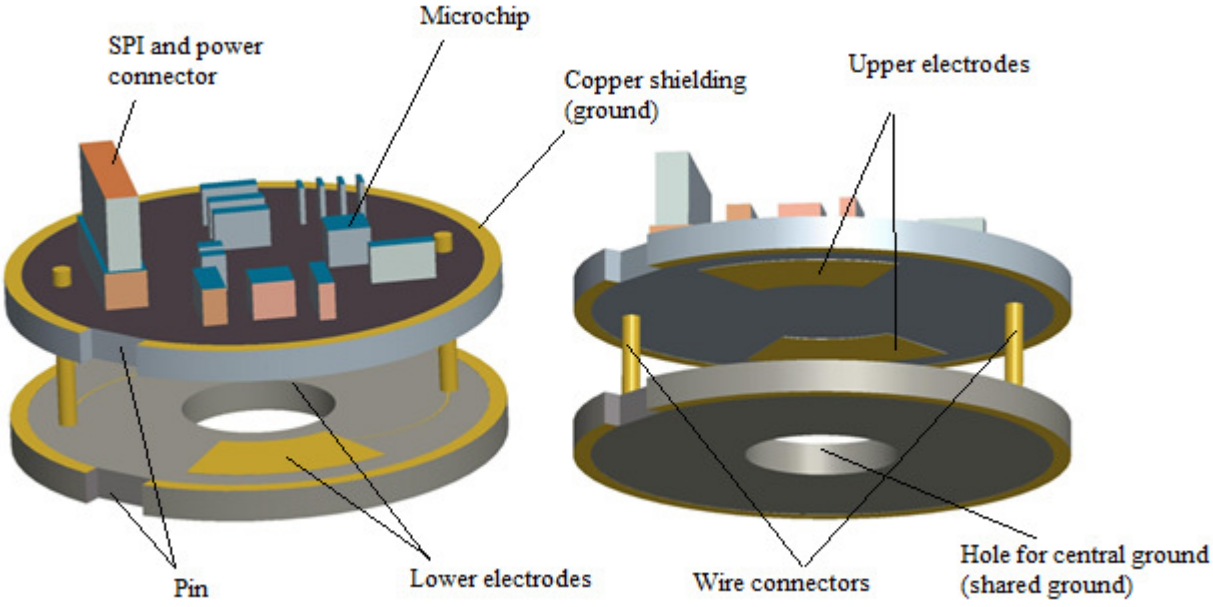

Fig. 55: PCB and electrodes of sensors

between electrodes and it is shared by all positive electrodes. The lower electrodes were connected by wire connectors with the upper PCB and there to the microchip. Upper electrodes were connected directly to the chip by signal traces etched from copper sheets laminated onto a non-conductive substrate FR 4.

Connectors

The connector was used to connect lower electrodes with the microchip. The first consideration was to use some catalog connectors. A problem was that for 6 mm distances between sensors it wasn't possible to find one. Tin wire was used, but the vibration of the tube had a negative influence on the signal. After the change of wire to a thicker one, there was a measurement without negative influences. This was a little bit of an uncomfortable solution, because during every disassembling it was necessary to solder the wire to the top PCB. The length of all connectors or copper traces was the same for all sensors. Capacitance is properties each conductor and this was a symmetrical solution for next measurement of capacity.

Shape of electrodes

The final shape for the positive electrode was designed and calculated. The maximal difference of capacity was most important factor for the construction. Focused

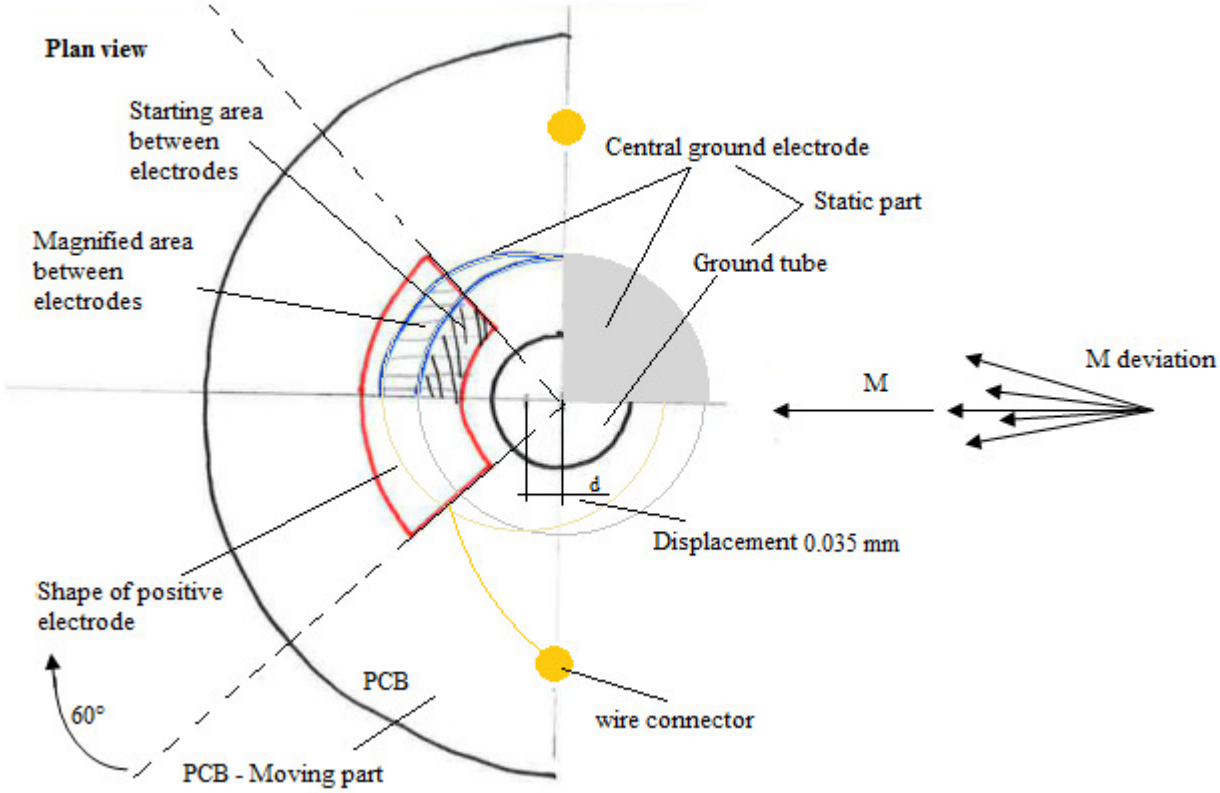

Fig. 56: Shape of electrodes

on the moment the maximal displacement was calculated as 0.035mm for one direction with spacing variation 0.01mm as from FEM.

Several types of shapes are in attachment A3. The calculations of some of them are in Tab. 7. The size of starting area is for comparison same. ProEngineer was used for calculations. From Attachment 3 shape ”j 60°” was chosen, because shape ”a“ was non-symmetrical to the ground (the ground is circle). More shapes had this problem. Sometimes the moment M had changed direction (Fig. 56) and it was an important factor. M deviation means that the moment is not exactly direct for repeatable measurement. The best result shape ” j 90° ” was the nearest from the connector and should have negative influence on capacity there (nonlinearity etc.).

The designed final shape of the positive electrode is in Fig. 56. This is the plan view. Some parts are shown in the cut for easier understanding. In this design one sensor is shown. The dimensions of electrodes were symmetrical and circular. This had reason to compensate the measurement for negative deviation of the moment. The lower PCB with electrode changed the displacement during deformation. The upper ground electrode was static. It extended the area for sensing (overlaid area – Tab. 7) between electrodes. The electric field and the capacity were changed by this bigger overlaid.
Calculation of the capacity difference for the several shapes:

Shape	S [mm2]	S2 [mm2]	S3 [mm2]	C2 [pF]	C3 [pF]	ΔC [pF]	≈ Δ %
A3	starting area	overlaid area	+Spacing var.	overlaid area	+Area - 0.01 mm		
			0.035mm		+Spacing + 0.035mm		
a	167.552	58.024	58.766	1.027	1.062	0.034	3.346
b	167.552	83.776	84.229	1.484	1.522	0.038	2.593
j 60°	167.552	70.686	71.273	1.252	1.288	0.036	2.888
j 90°	167.552	68.330	69.210	1.210	1.251	0.041	3.355
k	167.552	83.776	84.056	1.484	1.519	0.035	2.382

Tab. 7

Electronics

The electronics module on the upper PCB had same components such as the PC01-AD Plug-in module. Structure and connections were only redrawing from the chapter 3.1.3. The SPI communication was used. The drawing is in attachment A3 too.

FEM visualization of electric field

The FEM model of electric field in Fig. 57 was prepared for a better understanding of the influence of the electric field between the sensor's electrodes and middle ground. The material was titanium for ground and cover, PCB from FR4 and copper electrodes. On parallel electrodes was el.potential 3V and 0V and it is visualized in the coloured range. The dielectric between electrodes plates was, for both sensors, 0.25mm.

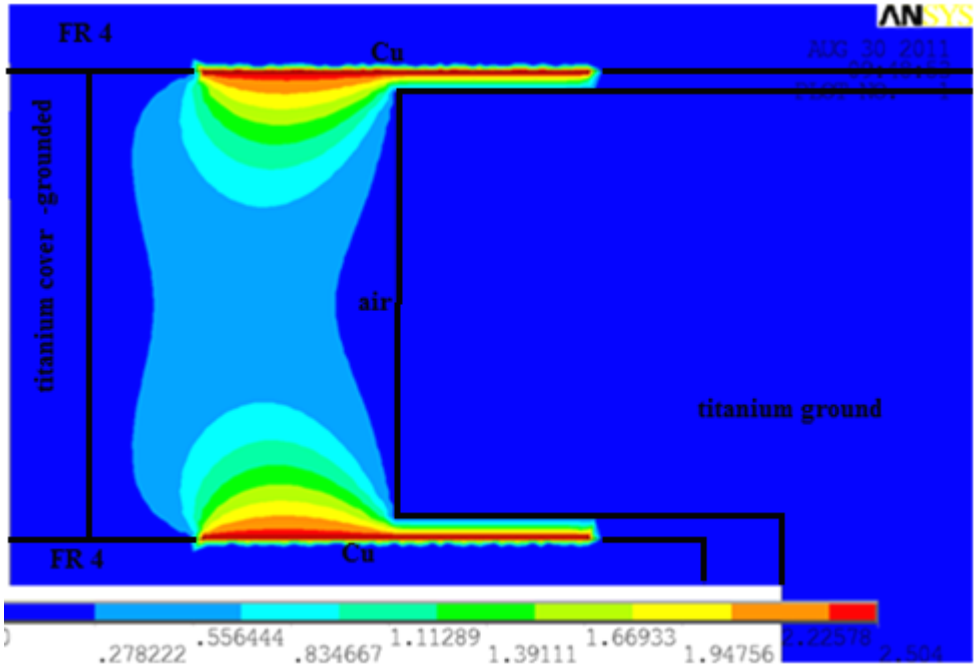

Fig. 57: Electrical field of capacitors

In Fig. 58 was set the electrode dielectric difference 0.1mm with a change of space of 0.01mm and area displacement 0.035mm. The electric field was strongest to the left top sensor where there was the highest area of electrodes nearest.

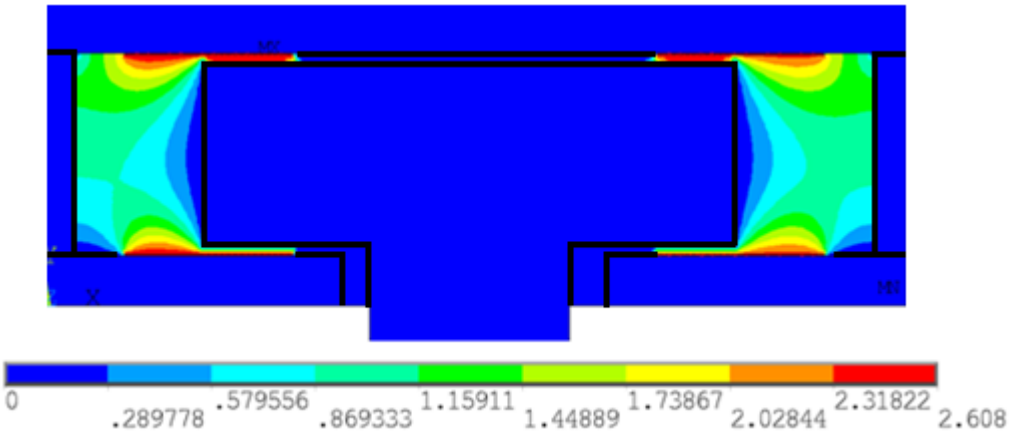

Fig. 58: Electric field with displacement

A greater overlap with the smaller electrode distance produced a larger and stronger electric field in the sensor. In this analysis it was calculated only with vertical and horizontal movement. The real process was influenced by the moment – for idealization it was possible to substitute the rotation (moment) for horizontal movement, because the changes were really small.

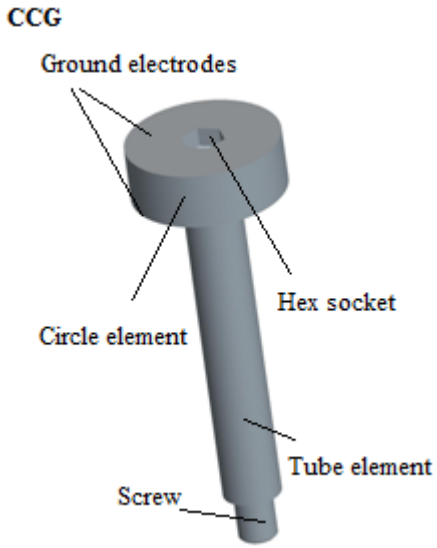

Fig. 59: Central circle ground (Titanium)

Central circle ground

This element visualized on Fig. 59 is the second ground electrode from the parallel-plate capacitor. It had a circular dimension – circular element for the symmetrical electrical field Fig. 59 and grounded tube element. The next advantage of this element was system mounting to the bottom surface in the adapter`s main body. A screw used. The part was the same for each direction after the screwing. It was a static part. The first was the prepared model from two elements (separate circle element and tube element) connected by thread for the calibration of same size of dielectric. After the first tests there was a change of the structure of two separate elements on one complete element. This part made the initial dielectric difference 0.25 mm. This issue will be described in more detail in the measurement and testing part later.

4.3.1. Next internal elements

Titanium ring

The titanium ring on Fig. 60 was made for creating the space between the sensors. The dimension of the ring was the same as the PCB and the edge was real connected into construction with the PCB copper shielding as a ground. There were two special pins for fixing the ring and PCB with right direction. Torsion and rotation were eliminated by this system.

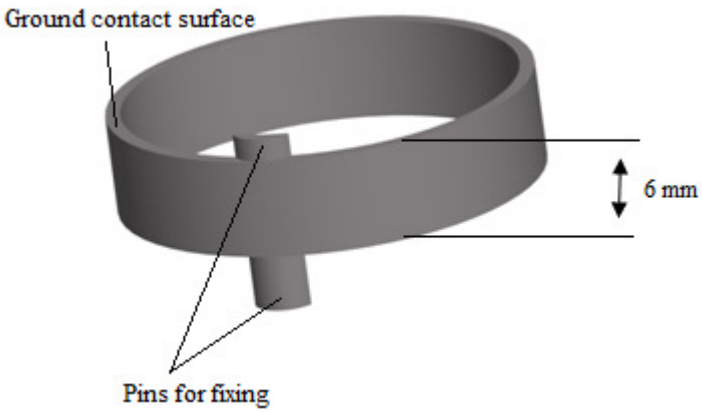

Fig. 60: Titanium ring

Cover and bushing

Fig. 61: Cover with bushing

The cover had a roundish shape as in Fig. 61. On the outside surface was the thread. The whole cover was screwed inside the top part of the main body and completely held the PCB, ring and electronics. Maximal stress was necessary, because the maximal fixation of the PCBs was needed. The hold element for the cable was on the top of cover. A plastic metric cable bushing M12 4-7 mm MBF12 was from catalog and used for screwing the cover and fixing the data cable from the electronics on the PCB.

4.4. Visualize extrude of adapter

4.4.1. Inside describing

The structure of the sensors with sharing central circle ground (CCG) is in Fig. 62. These parts were contactless, separated by a grounded titanium ring.

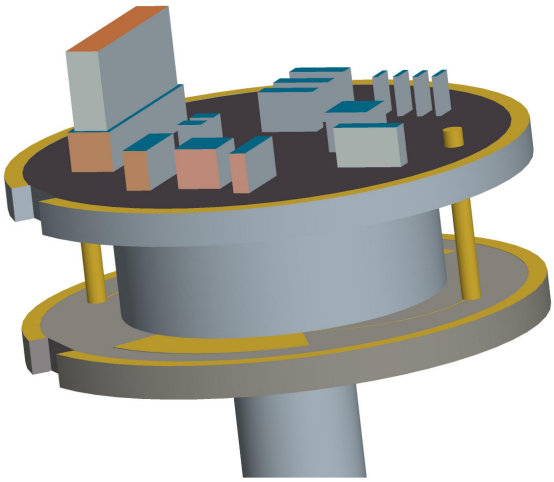

Fig. 62: Assembly of electrodes

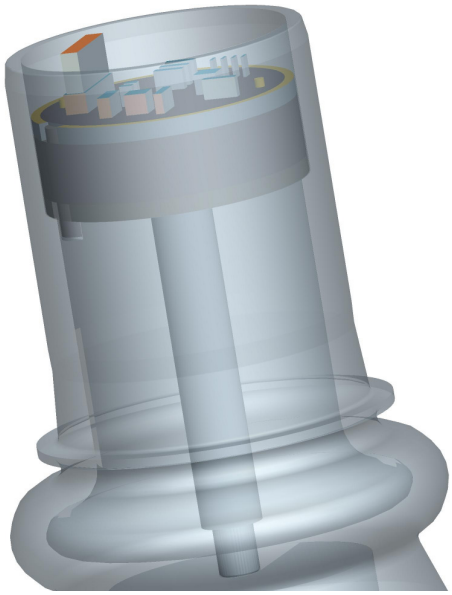

Fig. 63: Fixing the sensors

In Fig. 63 is shown fixing the inside structure in the main body of the adapter.

4.4.2. Complete extrude

Into the Main body (1) was first fixed the lower PCB (2) with electrodes and wire connectors. Then was inserted the CCG (3) (one or two elements) and screwed to the bottom of main body. The Titanium ring (4) was used to separate the space between sensors. The upper PCB (5) with the next two electrodes and electronics was fixed on the ring by a pin. The data cable was connected into the connector. The electrode connectors were soldered to the upper PCB. The cover with bushing (6) was screwed, finally the adapter was completely closed (7) and the data cable was tightened by bushing (Fig. 64).

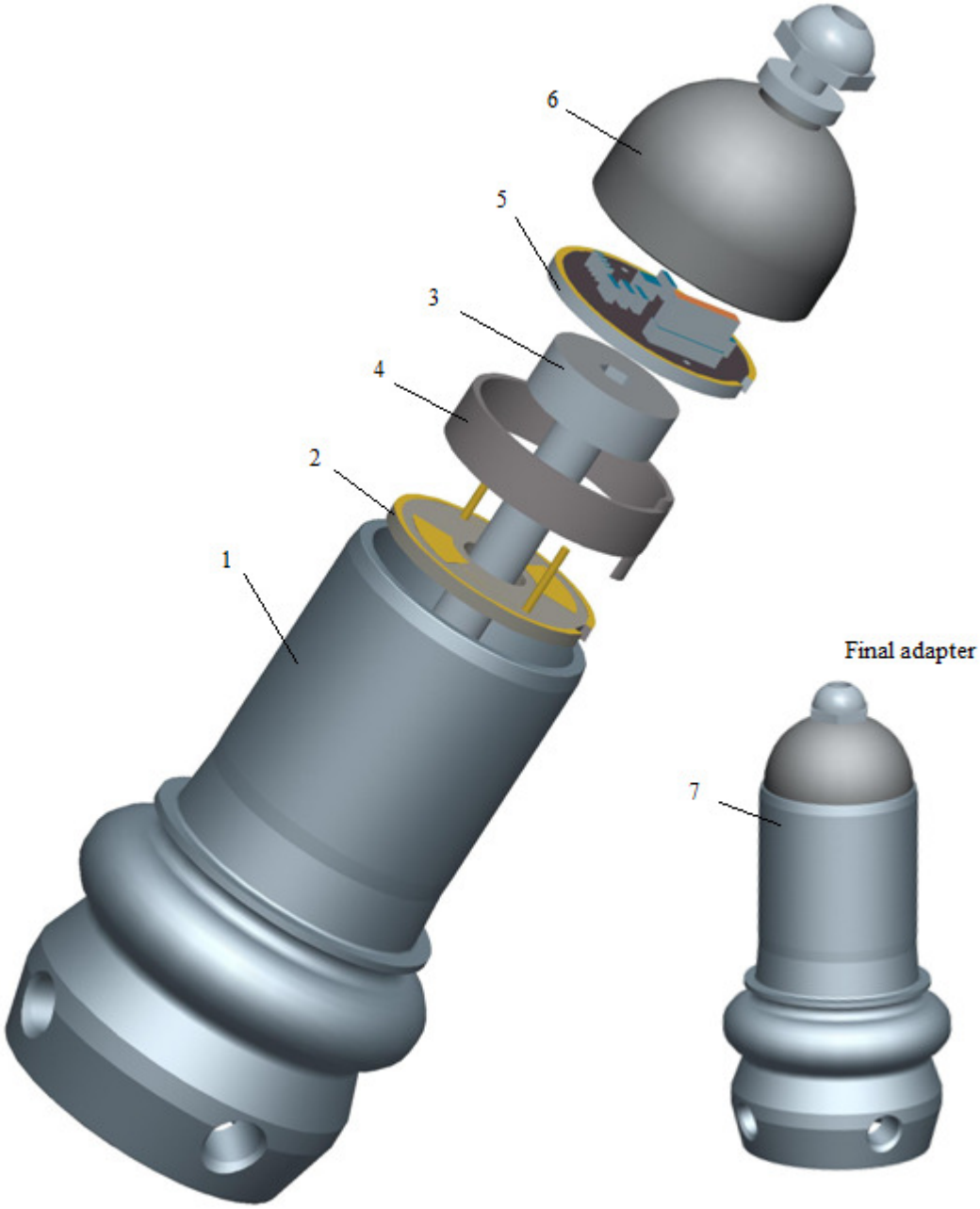

Fig. 64: Complete extrude with assembled adapter

4.5. Measurements and tests

The testing tube was connected to the adapter. The adapter was fastened on the steel testing desk by four hexa screws. The cable from the adapter was connected with the motherboard by SPI communication. For evaluation, the same measuring equipments were used as in the EBWorkspace in chapter 3 (PicoCap microchip, same motherboard, Programmer etc).

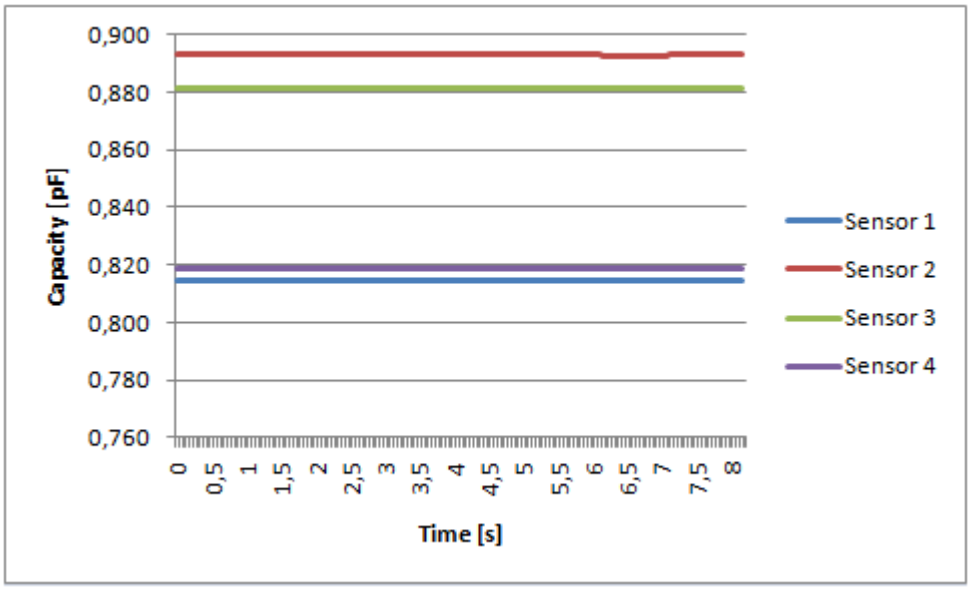

Graph 16: Uncalibrated signal

The measurement after the first load test of vertical force and moment showed a significant problem with the quality of the signal. After the re-measuring of the electronics parts, a defect was found on the PCB. The resistor, as in Fig. 65, was destroyed.

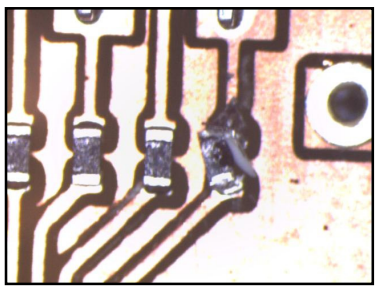

Fig. 65: Resistors under the microscope

The reaction on the vertical load and moment after the change of resistor was very good and was similar to the FEM analysis from the ProMechanic program. Uncalibrated signals are in Graph 16. The moment and vertical force differences for higher range between the channels was not seen. The different width of the dielectric between the upper and lower electrodes was evident in this graph. This problem was permanently solved and it was influenced by the material properties of PCB. By settings

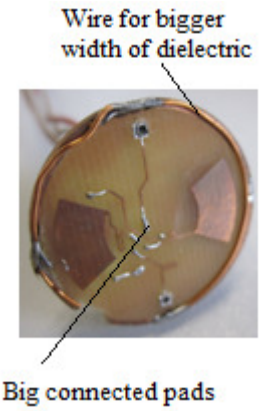

Fig. 66: Laboratory PCB

in PicoCap software it was possible to change the sampling frequency on the requirement value. The PCB was made in the electronic laboratory in the OttoBock company. The two big pads on the bottom of upper electrode (Fig. 66) caused during higher load a fatal error of measurement. It was found that some pads were connected with the CCG during the movement of the electrodes in the centre of the adapter. Since the first measurement was prepared for a difference of electrode of 0.25 mm this was problem – especially for the future measurement with a smaller width of the air dielectric. A manufacture PCB was ordered (without pads) for improving the measurement and removed this error (Fig. 67). The copper electrodes and signal traces etched from copper sheets were covered with a special varnish. The purpose was to protect it against oxidation and mechanical damage. The varnish was also a dielectric.

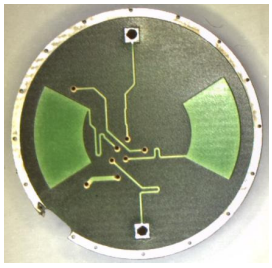

Fig. 67: Manufactured PCB

4.5.1. Width of the dielectrics

In chapter 4.3.4. the CCG is shown. The design solution of this part was more complicated. The interesting solutions will be shown in the following text.

Two elements structure

The first assumption was to do this part from two elements. First- the grounded tube element was strongly fixed on the bottom of main body. The second part of the CCG was the circle element (CE) and was screwed to the tube element (TE) on the top (Fig. 68). To create symmetrical width of dielectric it was necessary to put the CE to the centre, exactly between the sensors. In this case the dielectric width was 0.25mm for all sensors (Fig. 57) and the measurements initial capacities had the same values.

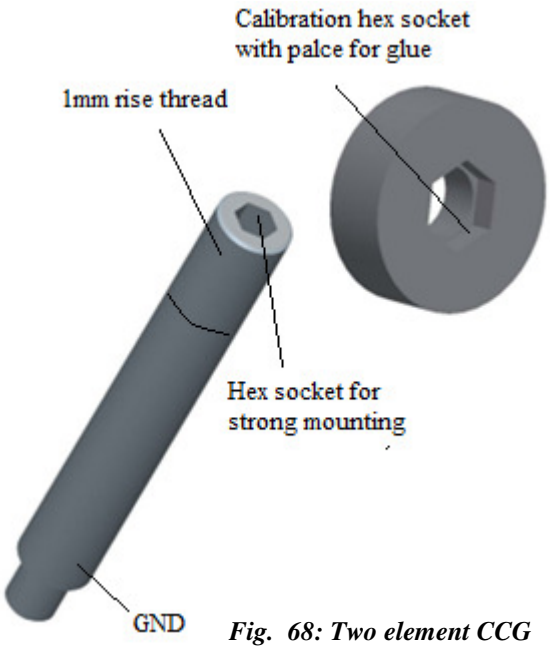

Fig. 68: Two element CCG

The procedure of construction: the thread had risen 1 mm on one turn (360°). The circle element was screwed on the lower positive electrode, after this unscrewed a half turned back (180°). The fix of CE with the TE by glue was later necessary. There was a big vibration and measurement noise without glue fix (Fig. 68). The position was set by this system directly 0.25 mm between the electrodes.

The locking position by glue was problematic, because the thread was free and the fixation was not symmetrical – the circle element did not have a right angle to the tube element. It means that the initial capacity for each sensor was different, but for the first testing measurement it was sufficient and negligible.

One element structure - with locknut

The smaller width of the dielectric was, theoretically for the measurement (in future practically), better. The one element structure was used for the width of the dielectric of 0.1 mm. It was manufactured by the same design, but only one element structure, for better positioning of the CCG. The design was prepared with good accuracy for screwing the element in to the main body. The locknut in Fig. 69 was on the bottom of the main body in the space for fixing the adapter by pyramid adapter. The width of dielectric was calibrated during the program setting part in live mode. According to the visualisation on the software, was set a right tension the locknut on the CCG. It was possible to make a similar signal without bigger deviation. As the locknut operated against the thread of CCG, during one of the settings the CCG was partly damaged - was used to big tension on the screw. After this accident, a different and more robust final solution was prepared.

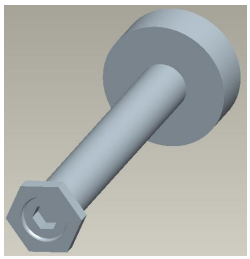

Fig. 69: Locknut

One element structure

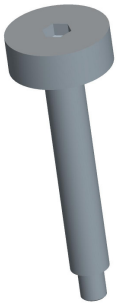

Fig. 70: One element CCG

The final CCG on Fig. 70 was manufactured with maximal accuracy for the measurement dielectric width 0.05mm as one element. The problem with this design was the different width of FR4 material in PCB (1.5mm ± 0.005), the copper had a different width (0.035mm ± 0.002mm). The width of the varnish was significant too. The copper ground layer and varnish were deformed during the mounting and screwing of the cover part on the PCBs.

It was difficult to find the right maximal torsion for the fix of PCB by

titanium cover. This solution was, in the end, the best because the highest value of the signal was measured, this meant the highest difference of the capacity which was possible. The problem was only with the size of each signal and it was necessary to calibrate them.

4.5.2. Moment measurement

A 1m long aluminium moment arm was made (MA) as in Fig. 71 for the moment measurement, which was connected by pyramid adapter on the testing tube. The testing tube was connected with the C-Leg adapter as in chapter 4.3.1. The length of 1 m allowed measure of the moment directly in [Nm] unit. Positive or negative moment was made by pressing the MA. For measurement of the load (weight) several weights were fixed on the MA in distance 1 m. The MA is aluminium and it is deformed, bended etc. This was neglected during measurement.

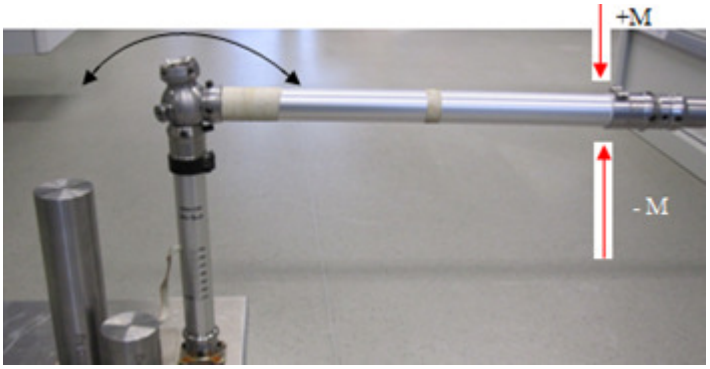

Fig. 71: Moment measurement

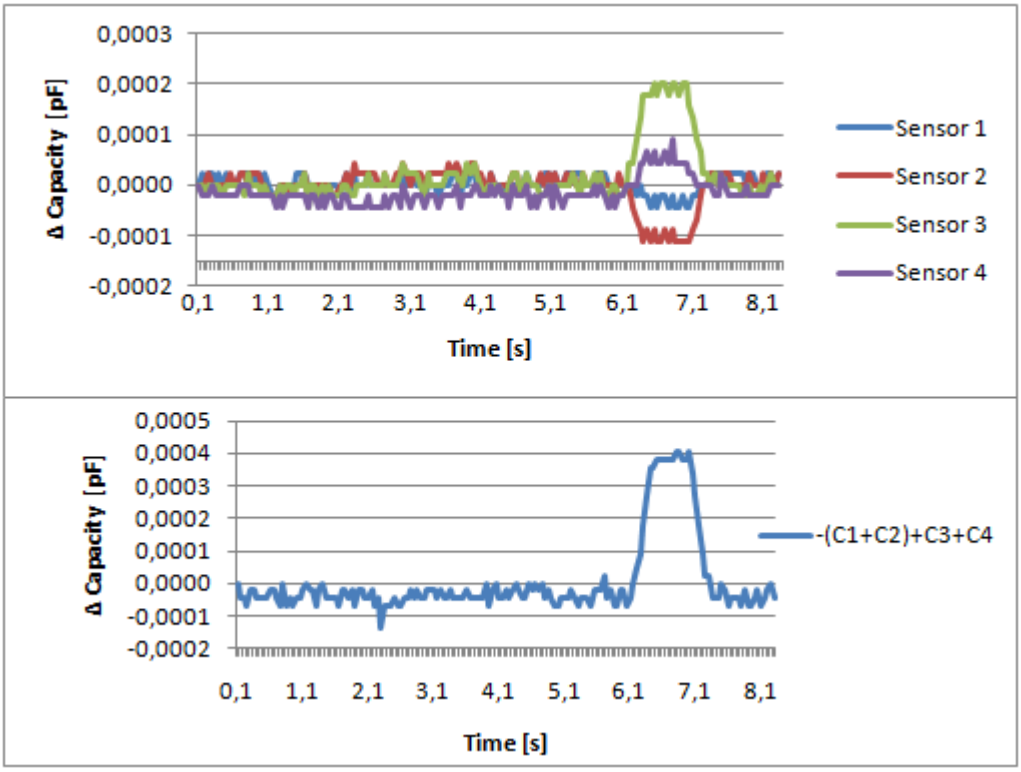

Graph 17: Test of moment

The moment was calculated by equation in chapter 4.2.1. In Graph 17 is shown an assumed result – the process of moment measurement. The data was calibrated by zero offset. In the upper part all characteristics of the sensors in the adapter are visualised. In the lower part of the graph is a final moment expressed as a maximal sum of the capacity according to chapter 4.2.1.

The same settings for measurement were necessary for repeatable tests. It was possible to measure the moment difference around minimal 1 Nm, but the change of signal was low.

4.5.3. Vertical force measurement

On the testing tube (without the moment arm) the weight was sequentially increased. The critical vertical force worked in the centre of the testing tube, as in Fig. 72. The weight was concentrated symmetrically to this centre. The testing tube with the adapter had to aim directly perpendicular. The process of the vertical force acting on the sensors is in Graph 18.

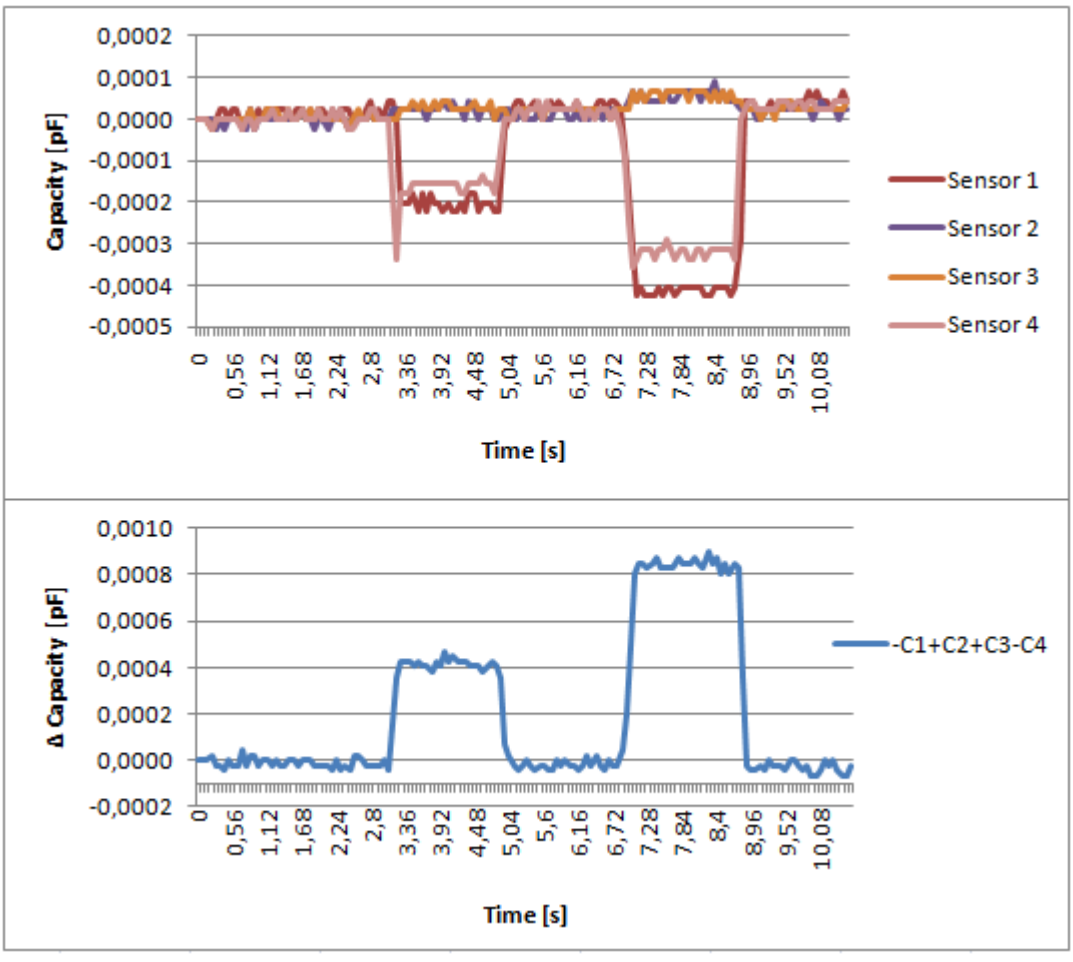

Graph 18: Test of vertical force

Fig. 72: Vertical force measurement

The signals in Graph 18 were not ideally measured, because the increase and decrease of the capacity in each sensor is not symmetrical. The different width of the dielectric was evident here. The sensor 2 and sensor 3 should have a bigger signal. In the other case it was not necessary to have the same dielectric width, because the vertical calculation worked well. The vertical force was expressed as a sum of maximal value of capacities in the correct position.

With PicoCap microchip, it was possible to measure a minimal load from 1 N.

The data from the measurements with different CCG – different width dielectrics are compared in Tab. 8. The change of the difference of capacity on the width of dielectrics was visible. The vertical force had a 10x smaller change of capacity. This was according to the FEM analysis being correct.

	Width			**Sum of capacity differences**	
	CCG - Circle element	Titanium ring	**Dielectric** of 1 sensor	Sum of capacity differences of vertical force for 9.57 N	Sum of capacity differences of moment for 9.57 Nm
Units	[mm]	[mm]	[mm]	[fF]	[fF]
Two element structure	5.50	6.00	0.25	0.03	0.99
One element structure - locknut	5.80	6.00	0.10	0.18	6.12
One element structure	5.90	6.00	**0.05**	0.49	9.30

Tab. 8

Result

The vertical force and the moment were connected together every time. The final signal was separated on the vertical and moment component in the assumed practise use. The minimal values were measured by all sizes of CCG, but for the better signals

the CCG was adjusted for the next tests on the width of dielectric **0.05 mm**. The weight tests on the prosthesis adapter were prepared according a norm ISO 10328 too.

4.5.4. Problems during measurement

Unexpected problems were common. The hardware properties were consulted with the manufacturing department and adapted gradually. The biggest problems that were detected during the measurement or testing of new C-Leg adapter are described in the following text.

Vibration

For example, for the CCG with circle element without glue fix was measured the vibration on Graph 19. The vibration was tested by knocking a metal object on the testing tube. Maximal vibration on the Sensor 1 (C1) is in Tab. 9 (but it depended on the strength of strokes). The vibration in this case were spacing and area movement – it was problem separated the movement and negative vibration.

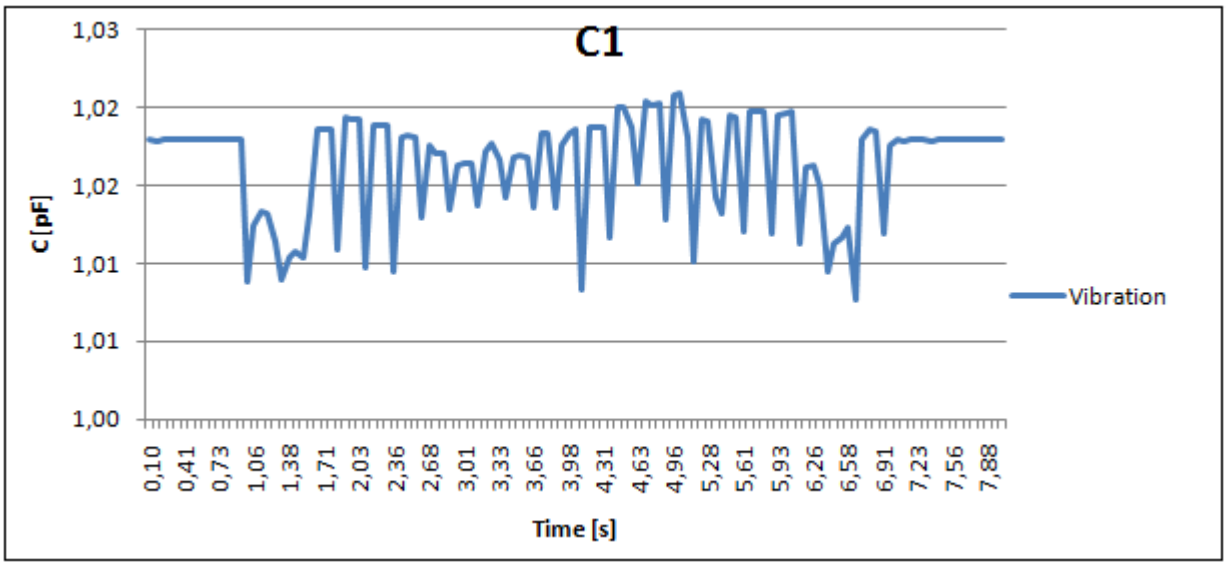

Graph 19: Vibration – two element structure

About the equation in 4.2.1., the vibration coefficients for moment and vertical force were calculated in Tab. 9. The stroke was made by hand and the same steel tool was used for all sizes of CCG. The hand measurement was a little inaccurate, because the exact same strength was not always used. For theoretical verification it was sufficient.

The maximal difference of capacity and capacity coefficients from the vibration measurement are in Tab. 9. The one element structure had the smallest vibration.

	Initial capacity [pF]	Max. Δ C from initial C [pF]	Maximal vibration Δ [pF]
Two element structure (without glue) Only signal from sensor 1 (Graph 19)	1.0181	1.0077	0.0103

	Coefficient [pF]	Maximal coefficient [pF]	Maximal vibration Δ [pF]
One element structure - locknut	0.8152	0.8186	0.0034
One element structure	0.6650	0.6659	**0.0010**

Tab. 9

The system was completely resistant for smaller vibration after fixing the TE and CE with glue. The higher vibration was for smaller load problem, especially for the vertical force calculation.

Signal noise

For finding the value of a signal noise it was necessary to measure the minimal loading and do recalculation for the moment and vertical force. The microchip signal noises properties were on the end compared.

On Graph 20 it is shown the moment step according to Tab 10. Dielectric width of 0.05 mm was used for higher signal as was explained in Tab. 8.

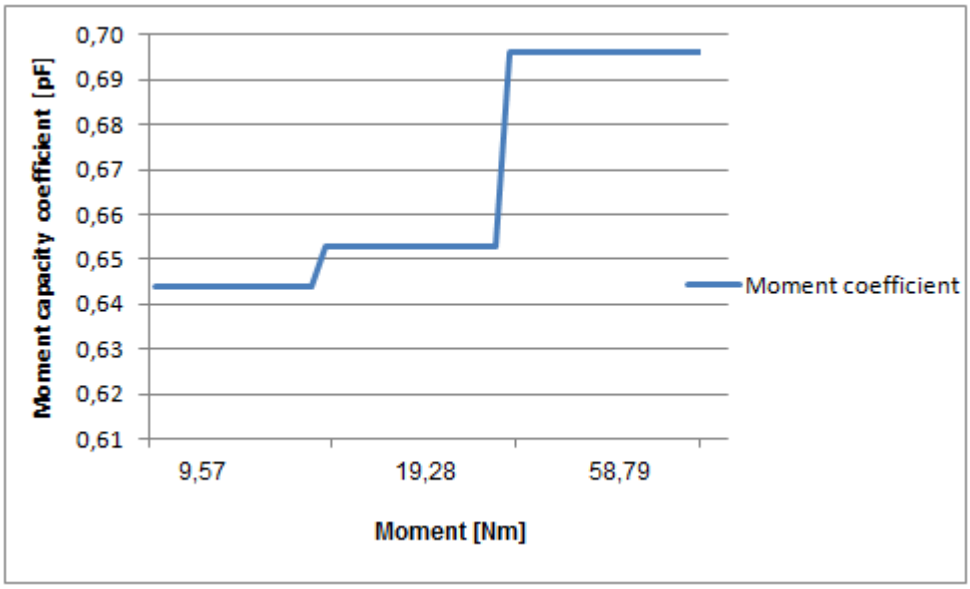

Graph 20: Moment steps

The minimal measuring moment was optimal according to Tab.10 – highlighted. Separate the vibration component from the moment from table was under the Δ coefficient problem.

Moment [Nm]	Sensor 1 [pF]	Sensor 2 [pF]	Sensor 3 [pF]	Sensor 4 [pF]	Moment capacity coefficient [pF]	Δ coefficient [pF]
9,5700	1,9294	1,0303	1,0111	1,3049	0,6437	0
19,2800	1,9307	1,0307	1,0109	1,2975	0,6530	**0,0093**
58,7900	1,9376	1,0326	1,0095	1,2647	0,6960	0,0522

Tab. 10

The process for the vibration in vertical force measurement was same as in moment one. The minimal measured value protected against the vibration was highlighted in the Tab. 11.

Vertical force [N]	Sensor 1 [pF]	Sensor 2 [pF]	Sensor 3 [pF]	Sensor 4 [pF]	Vertical force coefficient [pF]	Δ coefficient [pF]
0	1.9301	1.0213	1.0091	1.2994	1.1991	0
9.5700	1.9300	1.0214	1.0091	1.2991	1.1986	0.0005
48.8500	1.9298	1.0214	1.0091	1.2985	1.1978	**0.0013**

Tab. 11

When the adapter with sensor was loaded more than 48.85 N of the vertical force and 19.28 Nm of the moment, there was a signal stronger than the vibration influence as in the Tab. 9. This result was acceptable.

It was a problem made vibration which could be real in the C–Leg prosthesis. The vibration measurement in Graph 19 and earlier tables were probably overloaded, but for basic description it was sufficient.

Signal noise (vibration suppressed)

Measuring rate [Hz]	RMS Noise [fF]	Δ capacity coefficient for requirements vertical force resolution **1N** [fF]	Δ capacity coefficient for requirements moment resolution **1Nm** [fF]
6,10	**0,01288**	**0,0600**	**1,0770**

Tab. 12

Root mean-square (RMS) noise in fF as a function of output data rate in Hz, measured at 3.0 V supply voltage using the maximum possible sample size for in-chip averaging at the minimum possible cycle time. [10]

The signal noise for data rate from Tab. 12 was, according to the datasheet from Acam [10], recalculated. The signal noise is smaller than the minimal resolution of the sensors as in Tab. 8! Data was calculated by linearization from Tab. 10 and Tab. 11.

Copper dust

There was micro copper dust during the screwing and unscrewing of the adapter. The friction of materials deformed and polluted the copper grounding edge of the PCB. These micropieces of copper connected some electronic parts on the PCB. This made a big signal noise on the sensor 1. A new PCB was fitted with a new microchip and electronics. The PCB was completely cleaned with a special cleaning liquid after each disassembly. After this method the problem with negative noise on the sensor was eliminated.

Material hysteresis and deformation

The material hysteresis and deformation is evident in Graph 21. The material – titanium has got very small hysteresis. The PCBs were fixed by cover pressure. Small movement and deformation of the copper layer was possible. The problem was during the measurement. While the measurement was quick, the materials had small hysteresis elasticity. Repeatable measurement made small deformations.

These were negative properties of the system. Unfortunately, this could be solved only by making a new structure of the measuring system inside the adapter.

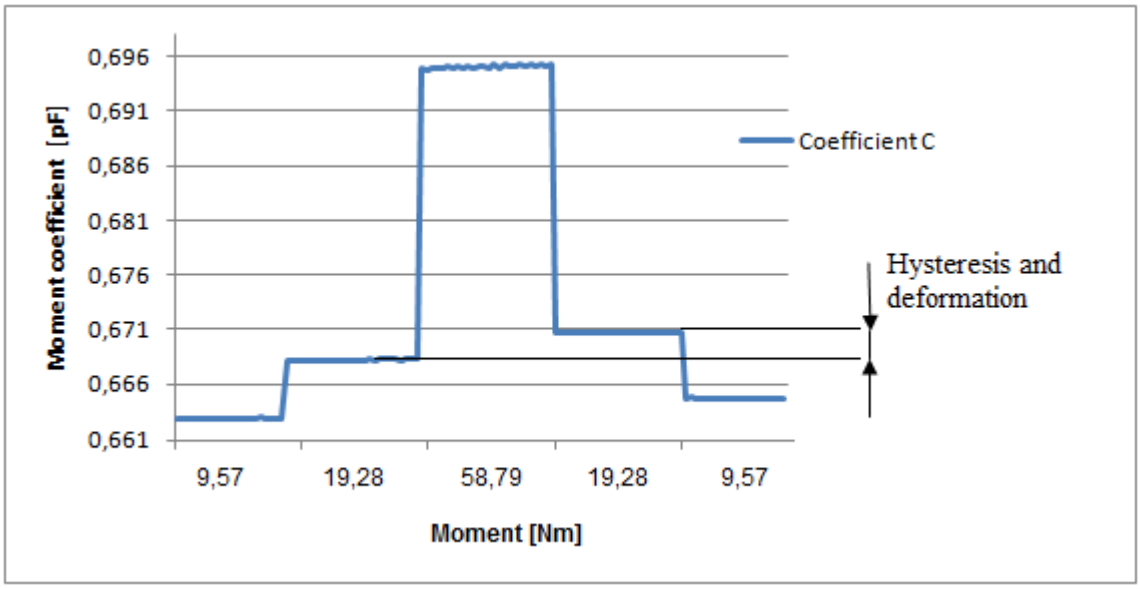

Graph 21: Hysteresis and deformation

This error was not measured repeatedly, only for the tests of moment. In Graph 21 was the maximal error for 19.2800 Nm 0.0178 pF (0.9fF/1N). This wasn't in range of measurement as in Tab. 10, but for higher optimal moment more than 50 Nm it was acceptable.

Temperature bridge connection

- Compensation of temperature and humidity

During the test it was assumed that the temperature and humidity distribution is theoretically homogeneous. From this case it was designed and used with a connection of sensor to the bridge, for compensation temperature and humidity.

A big nonlinearity of the sensors and different non-repeatable coefficients, calculated according chapter 4.2.1. with the temperature change, made the presumption of the inhomogeneous temperature and humidity field inside the sensor. This assumption of inhomogeneous field was later proved to be wrong.

4.6. Linearization methods

Capacitive sensors usually show an inherent non-linearity which varies over their capacity range, i.e. there is a varying deviation from the nominal value over the applicable capacitance of the sensor.[29] From the 3.1.5. and 3.1.6. it was known that the capacity depends on the temperature and humidity too. The capacity dependency of the area and spacing variation was known from the 2.3. For the measurement in the new C–Leg adapter a calculation systems was prepared in Microsoft Excel. There were compensated all non-linearity. Excel spreadsheets are in the attachment on the CD.

Polynomial approximation:

A non-linear function can be described by mathematical equations which approximate the characteristic of the curve. Thereby, the description of the non-linearity under consideration gets better the higher the order of the polynomial.[29] But a higher degree of polynomial can be difficult for the future processing data in the microchip. Because the capacitive sensors are non-linear – like the one outlined earlier – a polynomial compensation was chosen. For linearization the 2th and 3th order polynomial were used.

The basic equation for polynomial function can be written as:

$$y = a_m x^m + a_{m-1} x^{m-1} + \cdots + a_1 x + a_0$$

Where the x is variable and $a_m;\ a_{m-1}; \ldots a_1;\ a_0$ are real and m is the inherent number. [30] Linear approximation was calculated too in some cases where it was more suitable.

Final design

A hardware modification was made for the final linearization. The original OttoBock working aluminium tube (AT) was connected with the titanium adapter (main body) in the manufacturing department. Special two component glue was used. The mounting was heavier and stronger than in the testing tube. This connection worked like one element. The design of the next elements stayed unchanged.

4.6.1. Calibration of load

Calibration of load was based on the polynomial calculation of the right moment and vertical force from the measurement. Each coefficient had its own value for load. Equations from chapter 4.2.1 were used.

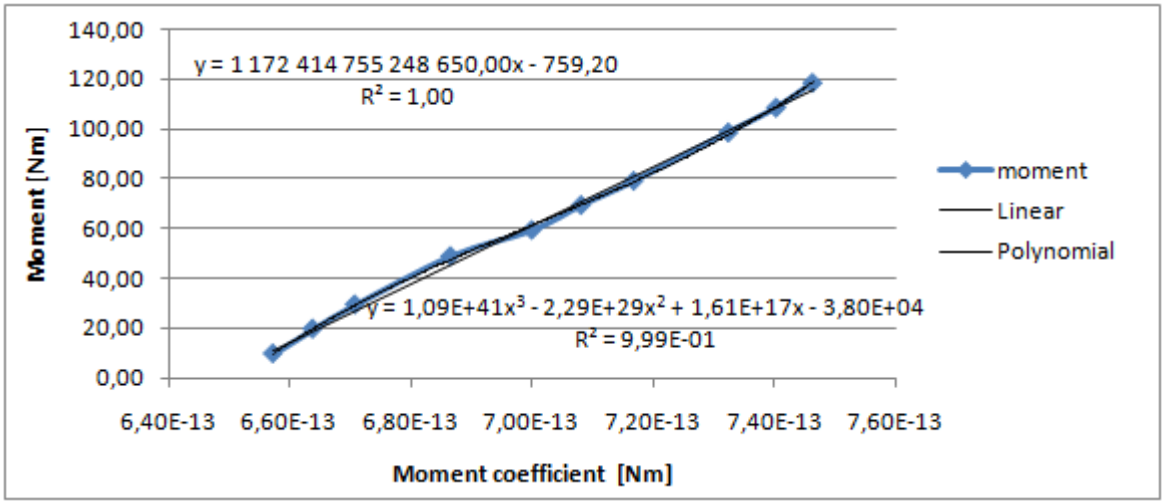

Graph 22: Moment approximation

The moment was measured according to Tab. 13. The moment on the testing tube and adapter was continually increased (Fig. 71). The coefficients were prepared from this measurement and from them the polynomial approximation, as is illustrated in Graph 22.

Coefficient	Weight [kg]	Moment [Nm]	Measured Moment [Nm]	**Deviation** [Nm]	Deviation [%]
6.57E-13	0.00	9.50	9.66	0.16	1,73
6.64E-13	1.00	19.51	19.64	0.13	0,68
6.71E-13	1.98	29.29	29.10	0.19	0,64
6.87E-13	3.93	48.80	47.45	1.35	2,77
7.00E-13	4.98	59.34	61.24	1.90	3,20
7.08E-13	5.99	69.35	69.51	0.16	0,22
7.17E-13	6.96	79.13	78.72	0.41	0,52
7.32E-13	8.91	98.64	97.65	0.99	1,00
7.40E-13	9.91	108.63	109.04	0.41	0,38
7.46E-13	10.91	118.64	118.84	0.20	0,17
Linear approximation			y = 1 172 414 755 248 650.00x - 759.20		
Polynomial approximation			**$y = 1.09E+41x^3 - 2.29E+29x^2 + 1.61E+17x - 3.80E+04$**		

Tab. 13

From the characteristic equation it was easy to find the correct moment for all process of measurement. The spacing variation should be less than 0.07 mm.

Linear approximation and the polynomial one were possible for linearization. The results were similar, a little bit better by polynomial approximation. The error or nonlinearity in the middle of measurement was made by a big change of the moment (change of type of weight). Here were the negative influence of the material hysteresis and deformation as was described earlier. For this reason is the characteristic a little bit nonlinear.

Vertical force calibration

As in the moment the vertical force was also calibrated by a system of increasing weight on the sensors in the vertical plane. The characteristic equation is in Tab. 14 and Graph 23. The capacity in this case had a linear progression.

Area variation should be max. 0.01 mm for vertical force for this measurement.

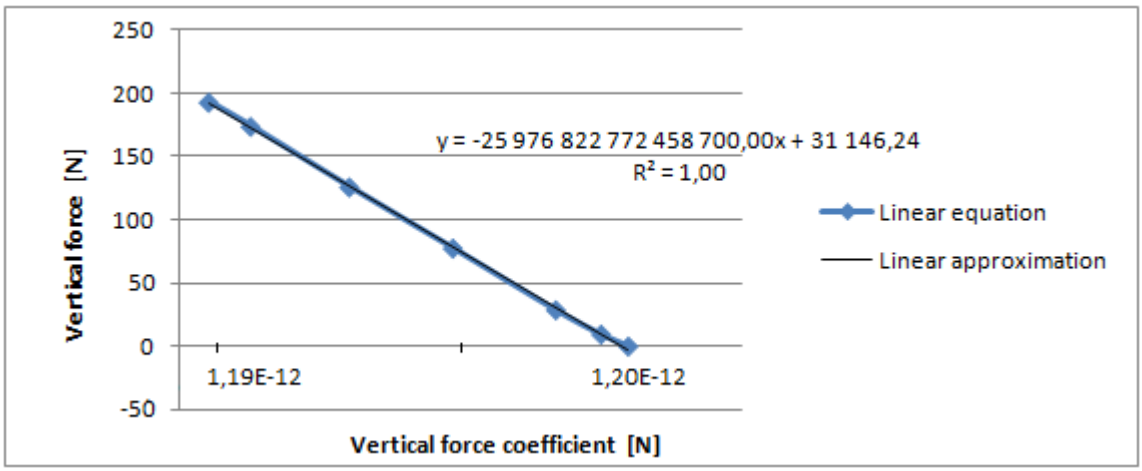

Graph 23: Vertical force approximation

Coefficient	Weight [kg]	Vertical force [N]	Measured vertical force [N]	**Deviation** [N]	Deviation [%]
1.20E-12	0	0	0	0	0
1.20E-12	0.98	9.59	9.84	0.24	2.55
1.20E-12	2.94	28.79	30.85	2.06	7.14
1.20E-12	7.92	77.69	78.84	1.16	1.49
1.19E-12	12.85	126.04	127.04	1.00	0.80
1.19E-12	17.73	173.96	172.95	1.01	0.58
1.19E-12	19.68	193.10	192.48	0.62	0.32
Linear approximation		**y=-25 976 822 772 458 700.00x + 31 146.24**			

Tab. 14

As is evident from Tab. 14 the deviation with the higher load is smaller from the set value. The deformation of material is bigger and the change of capacity is higher.

The theoretical assumptions were the non-linear dependency of capacity on the width of dielectric, but the approximation characteristic is for this very small range of the movement, **linear**.

4.6.2. Temperature and humidity Calibration

Theoretical assumption was that the temperature inside the adapter will influence the capacity on the sensors. As it is known from the earlier development, the temperature and humidity are non-linear with the capacity. For this reason the PCB was improved by the temperature aluminium strip with TK ≈ 2800 ppm/K and a polysilicon resistor with TK "close" to zero as a reference sensor directly placed on the microchip. The external 33 nF C0G capacitor was connected for discharge time measurements.[10] The temperature was measured by recalculation on the reference resistor. The resistivity was used for direct calculation of temperature coefficients.

The temperature coefficients were made in the climate box WKL64/40 as in chapter 3.1.5. in temperature range 60 °C to -10 °C. The gradient of the change of temperature in time was 0.4 K/min. This was enough time for creating the constant value of temperature inside the new C–Leg adapter. A signals with offset are in the Graph 24. Incorrect width of dielectric made a different electric field – different sensitivity of capacitive sensors – different ranges of the capacitive sensors.

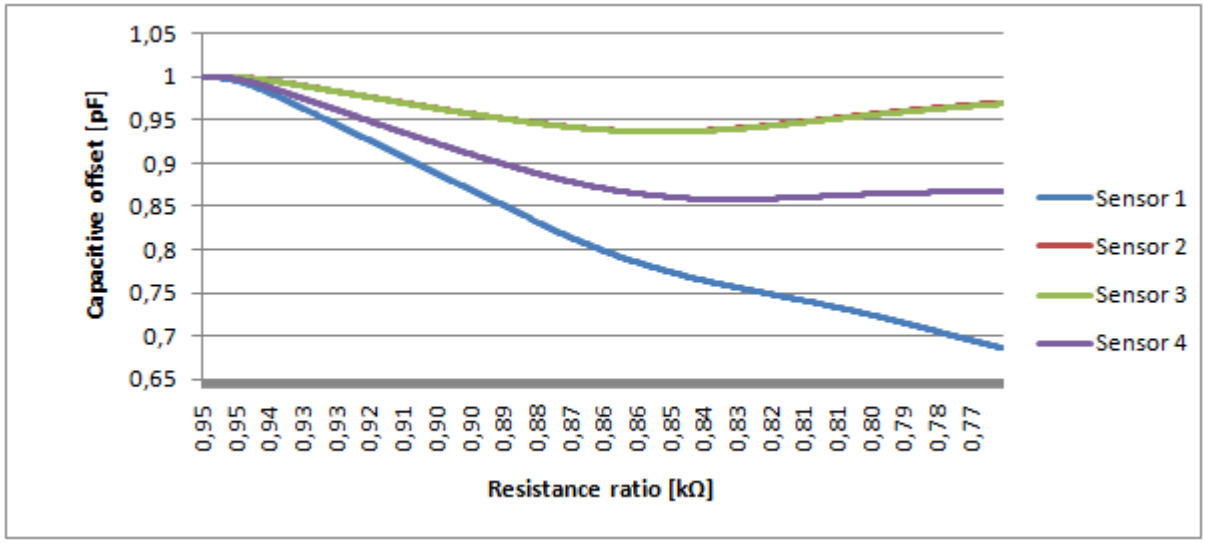

Graph 24: Clima box measurement

Absolute humidity was constant, because the system was completely closed by the titanium cover with bushing and special glue. Of course, the relative humidity influenced the measurement with temperature change , but the results were the same during repeat measurement.

The change of temperature was linear. The process is in Graph 25. The preheating was one hour before the measurement. This was necessary for a stable temperature in the climate box and adapter.

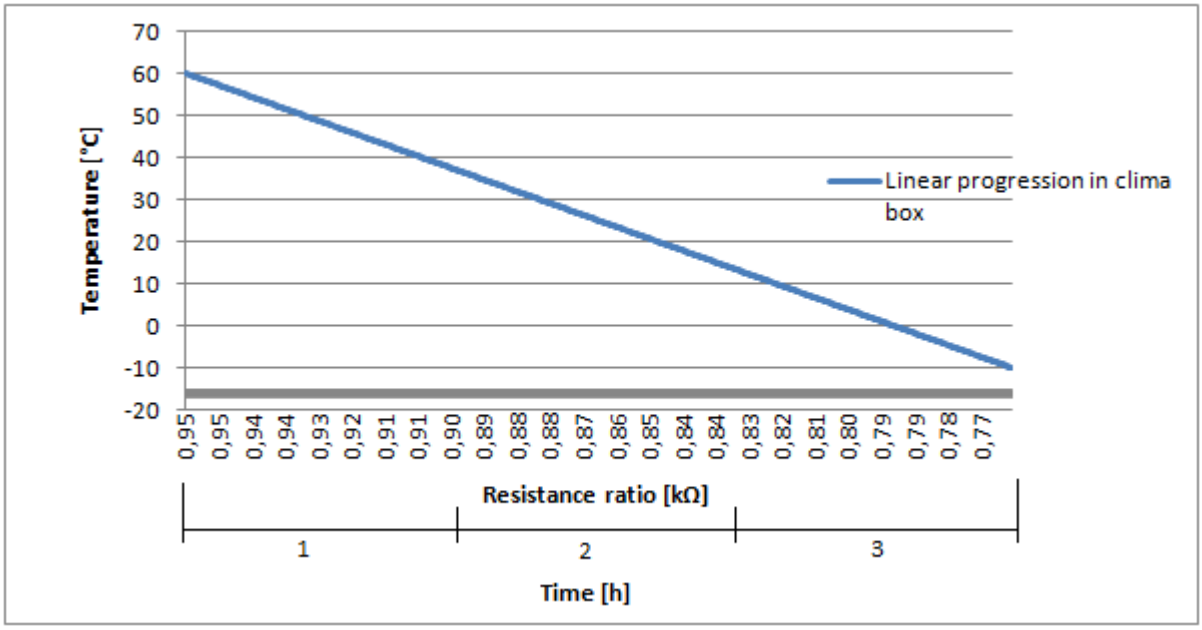

Graph 25: Relationship of the temperature and resistance

Characteristic polynomial equations

The polynomial approximation was made for all four capacitive sensors in the temperature range from climate box as in Graph 25.

Sensor 1 polynomial	**C1 constant**
$y = 6{,}98537E\text{-}12x^2 - 1{,}03111E\text{-}11x + 5{,}66527E\text{-}12$	1,93478E-12
Sensor 2 polynomial	**C2 constant**
$y = -4{,}18306E\text{-}10x^4 + 1{,}43875E\text{-}09x^3 - 1{,}84658E\text{-}09x^2 + 1{,}04828E\text{-}09x - 2{,}21094E\text{-}10$	1,00324E-12
Sensor 3 polynomial	**C3 constant**
$y = -4{,}11285E\text{-}10x^4 + 1{,}41470E\text{-}09x^3 - 1{,}81580E\text{-}09x^2 + 1{,}03083E\text{-}09x - 2{,}17422E\text{-}10$	9,83231E-13
Sensor 4 polynomial	**C4 constant**
$y = -4{,}71804E\text{-}10x^4 + 1{,}62984E\text{-}09x^3 - 2{,}09919E\text{-}09x^2 + 1{,}19540E\text{-}09x - 2{,}52788E\text{-}10$	1,27138E-12
Resistance ratio for 20°C:	0,84334

Tab. 15

The characteristic equation is in Tab. 15. Resistance ratio was chosen for 20 °C and for this temperature were chosen the sensor constants (C1-C4).

The data from the Acam PicoCap software was recalculated according to the polynomial equation. This equation was used for each following measurement. All data was calibrated on one resistant ratio value. Therefore, for temperature 20 °C.

4.6.3. Results of complete calibration

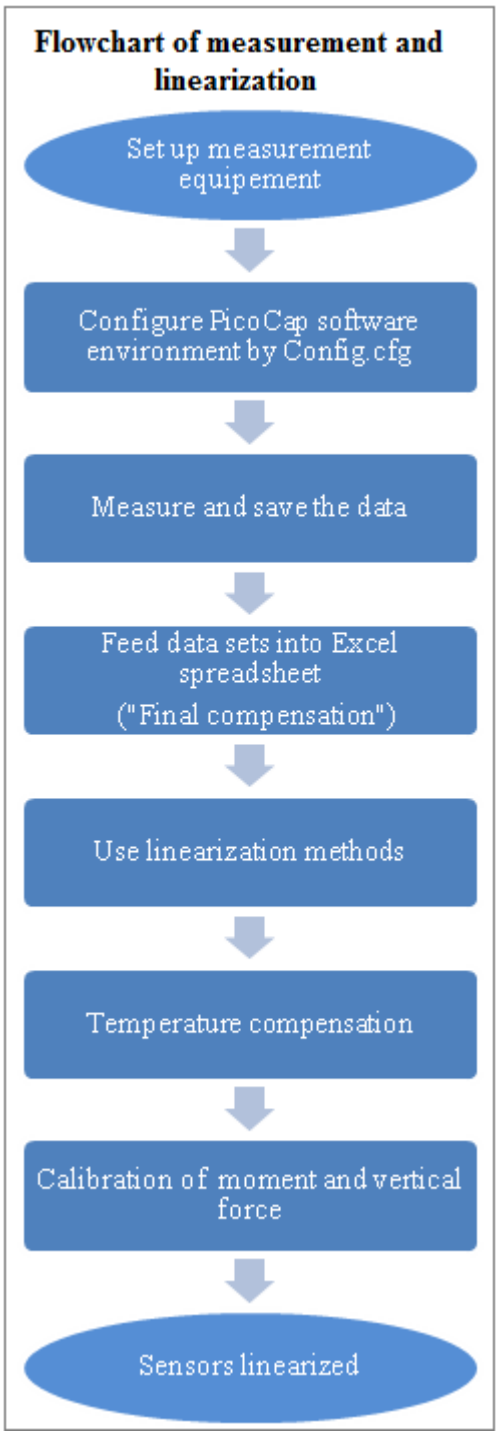

In Microsoft Excel was made "Final compensation" and calibration spreadsheet program. First calibration of temperature as in the earlier description in chapter 4.6.2. was made, then the next calculation for vertical force and moment calibration was prepared. This was made according to chapter 4.6.1. Capacity offset calibration was not necessary, because **it was calculated with coefficients according chapter 4.2.1**. These coefficients of moment and vertical force were the same for all testing measurements and prepared for comparison with the data from tests.

Tests

For linearization it was necessary to copy the data into the spreadsheet. Excel automatically recalculated and compensated the data according to the earlier explanation.

The results could possible visualised in graph form. All linearizations were calculated offline and Excel was chosen for universal use of the other users – especially in the OttoBock company.

The results from one of the tests, after the compensation, are in Graph 26 and Graph 27. Theoretical offset had to be zero, but real measurement and compensation found extreme errors!

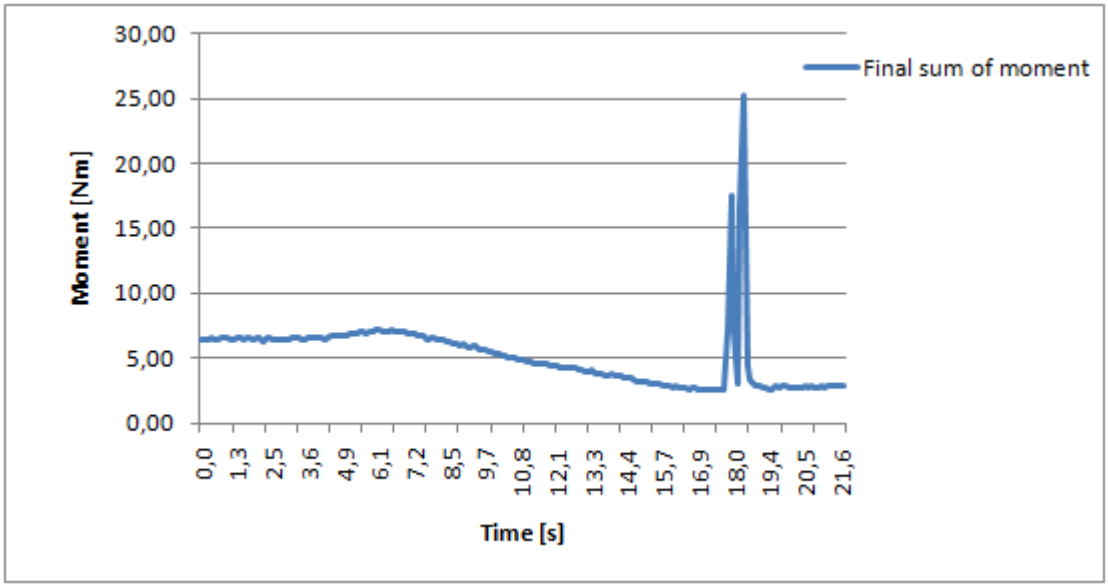

Graph 26: Test measurement of moment with hand heating

This measurement simulated the real change of signal during the gate (the time is idealised). The measurement was separated on two components as could be in the real process. By comparing the signals with the resistance ratio characteristic (Graph 28) we can see that the linearization wasn't working! This problem and result were in other tests too.

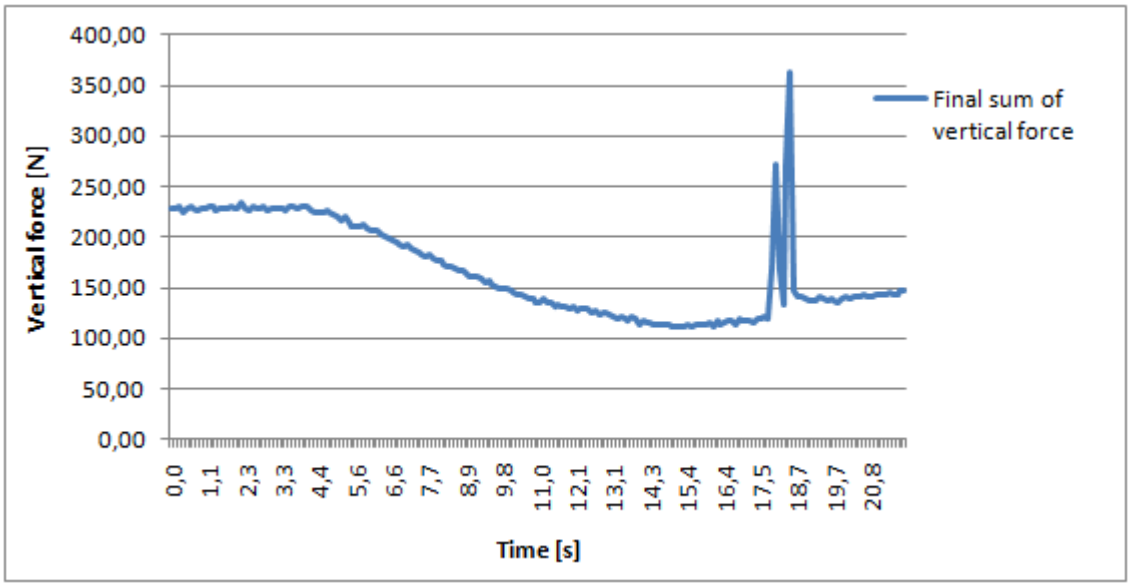

Graph 27: Test measurement of vertical force with hand heating

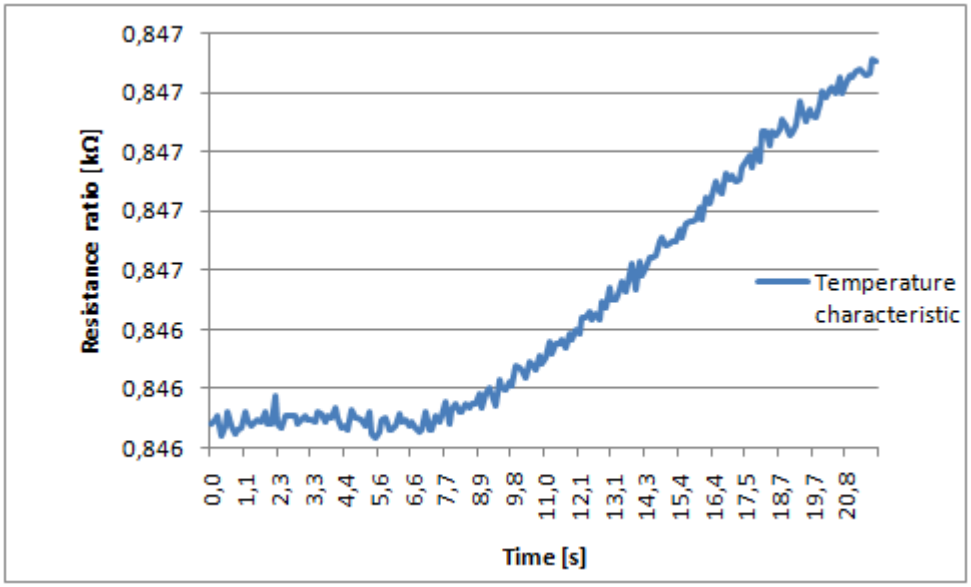

Graph 28: Hand heating of AT and adapter

4.6.4. Solving the problem of linearization

About theoretical assumption was the linearization very good and should to working, but during the tests there was a problem to compensate the temperature according to the temperature and humidity bridge and by coefficients from temperature sensor. The calculated coefficients were different than the assumed coefficients from the basic calibration and compensation by polynomial equation as is in Tab. 13 and Tab. 14. Several tests had different results and the same negative results.

For understanding where the error was or what the problem was of the negative results it is necessary to go back to Graph 24. Signal of Sensor 2, 3 was taken from this graph to the following Graph 29.

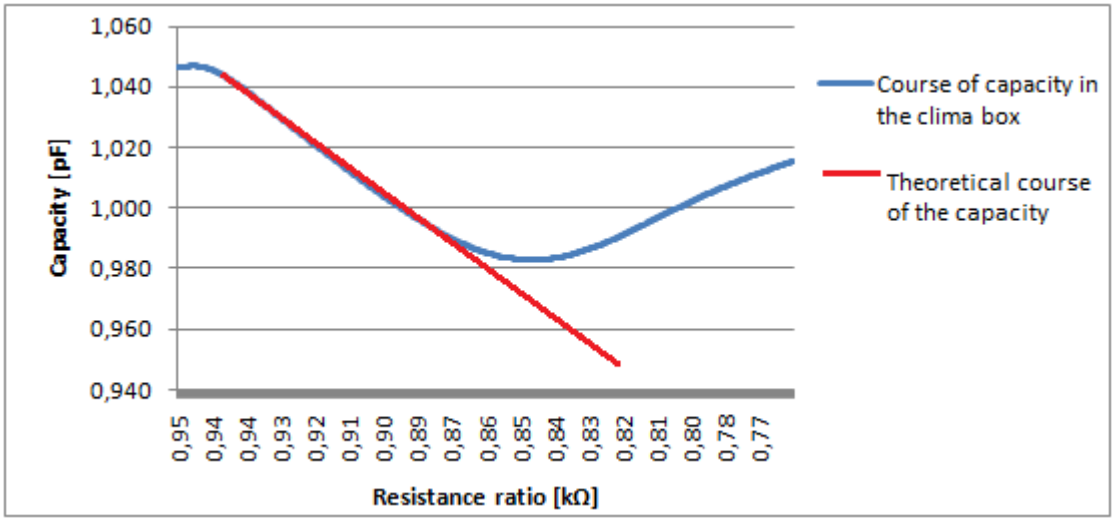

Graph 29: Sensor 2, 3 in the clima box

The capacity is changing with the changes of the temperature. From the Graph 29 it is evident that this was not in our measurement in the climate box. The outside temperature changed the temperature of AT and MB by different temperature gradients. The different temperature with different temperature gradient was distributed into the inside air exactly into to the temperature sensor on the microchip. There is a big temperature delay between the heating of the microchip and the material of the AT and adapter.

The thermal expansion and contraction of material was the biggest problem of this measurement! The AT and titanium main body expanded with the increased temperature to the length and this material properties was a bigger negative influence than the changes of temperature or humidity! The problem is described in Fig. 73.

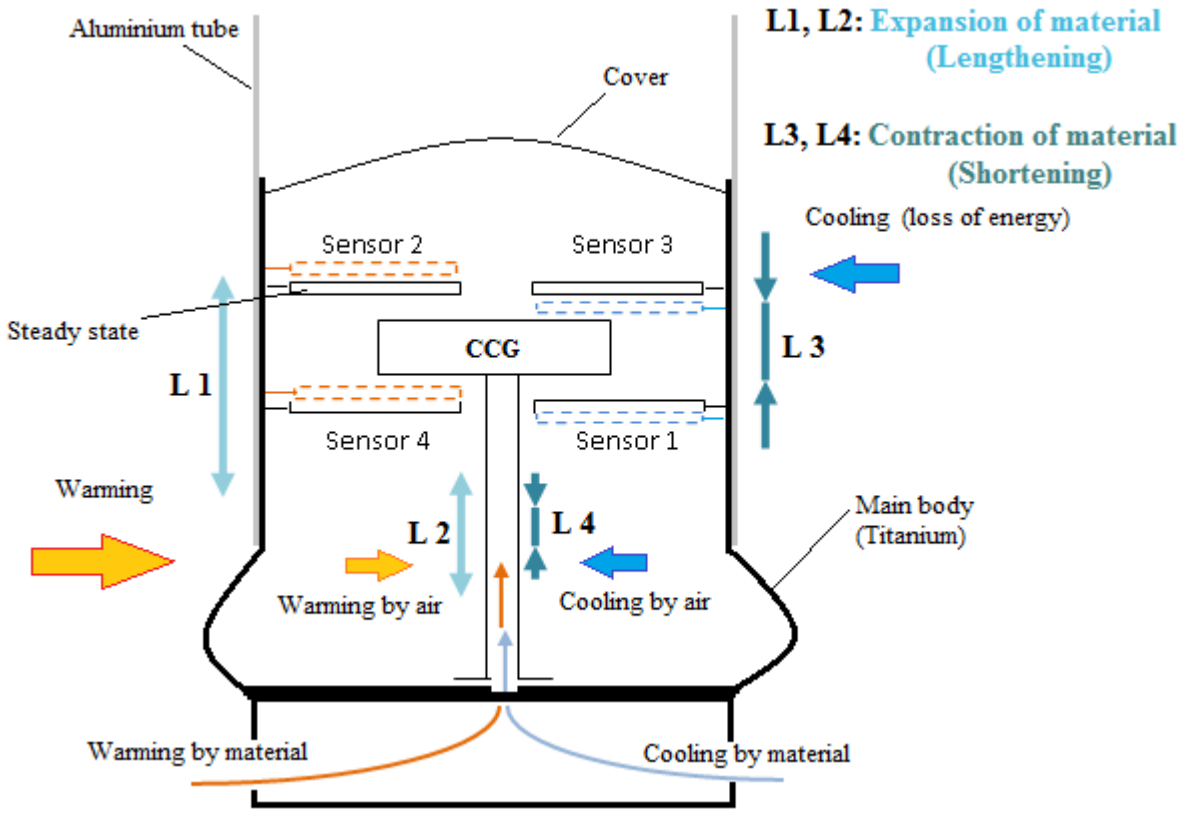

Fig. 73: Expansion and contraction of the different elements in adapter (cut)

The temperature on the main body was changed faster than the temperature on the CCG. There was d**ifferent temperature gradient**, different expansion or contraction of the materials and different width of the dielectrics.

The material expansion L1 of the main body and AT was faster and bigger with the increasing temperature from the steady state, because the changes of temperature on the CCG took a longer time and the expansion L2 was slower and smaller. The upper electrodes 2 and 3 increased the capacity, because dielectrics had smaller width. Conversely, electrodes 1 and 4 lost the same capacity.

The cooling of the adapter under the calibration resistant ratio (20 °C equivalent) was made contraction (L3) of material and the capacity increased on upper sensors as in Fig. 73. A contraction (Shortening L4) on CCG was slower than in the material of the main body (Shortening L3).

The gradient of temperature was different for different parts of the adapter. There were different expansion and contraction of material. The air temperature was different than the temperature on the solid parts of adapter. It was not possible to make the temperature calibration by temperature sensor of air. The expansion or contraction of material was bigger than the change of temperature of the air.

Sensor's reactions

Sensor's reactions on the expansion and contraction (loss of energy) of the material were documented in the measured test. The steady state was the same for CCG and MB with AT. The adapter was warmed by hand from the steady state. After approximately 40 s the warming stopped and the system was cooled by outside air. On Graph 30 is shown the air temperature inside the adapter.

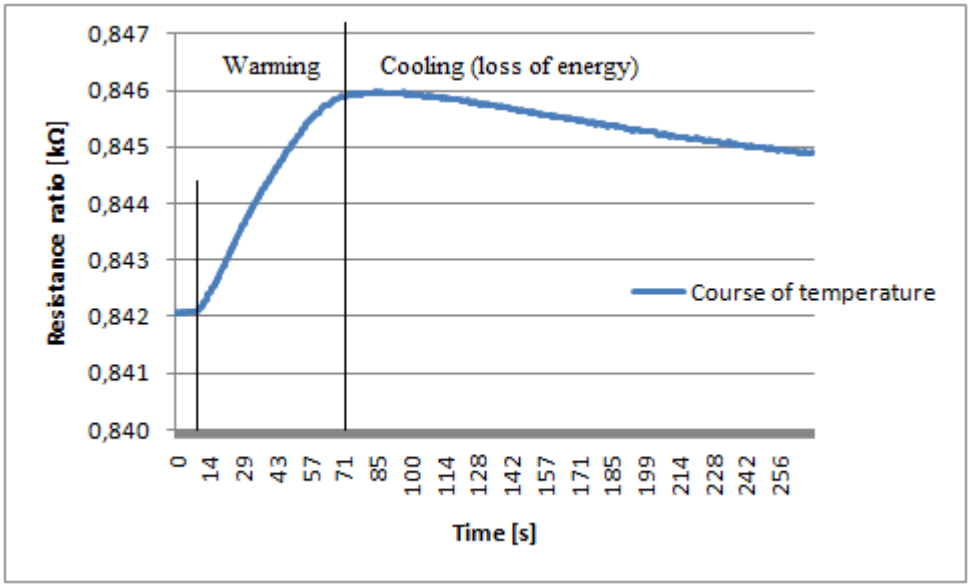

Graph 30: Temperature sensor -Test

The time delay of temperature is evident with the comparison of this graph with Graph 31 and Graph 32.

For illustration Sensor 3 and 4 in Graph 31, 32 were chosen. Here is explained the earlier material problem. With the increasing temperature, the material on the MB expanded, the tube was longer and the sensor was shifted up. It meant the dielectric was wider and the capacity was decreasing as in Graph 31.

After stopping the warming, the tube was cooled by air. The width of the dielectric got smaller. The capacity was coming back to the steady state.

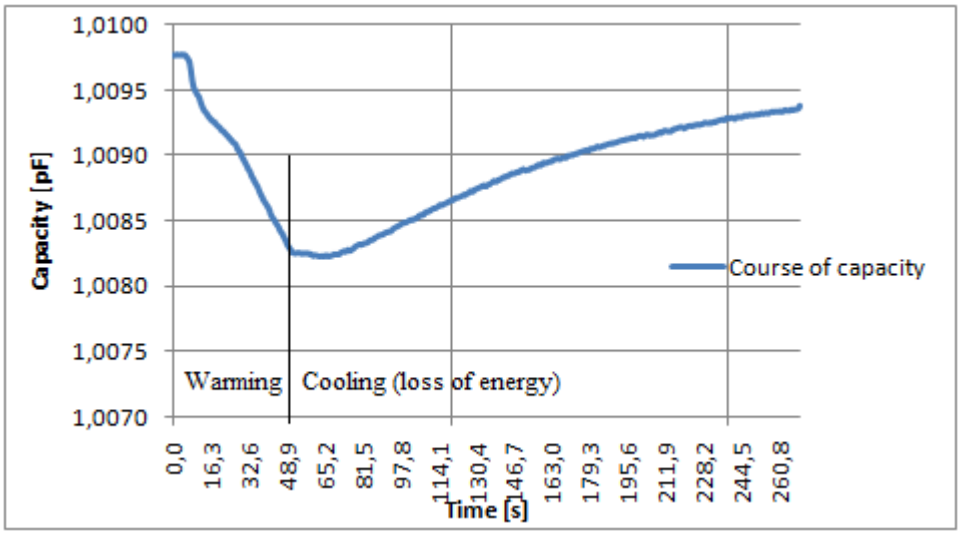

Graph 32: Sensor 3- Test

The opposite process of capacity is in Graph 32. With the lengthening of the tube was a smaller dielectric width and higher capacity. When the system lost energy, the electrode width was bigger –and capacity smaller. Both graphs correspond with Fig. 73.

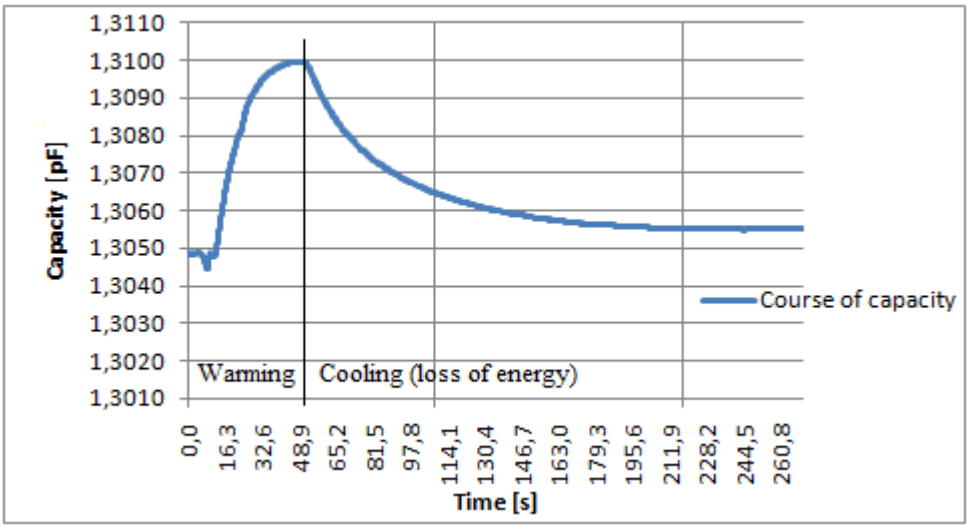

Graph 31: Sensor 4-Test

Result

The material properties were the biggest problem for the compensation in the adapter. The bridge compensation and calibration by temperature sensor on the microchip probably worked well, but the temperature instability of materials had a much bigger influence. It was not possible to create good sensor's calibration for this construction of model.

4.7. Possible solutions

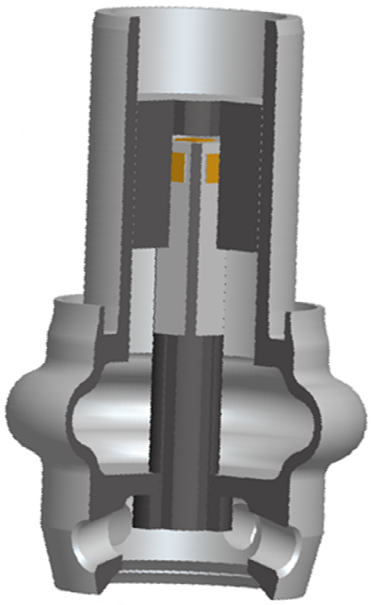

Fig. 75: Moment sensor

From the design structure in chapter 4.1. it is possible to make a moment sensor adapter with the expansion calibration. The expansion, as was written earlier, increased the length of the tube with adapter. If the structure of sensor is as in the following Fig. 75, it should be possible to compensate the vertical shift created by temperature. The sensor can measure only the moment component with compensation of thermal expansion and contraction of material.

The vertical force is measured on the top of the central element as in Fig. 74, but there is no compensation and the result can be with the same error as the testing new C-Leg adapter.

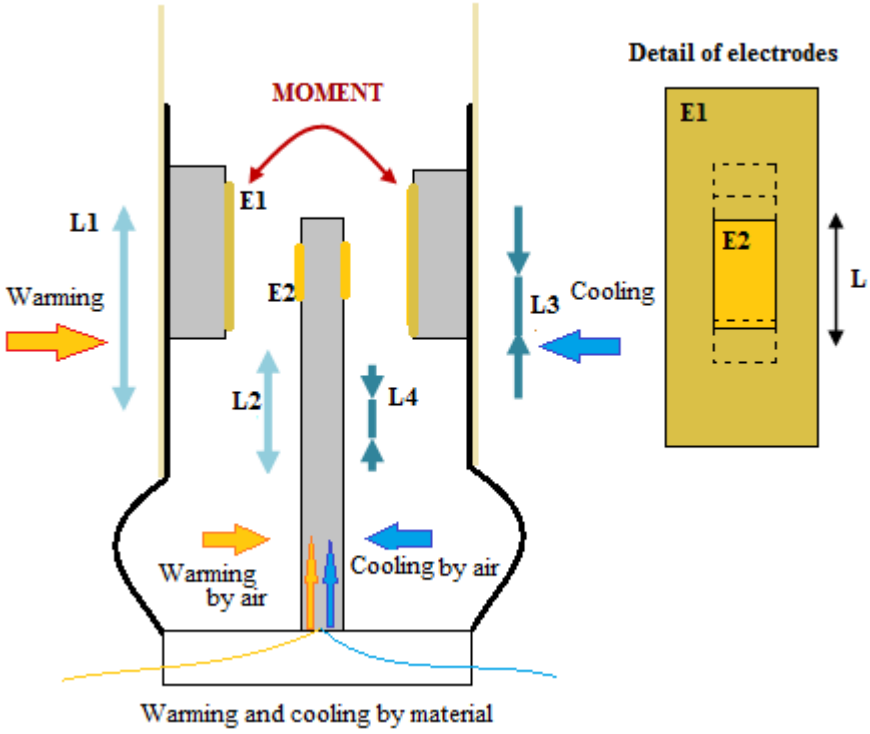

Fig. 74: Compensation of expanding and contraction - cut

As a real solution it is necessary to find the right design of model. It is necessary to find a place where there is not a deformation of material during load, but only material expansion or contraction with temperature influence. On this place can be implemented another capacitive sensor that can measure the difference of the material during warming or cooling exactly during expansion or contraction of material. The deformation of material is lengthening with the growing temperature and here it can be possible to measure a different width between electrodes. This is not an easy problem, but it is not impossible to solve it.

The adapter (main body) made by two materials with the positive and negative reaction on temperature (with increasing temperature – one material expansion and second contraction) could be much better solution. In this type of design have to be calculated right ratio of thermal expansion coefficient (WAK) [10-6/K] for "normal" material and ,material with negative thermal expansion (NTE). If is this ratio zero, we don't have expansion of material and it is possible compensate only the air inside adapter by some connection of temperature bridge or temperature sensor as now. The NTE materials are very interesting for research as describes John S.O. Evans[35]. This materials contracts when heated! Cubic Zirconium Tungstate (ZrW_2O_8), contracts continuously over temperature range of 2 to 1050 K. Matherials as $A_2M_2O_7$ and $A_2(MO_4)_3$ phases are also under investigation.[35] The cost and technology for developement of the MB by this new types of material is on discussion.

The next possibility how to improve this system for calibration is by adding some strain gauge sensor bridge on the MB and compensating the temperature directly on the material. This solution is made in C–Leg prosthesis now in manufacturing, but in this case the benefit of measurement only by capacitive sensors is lost.

Final result

New C–Leg working tube and adapter with capacitive sensors are in Fig. 76 shown.

Fig. 76: Final result

5 Discussion

Teoretical knowledge in the first two chapters have been used for a design of the capacitive sensing for equipments in prosthetics. During the development of the first Evaluating board it was achieved of very valuable results, applied later for a design of a new adapter for C-leg prosthetics.

According to the first measurement on Evaluating board it was neccesary to connect the sensors to Ground mode. An advantage was a better protection of a signal against the vibrations by ground mode and especially the benefit was a higher number of measurement channels. After several tests I made a conclusion that the system of sensors, which is described by Patric Biemuller is generally correct, but in this hardware solution is insoluble. Four sensors are insufficient for the total description of searched center of pressure. I developed during my measurements that the values of coefficients are too small and not unique for the searched position on the Evaluating board. According to the methodes of coordinates and coefficients it is not possible to exactly determine where the center of pressure is located and how much force we used. Temperature and humidity compensation was successfully solved by using a special calibration in the climate box. The system with the referential capacitor operated properly. It worth trying to replace it by temperature sensor on the microchip. The biggest disadvantage which influenced a whole result was using of rubber rollers as deformative element for separating the electrodes of sensors. These rubbers rollers has a thread and a lock screw for fixation in Evaluating board. This solution showed extreme nonlinearity and especially strong material hysteresys. This material is entirely unsuitable for futur commercial use in Evaluating board. As a possible improvement it would be appropriate to replace these elements by system of many springs located in the concentric cylinder. The movement would be eliminated in horizontal plane and it would be measured only the vertical force. The hysteresys has to be minimized and load of Evaluating board has to fully resemble to the linear progression. The device is functional and as long as a problem with rubber elements is eliminate in future, conditions for very high accuracy of measurement will be possible to create by calibration and coefficients.

Knowledge from previous test-device (Evaluating board) was also used for a design of C-leg adapter. It was needed to find a measure system, which would be able to

measure the vertical force and the moment. The Model was designed on the basis of deformation of the main adapter body in ProEngineer program. Finite element method analysis in ProMechanica program preliminary confirmed a functionality during the load. From many of variants it was chosen a system of four sensors, which compensate a temperature and humidity by bridge connection. The final vertical force and moment is created by sum of signals from all four sensors according to the particular connection. After the construction of necessary parts in manufacture department was whole system assembled and tested. The production of a printed circuit board was complicated and during repeated testing the copper parts were deformed. These problems were solved by professional production. The shape of electrodes was consulted with specialists and showed to be correct. Important part was choosing the central circuit electrode in ground connection, which made four sensors. The most appropriate option was the one with the smallest dielectric. It makes higher sensitivity of the system. This presumption was checked by Finite Element Method analysis in a program Ansys. Due to the strong nonlinearity of signal during first measurements I supposed that the humidity and temperature in adapter influences negatively the measurements. For this reason was the compensation extended to measurement by temperature sensor in the microchip. Program Microsoft Excel includes linearization process, which can compensate the temperature by coefficients from temperature sensor. The calibration of device for vertical force and moment has got higher accuracy with increase load.

I discovered that the linearization of temperature is incorrect. The reaction of capacitive sensors was different from the theoretical assumption due to temperature changes. An error was found in wrong fixation of tube element to adapter. After the fabrication changes it was discovered that the measurements were vey precise. The main problem was in relation between the material propertz of the main body and the temperature. Expansion and contraction of the material cause to shift of electrodes opposite ground and this makes the measurement strongly non-linear. There is a different thermal gradient for different elements inside the adapter. This material negative property was not recognized in previous measurements. As already mentioned, there was a problem with fixation of the aluminium tube element and adapter. Assumption of the non-homogenous temperature field and humidity inside the adapter was wrong. Main supply of linearity error is earlier described problem with expansion of material. This material property has much stronger impact on the result than own

temperature and humidity influence. From the development in this new device I made conclusion, that the problem with thermal expansion and contraction of material is displayed also on the rubber rollers for Evaluating board.

One of the option is to create a new inner structure of C-Leg adapter focused only on the moment component which is possible compensate easier. There is also another option in finding two materials with the same positive and negative thermal expansion.

Compared with strain gauge sensor, which are now used in C-Leg prosthesis, is compensation of material temperature extension more complicated. The benefit of contactless is overshadowed by direct measurement of material temperature as it is with strain gauge sensor. Here is used compensation by temperature bridge. However, the technology of capacity sensing is much cheaper and more available for manufacture field.

Conclusion

This thesis is concerned with capacity sensors in prothesis. After the detailed introduction, where the attention is focussed on biomechanics, prosthetics, prosthesis, properties and basic use of capacitive sensors, the implementation of capacity sensing in prosthesis devices is solved.

From the previous device for sensing the location of human feet and legs was developed Evaluation board workspace. On this equipment the connections of capacity sensors and influence of temperature and humidity were tested. The grafical output in Matlab program was easy understandable and system of calibration and calculation was made for finding the centre point of pressure on the board.

The thesis consist of detailed design of a new adapter for C-leg prosthesis. After the assemble, the final product was functional, continuously improved and didn´t have any functional problems. Minor problems were eliminated or the solution was outlined. Compensation of various adverse ambient effects were solved in spreadsheets of Microsoft Excel. This problem was sufficiently described in details and the knowledge will be used in future improvement of this new C-leg adapter prototype. A task of the thesis was fulfilled.

The vision of using optical and laser sensing could be an interesting subject for next progress. Capacity sensors have a great chance to succeed in prosthesis and certainly their development will continue.

References and other documentation

[1] KNUDSON, Duane. *Fundamentals of biomechanics*. New York 10013 : Kluwer Academic/ Plenum Publishers, 2003. 349 p. ISBN 0-306-47474-3.

[2] R. MCNEILL, Alexander. Mechanics of animal movement. In *Current biology* [online]. Leeds LS2 9JT, UK : School of Biology, University of Leeds, Available online, 22 August 2005 [cit. 2011-12-13]. Available WWW: <http://www.sciencedirect.com/science/article/pii/S0960982205009012>.

[3] VAŘEKA I., *Sofistikovaná biomechanická diagnostika lidského pohybu* [online]. CZ.1.07/2.3.00/09.0209. 2009 [cit. 2011-07-13]. Dynamická plantografie. Available from WWW: <www.biomechanikapohybu.upol.cz>.

[4] BLUMENTRITT, S. Biomechanische Aspekte zur Indikation von Prothesenkniegelenken : Biomechanical Aspects Influencing the Indication of Prosthetic Knee Joints. *Orthopädie Technik*. 06/2004, no.6, p. 9-19. ISSN 646D203.

[5] PITKIN, PH.D, Mark R. *Biomechanics of Lower Limb Prosthetics*. Berlin: Springer, 2010. 142 p. ISBN 978-3-642-03015-4.

[6] DUNGL, P. and colleague. *Ortopedie.* Praha: Grada, 2005, 1280 p. ISBN 80-247-0550-8.

[7] PICO CAP ® : Preliminary Datasheet. In *PCapØ1-EVA-KIT : Evaluation System for PCap01A*. Stutensee, Germany : Acam-messelectronic gmbh, April 29th, 2011. p. 26.

[8] SHALLCROSS, David C. *Handbook of psychrometric charts: humidity diagrams for engineers*. Great Britain : Springer, 1997. 317 p. ISBN 0751404764, 9780751404760.

[9] Humidity at the flat and its determination. *Construction and interior* [online]. 2009, 7, [cit. 2011-08-17]. Available from WWW: <http://www.stavebnictvi3000.cz/vypocty/vlhkost-v-byte/>.

[10] PICO CAP® : Preliminary Datasheet. In *PCapØ1Ax-0301 : Single-chip Solution for Capacitance Measurement with Standard Firmware 03.01.02*. Stutensee, Germany : Acam-messelectronic gmbh, May 13th, 2011. p. 68.

[11] BLOHMKE, Fritz; NÄDER, E.H. Max ; NÄDER, Hans Georg . *Prosthetic Compendium : Lower Limb Prostheses*. 3.revised and enlarged version. Berlin : Schiele & Schön GmbH, 2002. 127 p. ISBN 3-7949-0693- 4.

[12] GRONLEY, J.K.; PERRY, J. *Gait analysis techniques : Physical Therapy*. [c.l.] : [s.n.], 1984. 63 s. 1831-1838.

[13] WINTER, D. *Kinematic and kinetic patterns in human gait. : Kinematic and kinetic patterns in human gait.* . 3. [c.l.] : [s.n.], 1984. 102 p. 51-76.

[14] THOMPSON, Dave. *Moon.ouhsc.edu* [online]. Last updated 4-3-02 [cit. 2011-11-14]. Ground Reaction Force. Available from WWW: <http://moon.ouhsc.edu/dthompso/gait/kinetics/GRFBKGND.HTM>.

[15] BAXTER, Larry K. *Capacitive Sensors : Design and applications*. New York : IEEE PRESS, 1997. 305 p. Available from WWW: <http://www.capsense.com/capsense-wp.pdf>. ISBN 0-7803-1130-2.

[16] *Www.lionprecision.com : How Capacitive Sensors Work and How to Use Them Effectively* [online].TechNote, 2009 , LT03-0020 [cit. 2011-11-14]. Capacitive Sensor Operation and Optimization. Available from WWW: www.lionprecision.com.

[17] ALTENDORF, Roger. *Design World* [online]. North American Headquarters, Florence, Ky : 2011 [cit. 2011-11-16]. The Search for a Better Proximity Sensor Starts Here. Available from WWW: </www.designworldonline.com>.

[18] BIEMÜLLER, Patric. *Auslegung einer kraftmessplattform zur einfachen und preiswerten messung und anzeige des kraftangriffspunktes*. Hochschule Ulm, 2010. 136 s. Diploma Thesis. Hochschule ULm .

[19] ADÁMEK, Martin . *Internetová stránka Martina Adámka* [online]. 2007 [cit. 2011-11-22]. General properties. Available from WWW: <http://147.229.68.118/~adamek/>.

[20] HATZE, Herbert . The meaning of the term biomechanics. In *Journal of Biomechanics 7*. [c.l.] : [s.n.], 1974. p. 189–190.

[21] WINTER, David A. *Human Movement Science*. Volume 3, Issues 1-2. [c.l.] : [s.n.], 1984. 51-76 p.

[22] KETTELKAMP, D. B. , et al. *J.Bone Joint Surg.*. [c.l.] : [s.n.], 1970. An electrogoniometric study of knee motion in normal gait, p. A-52:775.

[23] LAUBENTHAL, K.N. *A quantitative analysis of knee motion during activities of daily living : Phys Ther 52(1).* [c.l.] : [s.n.], 1972. 34-43 s.

[24] PERRY, J. ; BONTAGER, E. *Development of a gait analyser for clinical use*. 2. Trans Orthop Res Soc : [s.n.], 1977. 48 p.

[25] JÍROVÁ, Jitka. *5_koleno_pohyb.pdf* [online]. 2009 [cit. 2011-11-22]. Biomechanika. Available from WWW: <www.mech.fd.cvut.cz>.

[26] KWON, Young-Hoo. *Kwon3d* [online]. 1998 [cit. 2011-11-29]. Force-Plate Issues. Available from WWW: <www.kwon3d.com>.

[27] DIETL, H, et al. C-Leg - Ein neues System zur Versorgung von Oberschankelamputationen. *Orthopädie Technik*. 1998, 49, p. 197-211.

[28] DUTTON, Mark. *Orthopaedics : for the Physical Therapist Assistant*. Allegheny general hospital, Pittsburgh : Jones & Bartlett Learning, 2011. 732 p. ISBN 978-0763797553.

[29] PICOCAP ® *: Linearization of Pressure Sensors with PCap01*. WP005_e V0.2. Germany : Acam-messelectronic gmbh, 2011. 34 p. Available from WWW: www.acam.de/fileadmin/Download/pdf/English/WP005_e.pdf>.

[30] KRYNICKÝ, Martin . *Učebnice matematiky a fyziky* [online]. 12. 2. 2009 [cit. 2011-12-12]. Racionální a polynomické funkce . Available from WWW: <http://ucebnice.krynicky.cz/Matematika/02_Funkce_a_rovnice/7_Mocnine_funkce_a_odmocniny/2705_Racionalni_a_polynomicke_funkce.pdf>.

[31] HIPPEL, A. Van. *Tables of dielectric materials*. Laboratory for Insulation research, 1944. 199 p. Final Report . Massasuchets institut of technology. Available from WWW: <http://www.dtic.mil/cgi-bin/GetTRDoc?Location=U2&doc=GetTRDoc.pdf&AD=ADA288986>. WL-TR-94-4125.

[32] NORDIN, Margareta ; FRANKEL, Victor Hirsch . *Basic biomechanics of the musculoskeletal system : M - Medicine Series*. 3. [c.l.] : Lippincott Williams & Wilkins, 2001. 467 s. ISBN 0683302477,9780683302479.

[33] *The Engineering ToolBox* [online]. c2011 [cit. 2011-10-02]. Elastic Properties and Young Modulus for some Materials. Available from WWW: <http://www.engineeringtoolbox.com/young-modulus-d_417.html>.

[34] Gaussova funkce. In *Wikipedia : the free encyclopedia* [online]. St. Petersburg (Florida) : Wikipedia Foundation, 13.4.2010, last modified on 18.3.2011 [cit. 2011-12-13]. Available from WWW: <http://cs.wikipedia.org/wiki/Gaussova_funkce>.

[35] EVANS, John S.O. *John Evans Research Interests* [online]. Chemistry Department at the University of Durham : 30-Oct-2011 [cit. 2011-12-16]. Negative Thermal Expansion Materials. Available from WWW: <http://www.dur.ac.uk/john.evans/webpages/research_nteintro.html>.

List of Figures

List of Graphs

Attachments

Content

CD contens:

Master thesis, PDF
Programs in Matlab
Programs in MS Excel

A1 Program code in Matlab "Mass Measurement-Gaussian function"

```
% - MASS MEASUREMENT -
%----------------------
% Connect evaluating board with the computer
% Start the measurement (better with lower measuring rate)
% Save data to file "data.txt" into your computer,where is your
% matlab file saved.
% Run Massmeasurement.m file.

% script for changin the comma to dot
file1='data.txt';
% replaces all occurences of comma (",") with point (".") in a text-
% file.
% Note that the file is overwritten, which is the price for high
% speed.
    file = memmapfile( file1 , 'writable', true );
    comma = uint8(',');
    point = uint8('.');
    file.Data( transpose( file.Data==comma) ) = point;
    delete(file)

%reading dat from .txt
clear all;
A = importdata('data.txt','\t',1);
offsetdata = A.data;

%Offset calculation
d1=offsetdata(1,1)-min(min(offsetdata));
d2=offsetdata(1,2)-min(min(offsetdata));
d3=offsetdata(1,3)-min(min(offsetdata));
d4=offsetdata(1,4)-min(min(offsetdata));

offsetdata(:,1)=offsetdata(:,1)-d1;
offsetdata(:,2)=offsetdata(:,2)-d2;
offsetdata(:,3)=offsetdata(:,3)-d3;
offsetdata(:,4)=offsetdata(:,4)-d4;


e=min(min(offsetdata));
offsetdata=offsetdata-e;

numdata=offsetdata;

[X,Y,Z] = peaks(24);
Z=zeros(24,24);
figure(1);
u=0.1;
b=min(min(numdata));
c=max(max(numdata));
```

```
%Gaussian function implementation for 4 channels
for i=1:size(numdata,1)   %for i=1:length(dat)
    Sx=6;   %x - center point of plotting
    Sy=6;   %y - center point of plotting
    for jx=1:12
        for jy=1:12
          Z(jx,jy)=numdata(i,1)*exp(-u*(jx-Sx).^2)*exp(-u*(jy-Sy).^2);
            %dat(2,i) - 2. line, i. column
            %u - speed of gradient of the curve
        end;
    end;
    Sx=18;
    Sy=6;
    for jx=13:24
        for jy=1:12
          Z(jx,jy)=numdata(i,2)*exp(-u*(jx-Sx).^2)*exp(-u*(jy-Sy).^2);
        end;
    end;
    Sx=6;
    Sy=18;
    for jx=1:12
        for jy=13:24
          Z(jx,jy)=numdata(i,3)*exp(-u*(jx-Sx).^2)*exp(-u*(jy-Sy).^2);
        end;
    end;
    Sx=18;
    Sy=18;
     for jx=13:24
         for jy=13:24
          Z(jx,jy)=numdata(i,4)*exp(-u*(jx-Sx).^2)*exp(-u*(jy-Sy).^2);
         end;
     end;

    %Graphical interface
    colormap(jet)
    figure(1);surf(X,Y,Z);
    axis([-3  3  -3  3  0  c])    %axes

text(1.5,1.5,c,strcat('CH4:',num2str(Z(18,18))),'HorizontalAlignment',
'left');
    text(-1.5,-
1.5,c,strcat('CH1:',num2str(Z(6,6))),'HorizontalAlignment','left');
    text(1.5,-
1.5,c,strcat('CH2:',num2str(Z(6,18))),'HorizontalAlignment','left');
    text(-
1.5,1.5,c,strcat('CH3:',num2str(Z(18,6))),'HorizontalAlignment','left'
);
    title('EVALUATING BOARD');
    zlabel('Capacity Difference [pF]');
    pause(0.2);      %speed
    disp(['Number of graphs shown: ',num2str(i)]);
end;
```

A1 Program code in Matlab “COP method of ratio”

```
% - MASS MEASUREMENT- COP ratio -
%----------------------
% Connect evaluating board with the computer
% Strat the measurement(better with lower measuring rate)
% Save data to file "data.txt" into your computer,where is your
% matlab file saved.
% Run Massmeasurement_point.m file.

%script for changin the comma to dot
file1='data.txt';
% replaces all occurences of comma (",") with point (".") in a text-
file.
% Note that the file is overwritten, which is the price for high
speed.
    file = memmapfile( file1 , 'writable', true );
    comma = uint8(',');
    point = uint8('.');
    file.Data( transpose( file.Data==comma) ) = point;
    delete(file)



%reading dat from .txt
clear all;
A = importdata('data.txt','\t',1);
offsetdata = A.data;

%Offset calculation
d1=offsetdata(1,1);
d2=offsetdata(1,2);
d3=offsetdata(1,3);
d4=offsetdata(1,4);

% Calibration on from 0
offsetdata(:,1)=offsetdata(:,1)-d1;
offsetdata(:,2)=offsetdata(:,2)-d2;
offsetdata(:,3)=offsetdata(:,3)-d3;
offsetdata(:,4)=offsetdata(:,4)-d4;



% Point
L1Total=250;
L2Total=400;
L3Total=250;
L4Total=400;
```

```
%stable kalibration of free board
%n=max(max(offsetdata));

for k=1:size(offsetdata,1)


L1=L1Total*(offsetdata(k,2)/(offsetdata(k,1)+offsetdata(k,2)));

L2=L2Total*(offsetdata(k,3)/(offsetdata(k,2)+offsetdata(k,3)));

L3=L3Total*(offsetdata(k,4)/(offsetdata(k,3)+offsetdata(k,4)));

L4=L4Total*(offsetdata(k,1)/(offsetdata(k,4)+offsetdata(k,1)));

        if offsetdata(k,:)<5e-014    % Calibration of measurement
    L1=250;
    L2=400;
    L3=250;
    L4=400;
        End

plot([400 0],[L1 250-L3],[400-L2 L4],[250 0],'Marker','.',
'LineStyle','-')
%     plot(Lx,Ly,'.','markersize',30);
    grid on
    axis([0 400 0 250]);
    title('EVALUATING BOARD-MASS-POINT');
    xlabel('Length [mm]');
    ylabel('Width [mm]');
    text(340,55,('+  CH1'),'HorizontalAlignment','left');
    text(60,55,('+  CH4'),'HorizontalAlignment','left');
    text(340,195,('+  CH2'),'HorizontalAlignment','left');
    text(60,195,('+  CH3'),'HorizontalAlignment','left');

    pause(0.01);
end
```

A1 Program code in Matlab "COP method of coordinates"

```
% - MASS MEASUREMENT- COP coordinates -
%----------------------
% Connect evaluating board with the computer
% Strat the measurement(better with lower measuring rate)with 4.885Kg
% in
% center of board for calibration.
% Save config in PicoCap software - use everytime same config as for
% calibration.
% Save data to file "data_reference.txt" into your computer,where is
% your
% matlab file saved. Do another measurement for free board and save
% the data
% to data_reference_free.txt. Start new real measurement,
% save the data to data.txtto same file.
% Run Massmeasurement_point_2.m file.

%script for changin the comma to dot
file1='data.txt';
% replaces all occurences of comma (",") with point (".") in a text-
% file.
% Note that the file is overwritten, which is the price for high
% speed.
    file = memmapfile( file1 , 'writable', true );
    comma = uint8(',');
    point = uint8('.');
    file.Data( transpose( file.Data==comma) ) = point;
    delete(file)


%reading dat from .txt
clear all;
A = importdata('data.txt','\t',1);
offsetdata = A.data;

% % Offset calculation
% d1=abs((4.0114E-12)-offsetdata(1,1));
% d2=abs((2.9248E-12)-offsetdata(1,2));
% d3=abs((3.9748E-12)-offsetdata(1,3));
% d4=abs((4.5095E-12)-offsetdata(1,4));
%
% % Calibration on from basic values of sensors
% offsetdata(:,1)=offsetdata(:,1)-d1;
% offsetdata(:,2)=offsetdata(:,2)-d2;
% offsetdata(:,3)=offsetdata(:,3)-d3;
% offsetdata(:,4)=offsetdata(:,4)-d4;

% Koeficient Weight + Length (from measured data)
KoefWL=offsetdata;
KoefWidth=(KoefWL(:,3)+KoefWL(:,4))./(KoefWL(:,1)+KoefWL(:,2));
KoefLength=(KoefWL(:,2)+KoefWL(:,3))./(KoefWL(:,1)+KoefWL(:,4));

% Load KoeficientWL (constant data for calibration)
B = importdata('koeficientWL5Kg.txt','\t',1);
koeficient = B.data;
```

```
% Load data_reference Free_EB(constant data for calibration of Weight)
C = importdata('data_reference_free.txt','\t',1);
ReferenceFree = C.data;
WeightRefFree=ReferenceFree(:,1)+ReferenceFree(:,2)+ReferenceFree(:,3)
+ReferenceFree(:,4);  % Reference capacity for 4.885Kg
WeightFree=1*10e-15;
WeightRefAvgFree=sum(WeightRefFree)./size(ReferenceFree,1);


% Load data_reference 4.885Kg(constant data for calibration of weight)
D = importdata('data_reference.txt','\t',1);
reference = D.data;
weightref=reference(:,1)+reference(:,2)+reference(:,3)+reference(:,4);
% Reference capacity for 4.885K
weight=4.885;
weightrefavg=sum(weightref)./size(reference,1);

WeightRange=weightrefavg-WeightRefAvgFree;


% Coordinates
for n=1:size(offsetdata,1)


completcapacity=offsetdata(n,1)+offsetdata(n,2)+offsetdata(n,3)+offset
data(n,4);
        completcapacity=completcapacity-WeightRefAvgFree;
        weightnew=abs((completcapacity*weight)/WeightRange);
                                          % Transform to the weight

        minnumberW =  KoefWidth(n,1)-koeficient(:,1);
                                        %Test of minvalue
        minnumberW=abs(minnumberW); % Array of results
        [r,c]=find(minnumberW==min(min(minnumberW)));  % Find a row
        x=koeficient(r,5);   % Find x from axes

        minnumberL =  KoefLength(n,1)-koeficient(:,2);
        minnumberL=abs(minnumberL);
        [r2,c2]=find(minnumberL==min(min(minnumberL)));
        y=koeficient(r2,4);

    plot(x(1,1),y(1,1),'.','markersize',30);
    grid on
    axis([-200 200 -125 125]);
    title('EVALUATING BOARD-MASS-POINT-2');
    xlabel('Length [mm]');
    ylabel('Width [mm]');
text(100,-150,strcat('WEIGHT: ',num2str(weightnew),'[Kg]'),
'HorizontalAlignment','left','BackgroundColor',[.9 .9 .7],'Margin',7);
       pause(0.1);

end
```

A2 Inside sensor structure

1.Design

Variant: a) one dimensional system - vertical force [y]
b) two dimensional system - vertical force [y], moment [x]
c) three dimensional system - vertical force [y], moment [x, z]

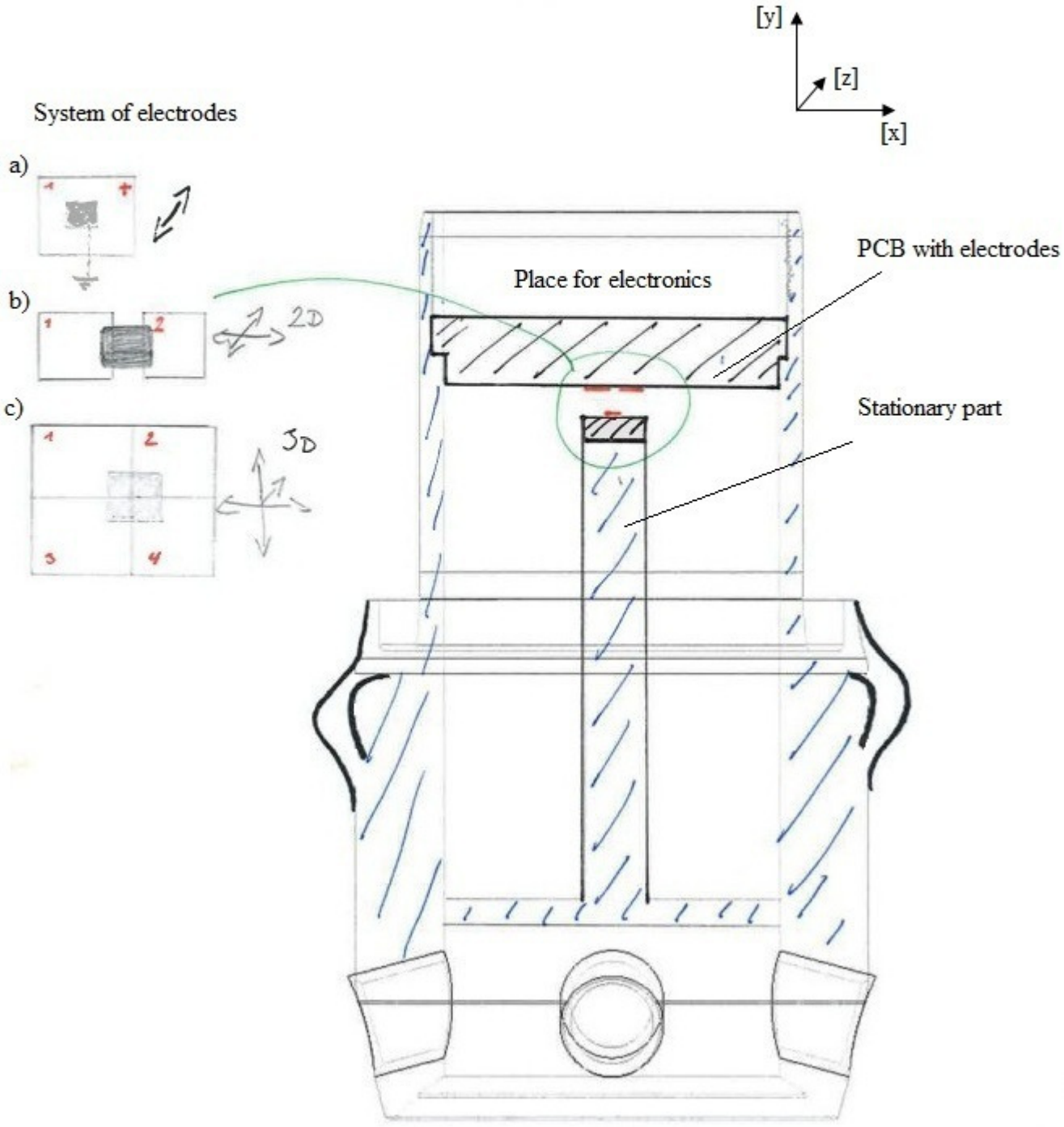

A2 Inside sensor structure

2.Design

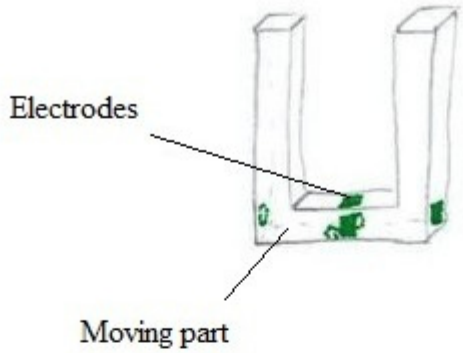

Three dimensional system
(Two dimensional variable)

[x] moment
[y] vertical force
[z] moment

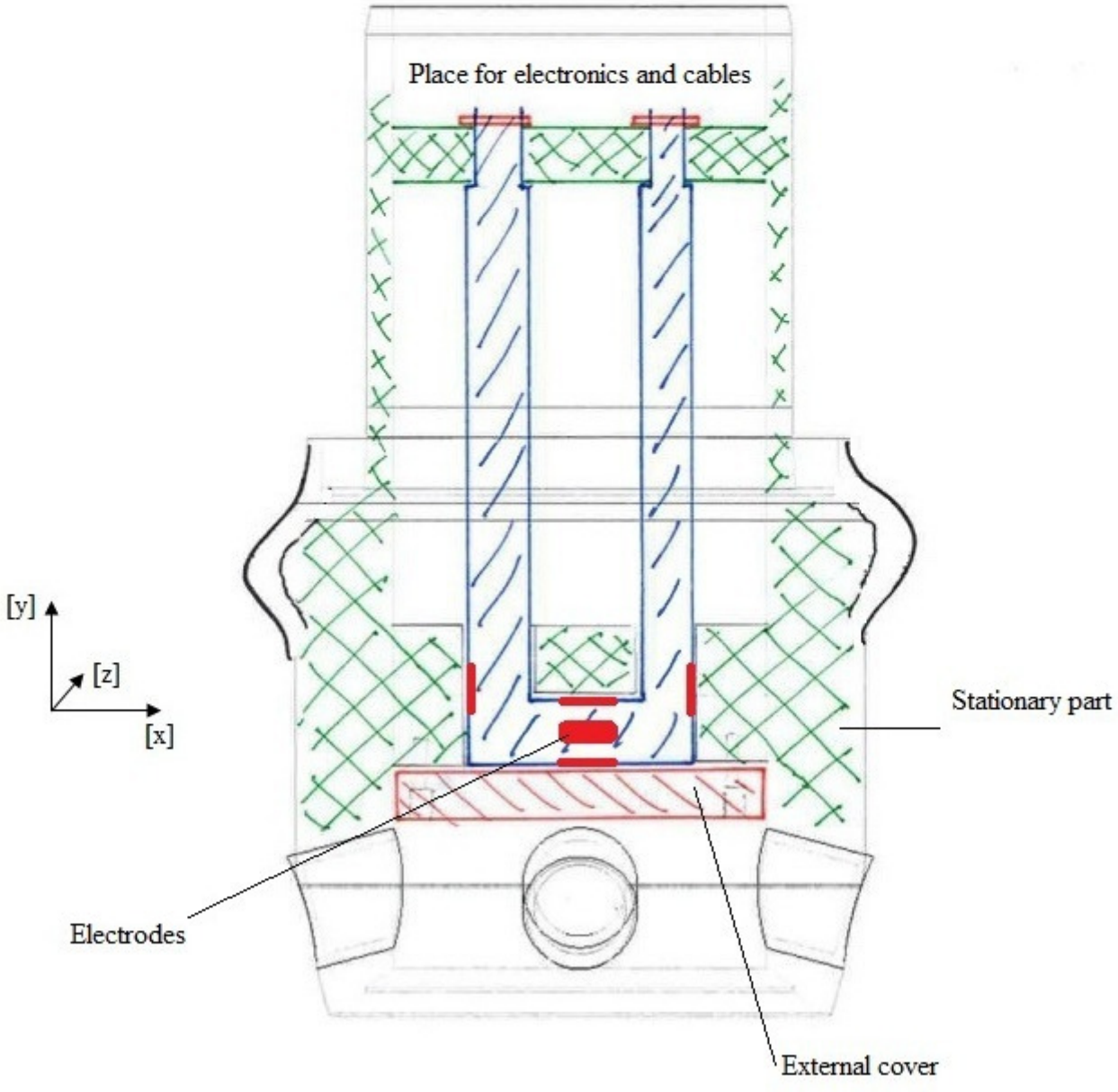

A2 Inside sensor structure

3.Design

Two dimensional system
(Three dimensional variable)

[x] moment
[y] vertical force

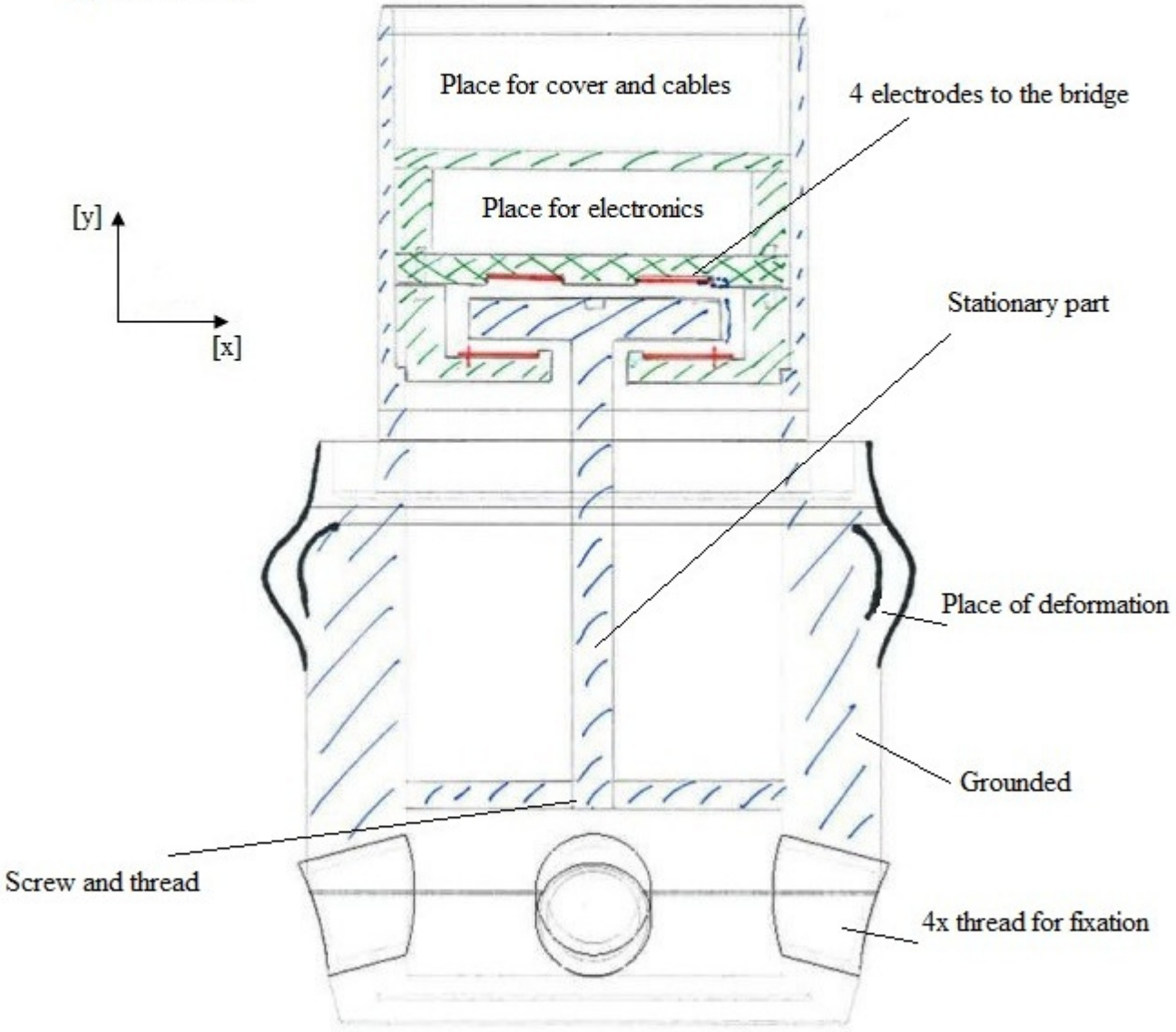

A3 PCB drawings

Shapes of electrodes

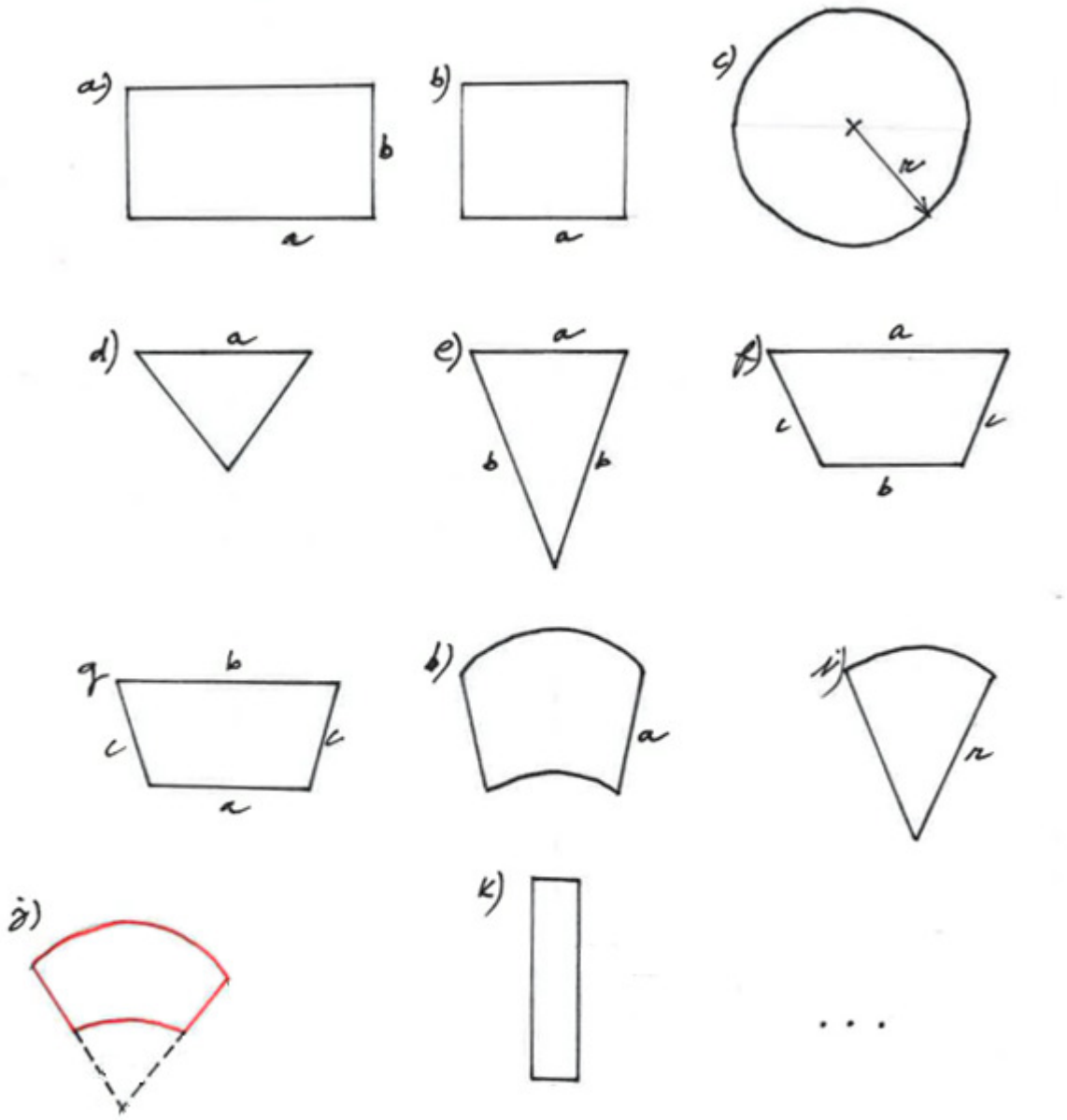

A3 PCB drawings

The winning shapes of positive electrodes:

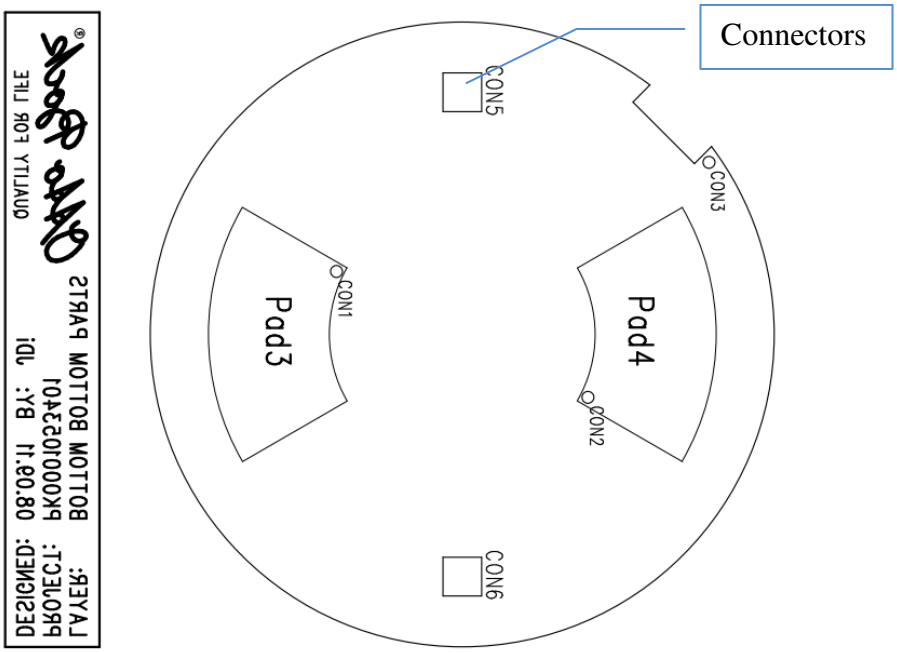

The Electronic on the top of the PCB: